Faculty of Science

Charles University in Prague

PhD Study Programmes in Biomedicine

Molecular and Cellular Biology, Genetics and Virology

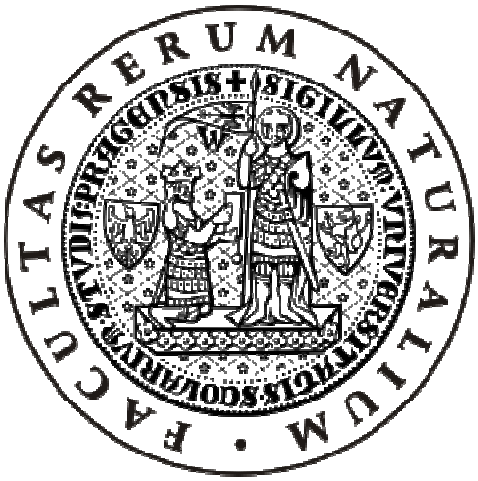

Regulation of pre-mRNA splicing in the context of cell nucleus

Jarmila Hnilicová

PhD Thesis

Scientific supervisor: David Staněk, PhD

Institute of Molecular Genetics

Academy of Sciences of the Czech Republic

Prague, 2011

Prohlašuji, že všechny použité zdroje a literatura byly řádně citovány a že jsem nepředložila práci ani její podstatnou část k získání jiného nebo stejného akademického titulu.

V Praze, 23.6.2011 Jarmila Hnilicová

Prohlašuji, že podíl studenta na výsledcích uvedený v kapitole „Commentary to the results“ je pravdivý.

V Praze, 23.6.2011 Mgr. David Staněk, Ph.D., školitel

Acknowledgement

I would like to thank my supervisor David Staněk for his ideas and enthusiasm. This PhD thesis would never be finished without his support.

Many thanks also belong to my colleagues for creating friendly environment and stimulating atmosphere in the lab.

Contents

List of abbreviations

ChIP	chromatin imunoprecipitation
ED-A, EDA	extra domain A
ED-B, EDB	extra domain B
FDA	Food and Drug Administration
FTDP-17	Frontotemporal dementia and Parkinsonism linked to Chromosome 17
HAT	histone acetyl transferase
HDAC	histone deacetylase
hnRNP	heterogeneous nuclear ribonucleoprotein
mRNA	messenger RNA
pre-mRNA	precursor mRNA
snoRNA	small nucleolar RNA
snRNA	small nuclear RNA
snRNP	small ribonucleoprotein particle
SR	serin arginine rich
tRNA	transfer RNA
U snRNP	uridine-rich small ribonucleoprotein particle
U2AF	U2 auxiliary factor

Abstract

Eukaryotic genes contain non-coding sequences - introns that are removed during pre-mRNA splicing by the spliceosome. The spliceosome is composed of five snRNPs (U1, U2, U4/U6 and U5) which assemble on pre-mRNA in a step-wise manner and together with additional non-snRNP proteins catalyse splicing. Mutations in splicing factors can cause severe diseases, for example a point missense mutation (called AD29) in hPrp31 (U4/U6 snRNP specific protein) induces retinitis pigmentosa, disease often leading to complete blindness. In this PhD thesis we show that the hPrp31 AD29 mutant is unstable and is not properly incorporated into spliceosomal snRNPs. In addition, the expression of the mutant protein reduces cell proliferation, which indicates that it interferes with cellular metabolism (likely splicing) and could explain the induction of retinitis pigmentosa.

Next, we focus on a role of nuclear environment in pre-mRNA splicing. It was shown that new U4/U6·U5 snRNPs are preferentially assembled in non-membrane nuclear structure - Cajal body. Here we expand this finding and provide evidence that Cajal bodies are also important for U4/U6·U5 snRNP recycling after splicing. In addition, we analyzed a role of chromatin and particularly histone acetylation modulates in splicing regulation. Using inhibitor of histone deacetylases we change alternative splicing of more than 700 genes. Specifically HDAC1 deacetylase activity regulates alternative splicing of the fibronectin gene. We provide evidence that HDAC inhibition induces histone H4 acetylation and increases RNA polymerase II processivity along an alternatively spliced fibronectin elements. In addition, HDAC inhibition reduces co-transcriptional association of the splicing regulator SRp40 with the fibronectin alternative exon. We believe that there is a potential to use HDAC inhibitors in therapy of splicing related disorders in the future.

Abstrakt

Eukaryotní geny obsahují nekódující sekvence – introny, které jsou z pre-mRNA odstraňovány sestřihovými komplexy. Sestřihové komplexy se skládají z pěti RNA-proteinových podjednotek (U1, U2, U4/U6 a U5), které postupně nasedají na pre-mRNA a jsou společně s dalšími bílkovinami nutné pro vystřižení intronu. Mutace v bílkovinách důležitých pro RNA sestřih mohou způsobovat vážná onemocněním, například mutace zvaná AD29 vedoucí k záměně jediné aminokyseliny v proteinu hPrp31 (tato bílkovina je součástí U4/U6 sestřihového komplexu) je příčinou nemoci retinitis pigmentosa, která často končí úplnou slepotou. Ukázali jsme, že hPrp31 AD29 mutant je nestabilní a není řádně začleněný do sestřihových komplexů. Přesto vadný hPrp31 zřejmě má vliv na metabolismus buňky, protože zpomaluje buněčný růst a dělení, což by mohlo vysvětlit, proč tato mutace vede k retinitis pigmentosa.

Dále se zaměřujeme na roli buněčného jádra v pre-mRNA sestřihu. Nové U4/U6·U5 snRNP částice jsou přednostně skládány v nemembránových jaderných strukturách - Cajalových tělíscích. Zjistili jsme, že Cajalova tělíska jsou také důležitá pro recyklaci U4/U6·U5 snRNP. Vedle toho jsme se zaměřili na roli chromatinu (především acetylace histonů) při regulaci alternativního sestřihu. Pomocí inhibitorů histonových deacetylázy jsme změnili alternativní sestřih více jak 700 genů. HDAC1 deacetylázová aktivita mění alternativní sestřih fibronektinu. Inhibice histonových deacetyláz zvyšuje acetylaci histonů H4 a procesivitu RNA polymerázy II na alternativně stříhaných exonech fibronektinu. Současně HDAC inhibice snižuje kotranskripční vazbu sestřihového regulátoru SRp40 na alternativní exon fibronektinu. Věříme, že je v budoucnu možné použít inhibitory histondeacetyláz pro případnou léčbu onemocnění souvisejících s pre-mRNA sestřihem.

Introduction

1. Eukaryotic genes are interspersed with introns

By the late 70s it was believed that the structure of eukaryotic gene is very similar to the structure of bacterial gene. It was assumed that the sequence of expressed protein corresponds to the entire sequence of the gene and both genes and proteins are collinear. However, in 1977 it was discovered that adenoviral mRNA does not matches completely the gene it is originally transcribed from and surprisingly, parts of the internal adenoviral gene sequence are missing from the mRNA (Berget et al., 1977; Chow et al., 1977). Soon it became evident that not only adenoviral genes but a majority of eukaryotic genes are split. These genes have introns or intervening sequences which are removed from the pre-mRNA in the cell nucleus by the process called RNA splicing.

Several types of introns and a number of splicing mechanisms have appeared during evolution. These include classes I and II introns, rare structured introns present in bacteria, in ribosomal RNAs in the nucleus of protists, fungi or plants and in eukaryotic organelles (Haugen et al., 2005; Lambowitz and Zimmerly, 2010). Group I and II self-splicing introns functions as ribozymes that are able to catalyse their own excision. Another special type of introns are introns found in tRNAs, that are removed only by protein enzymes. Most of the introns in eukaryotes are spliceosomal introns, that are spliced by large ribonucleoprotein complex named spliceosome. At least two different types of spliceosome have been described: major spliceosome recognizing introns starting with GU and finishing with AG, minor spliceosome recognizing AT-AC intron boundaries (Hall and Padgett, 1996; Tarn and Steitz, 1996) and spliceosomes that are able to perform trans-splicing where two RNA pieces originated from different RNA molecules are spliced together (Bruzik et al., 1988; Van Doren and Hirsh, 1988). The AT-AC introns are present also in human genome (e.g. *NOP2* gene encoding nucleolar protein), but they represent only a little more than 0,1 % of all our introns (Scherer, 2008). The trans-splicing was described for example in *Trypanosoma* (Campbell et al., 1984), *C. elegans* (Krause and Hirsh, 1987)

or sea squirt *Ciona* (Vandenberghe et al., 2001). The further text will be focused only on the most abundant type of splicing performed by major spliceosome.

It is not known how introns have evolved and what is their function. Current views hold the first introns are likely to have arisen very early in eukaryotic evolution and together with the spliceosome were present already in the ancestor of all contemporary eukaryotes (Rodriguez-Trelles et al., 2006). The introns-late hypothesis suggests intron acquisition occured together with the origin of eukaryotic cell and spliceosomal introns evolved from group II self-splicing introns which were present in proteobacterial endosymbiont – mitochondria. Group II introns invaded uninterrupted nuclear genes, then lost the ability of self-splicing and started to be spliced by spliceosome (Cech, 1986; Sharp, 1985). This concept is supported by the discovery of introns in primitive protists like *Giardia* (Simpson et al., 2002) or *Entamoeba histolytica* (Wilihoeft et al., 2001) or other deep-branching eukaryotes such as *Plasmodium falcifarum* and *Trichomonas vaginalis* (Vanacova et al., 2005). Noticebly, most of the spliceosomal components were found in all eukaryotic genomes sequenced so far (Collins and Penny, 2005). Alternative „intron-early“ theory postulates the presence of introns before the origin of eukaryotes, at the earliest stage of life evolution suggesting that the first protein-coding genes already had introns that facilitated recombination of sequences coding small protein modules and played a role in protein evolution (Rodriguez-Trelles et al., 2006). These introns were later lost in prokaryotes. „Intron-first“ model suggests that introns even date back to the RNA world. mRNA arose as a byproduct of ribozyme processing reactions and originally it is from unused genetic material (Poole et al., 1998). In eukaryotic genome, many small nucleolar RNAs (snoRNAs) – relicts of RNA world necessary for maturation of ribosomal RNAs are encoded in introns of ribosomal and heat-shock proteins. So, supporting the theory some ancient ribozymes survive in introns.

In human genome, intron lenght can be enormous. The largest human intron which is found in *HS6ST3* heparan sulfate sulfotransferase gene has 740 kb (Scherer, 2008). This is the size of minimal genome - it is for example approximately the size of the genome of Gram-negative bacteria

Wigglesworthia glossinidia brevipalpis living in the gut of tse-tse fly (Akman et al., 2002). Although most of the introns are shorter with an average lenght of 3.4 kb, they are still ten times longer than an average exon having the lenght of 145 bp (Lander et al., 2001). Spliceosome must recognize correctly introns and joint exons, although the exons represent actually only a small fraction of the genes.

2. Spliceosome: RNA – protein macromolecular machine

Spliceosome is one the largest molecular complex in the cell. It resembles the ribosome – not only with the size, but also with the composition. Both, spliceosome and ribosome are ribonucleoprotein enzymes with RNAs located in active sites and playing a direct role in catalysis of the reactions (Nissen et al., 2000; Valadkhan and Manley, 2001). It is estimated that more than 150 proteins participates in pre-mRNA splicing (Makarov et al., 2002) together with 5 small nuclear RNAs (snRNAs). snRNAs form with proteins small ribonucleoprotein complexes (snRNPs). The spliceosome is a dynamic machine building anew on pre-mRNA each round of splicing: the building blocks of the spliceosome are U1, U2, U4/U6 and U5 snRNP that assemble in ordered, step-wise manner on the pre-mRNA, see **Fig. 1** (Jurica and Moore, 2003; Wahl et al., 2009). snRNPs are named according to the snRNAs they are composed of – for example U1 snRNP is a complex of U1 snRNA and a specific set of proteins. The proteins are different for each different type of snRNP with exception of seven Sm proteins, which are assembled as a stable ring on each of U1, U2, U4 and U5 snRNAs. How is the pre-mRNA splicing performed? First, U1 snRNP binds to 5´splice site via the base-pairing between the U1 snRNA and the consensus sequence at the splice site. In the cell nucleus, U1 snRNP is much more abundant than other snRNPs, the interaction of U1 snRNP with pre-mRNA occurs within seconds (Huranova et al., 2010) and is ATP-independent. Then 3´splice site elements must be recognized by SF1 protein (that interacts with branch point) and U2AF subunits. At this stage the intron boundaries are defined (see **Fig. 1**).

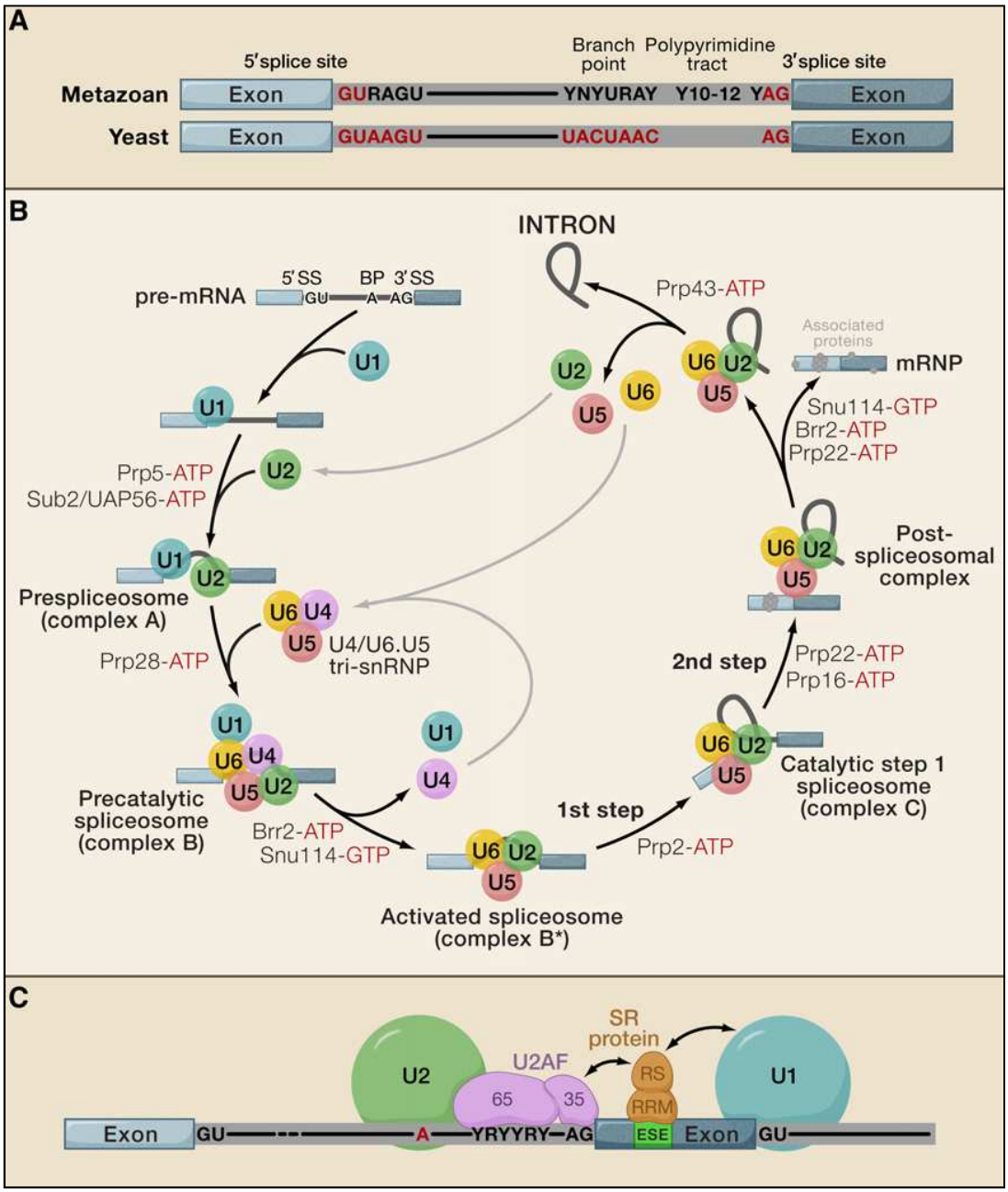

Fig. 1 Pre-mRNA splicing (Wahl et al., 2009)

(A) Consensus splice sites recognized by spliceosome.

(B) Step-wise spliceosome assembly on the pre-mRNA substrate, activation of spliceosome and disassembly of final products of splicing reaction. Prp22 RNA helicase and Snu114 GTPase will be discussed in experiments in Publication I and II.

(C) SR proteins help spliceosome to assemble on pre-mRNA. One of them, SRp40 was used to in experiments in Publication III.

After that U2 snRNP complex replaces SF1 protein and U2 snRNA directly base-pair with the branch point. Subsequently, the U4/U6 and U5 snRNPs are recruited as a preassembled U4/U6·U5 tri-snRNP, several compositional and conformational rearrangements occur (U1 snRNA interaction at 5´splice site is replaced with U6 snRNA and both U1 snRNP and U4 snRNP are lost from the complex) and spliceosome becomes competent to catalyse the first transesterification reaction. After the second catalytic step mRNA with ligated adjacent exons is released and U2, U5 and U6 snRNPs remain associated with the excised intron lariat. Thus, snRNPs must be recycled to allow a new round of pre-mRNA splicing.

Although two transesterification reactions that excise the intron do not themselves need ATP to proceed and can be reversible under certain ion conditions (Tseng and Cheng, 2008), the spliceosome assembly, multiple RNA-RNA rearrangements and spliceosome disassembly require ATP. Eight evolutionarily conserved DExD/H-type RNA-dependent ATPases/helicases (named after one of the consensus amino acid sequence motifs) participates in splicing (**Fig. 1**).

One of helicases is Prp22, that has several functions (see **Fig. 2**). Prp22 promotes the second transesterification reaction of splicing (Schwer and Gross, 1998), enhances fidelity of this reaction (Mayas et al., 2006), together with other spliceosomal proteins participates in splicing of atypical introns (Gahura et al., 2009) and importantly, Prp22 mediates the release of spliced mRNA from the spliceosome (Company et al., 1991; Ohno and Shimura, 1996; Schwer and Gross, 1998; Wagner et al., 1998). Prp22 disrupts contacts between U5 snRNA, Prp8 (U5 snRNP protein, **Fig. 3**) and spliced mRNA (Aronova et al., 2007). Thus, Prp22 is necessary for recycling of U5 snRNP components.

Prp43 is an RNA helicase important in the next step - it dissociates snRNPs from excised intron lariat (Arenas and Abelson, 1997). Postsplicing complex contains intron lariat with bound U2, U5, U6 snRNAs and some of the spliceosomal proteins (**Fig. 1**). These spliceosomal components must be removed before the free lariat is degraded by debranching enzyme Dbr1, which

specifically cleaves the branched 2′-5′ phosphodiester bond and induces intron degradation (Chapman and Boeke, 1991).

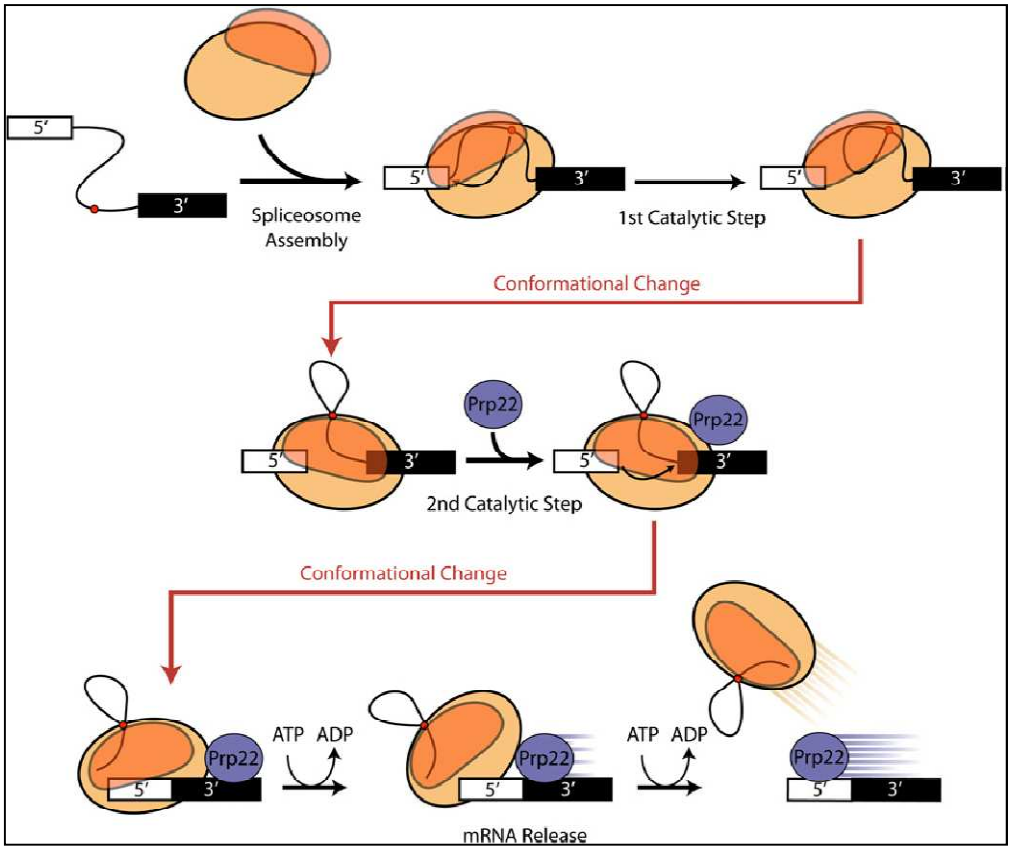

Fig. 2 Functions of Prp22 RNA helicase in pre-mRNA splicing

Prp22 discards spliceosome with intron lariat from spliced mRNA (McManus and Graveley, 2008).

Prp43 interacts with Ntr1 (human TFIP11) and Ntr2 proteins and these proteins are required for lariat release (Boon et al., 2006; Martin et al., 2002; Tanaka et al., 2007; Tsai et al., 2005; Tsai et al., 2007). Ntr1 recruits Prp43 to the postsplicing intron complex and stimulates Prp43 helicase activity which is necessary for efficient debranching and turnover of excised introns. Lack of functional Prp43 or Ntr1 causes intron accumulation and retention of snRNPs with the introns (Boon et al., 2006; Martin et al., 2002; Yoshimoto et al., 2009). However, after each splicing cycle, released snRNAs and spliceosomal proteins must be correctly reassembled into the active snRNPs.

3. snRNP recycling

The formation of U4/U6•U5 snRNP involves several distinc steps (for overview of tri-snRNP composition see **Fig. 3**).

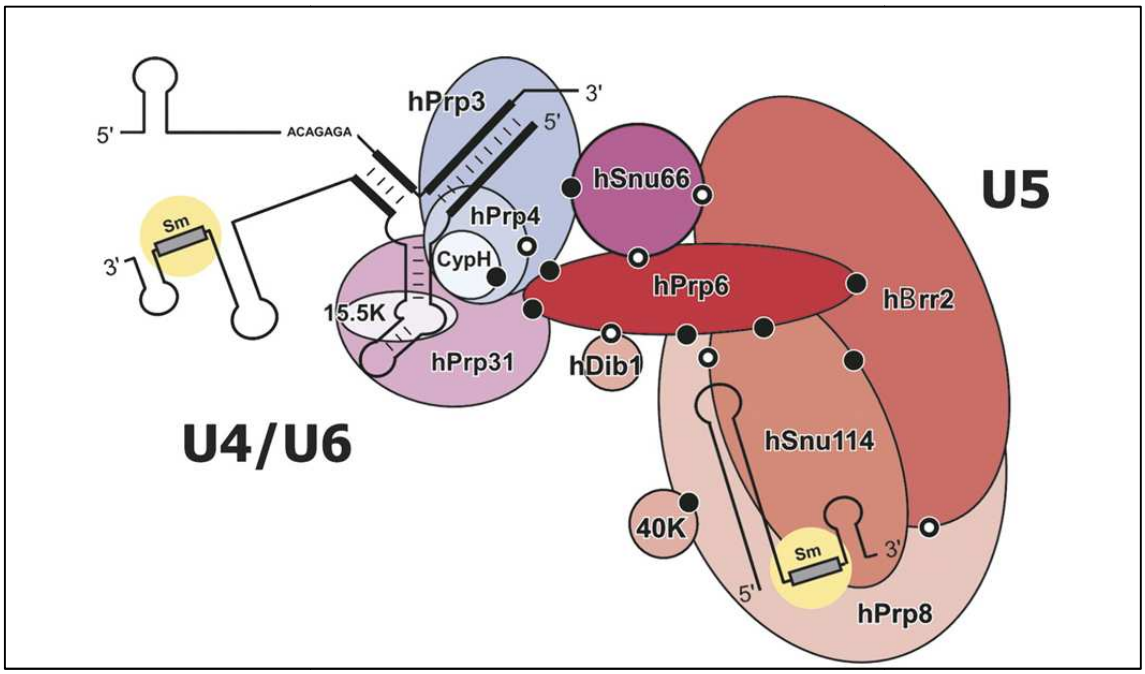

Fig. 3 Proteins of U4/U6·U5 tri-snRNP (Liu et al., 2006).

The dots indicate protein–protein interactions between individual proteins of tri-snRNP. The interaction between Prp31 and Prp6 is important for U4/U6•U5 snRNP assembly. Mutations in the gene encoding proteins Prp31, Prp8 and Prp3 cause retinitis pigmentosa.

During splicing U4/U6 snRNA base pairing is destroyed. Thus, the first step in tri-snRNP recycling is U4/ U6 snRNAs annealing. Prp24 (named hPrp24, SART3 or p110 in humans) is a splicing factor that that binds free U6 snRNA and reanneals U4 and U6 snRNAs during spliceosome recycling in yeasts and humans (Bell et al., 2002; Ghetti et al., 1995; Raghunathan and Guthrie, 1998). After that, Prp24 is released and does not associate with the assembled, complete tri-snRNP. U4/U6 snRNP specific proteins then bind to snRNAs in hierarchical way: 15.5K protein binds to the U4 5′ stem–loop (Nottrott et al., 1999) and this interaction is required for subsequent association of both the U4/U6 snRNP-specific Prp31 protein and the Prp3/Prp4/CypH protein

complex with U4/U6 snRNA duplex (Nottrott et al., 2002). U5 snRNP binds to U4/U6 snRNP via protein-protein interactions, see **Fig. 3** (Liu et al., 2006), especially via the interaction between Prp31 and Prp6 proteins. Depletion of the U5-specific Prp6 or the U4/U6-specific Prp31 inhibits tri-snRNP assembly and leads to the accumulation of U5 mono-snRNPs and U4/U6 di-snRNPs (Makarova et al., 2002; Schaffert et al., 2004). However, protein posttranslatinal modifications such ubiquitination have been also reported to affect tri-snRNP stability (Song et al., 2010).

In Publication I we focused on the question in what part of the cell nucleus spliceosome recycling takes place. Specific steps of the assembly of newly made spliceosomal snRNPs are localized in Cajal bodies. These are nonmembrane nuclear structures present in the nuclei of most cells. They were named after the Spanish neurobiologist Ramón y Cajal, who first observed them in 1903 (Cajal, 1903). Marker of Cajal bodies is coilin (Andrade et al., 1991; Raska et al., 1991; Tuma et al., 1993). Although coilin was identified 30 years ago, its function remains mysterious. During de novo assembly, snRNPs enter Cajal bodies, which contains Cajal body-specific RNAs (scaRNAs) that guide modifications of spliceosomal snRNAs (Darzacq et al., 2002; Jady et al., 2003; Kiss et al., 2002). snRNAs are extensively modified by both 2′-O-ribose methylation and pseudouridylation and these modified nucleotides influence snRNP and spliceosome assembly (Karijolich and Yu, 2010). There are several evidences that U4/U6 snRNP formatin occurs in Cajal bodies: There are present all components necessary for the assembly (SART3, U4 and U6 snRNAs as well as U6 and U4/U6 specific proteins are enriched in Cajal bodies (Stanek and Neugebauer, 2006) and transient assembly intermendiates were also detected there (Stanek and Neugebauer, 2004). The inhibition of the next step, tri-snRNP formation leads to accumulation of the U4/U6 snRNPs in Cajal bodies (Schaffert et al., 2004). The explanation for this observation can be that the tri-snRNP formation occurs also in Cajal bodies: U4/U6 snRNP is retained there and waits until the U5 snRNP joins and only after that mature tri-snRNP is released to the nucleoplasm. Publication I confirmed this hypothesis. Although there are some cells lacking Cajal bodies and tri-snRNP can be formed also in the nucleoplasm, tri-snRNP assembly in Cajal bodies is at least ten times

faster than in nucleoplasm (Klingauf et al., 2006; Novotny et al., 2011). Concentration of snRNP components in CBs helps to overcome rate-limiting assembly steps, increases the efficiency of snRNPs formation and expression of spliced mRNAs (Strzelecka et al., 2010).

4. Retinitis pigmentosa – disease connected with splicing

Retinitis pigmentosa (RP) is a hereditary eye disease that causes degeneration of photoreceptor cells in the retina. In many patients this disease leads to compelete blindness. It has a prevalence of approximately 1 in 4000 and at least more 1,5 million people worlwide are affected. Almost 50 genes were found to be associated with the retinitis pigmentosa – including visual transduction proteins such as rhodopsin, the first mutated gene identified in some of the patiens (Dryja et al., 1990), proteins involved in photoreceptor differentiation, trafficking or cytoskeletal proteins (Hamel, 2006). Interestingly, three proteins involved in pre-mRNA splicing also carry mutations causing retinitis pigmentosa. These proteins are Prp8, Prp31 and Prp3, ubiquitously expressed components of the spliceosome (Chakarova et al., 2002; McKie et al., 2001; Vithana et al., 2001), see **Fig. 3**. They are all parts of the U4/U6•U5 tri-snRNP and they are important for tri-snRNP assembly and stability. It is not known why mutations in general splicing factors cause only retina-restricted phenotype - specifically the loss of photoreceptors and degeneration of the retina. One of the reasons could be that retina has a high demand of snRNPs. Compared to other tissues, retina expresses the highest amount of snRNAs (Tanackovic et al., 2011). The expression of retinitis-pigmentosa associated genes Prp8, Prp31 and Prp3 is also significantly higher in retina than in other tissues of adult mouse (Cao et al., 2011). This suggests that retina needs higher steady-state basal levels of splicing components than other metabolically active tissues. Out of 30 different tissues, retinal cells were shown to have the highest level of spliced transcripts of housekeeping genes indicating a high level of splicing activity in retina (Tanackovic et al., 2011). The reason might be that photoreceptors must constantly renew their light-sensitive outer

segments and this requires continuous synthesis of membranes and many components of the cell metabolism.

There are several models how aberrant spliceosomal proteins can initiate the disease (Mordes et al., 2006). The first is the haploinsufficiency model. According to this model, mutated copy of the spliceosomal gene leads to the production of nonfunctional protein and this causes reduced level of functional snRNP and lack of snRNPs in retina. As mentioned above, the high amount of snRNPs is necessary for the metabolism of photoreceptors. To support this model, it has been observed in some of the retinitis pigmentosa patiens that the expression of Prp31 is lower (Vithana et al., 2003). The reduction of Prp31 protein level to 70% by morpholino in zebrafish recapitulates retinis pigmentosa disease – it affects photoreceptor morfology and causes defects in their visual function (Linder et al., 2011). In another model organism, in Drosophila, downregulation of Prp31 induces the absence of eyes or reduction of eye size connected with photoreceptor degeneration (Ray et al., 2010). The second model predicts the presence of specific factor in photoreceptors that would interact with spliceosomal proteins and that would be responsible for photoreceptor-restricted phenotype. However, any such factor has not been identified so far. The third model is based on the assumption that mutated spliceosomal proteins are toxic for the sensitive cells in retina and they function in a dominant negative way. This model is supported for example by the observation that heterozygous Prp3 knockout mice or zebrafish develop normally and do not show any defects in photoreceptors (Graziotto et al., 2008). In addition, overexpression of the retinitis pigmentosa - mutated spliceosomal proteins in the cells with two non-mutated functional copies of the gene can cause apoptosis or disease-like phenotype (Yuan et al., 2005).

Retinitis pigmentosa can be caused by the combination of these models. To elucidate this question, we have studied one of the missense disease-causing mutations called „AD29“, which is in exon 7 of Prp31 gene and swaps alanine to proline at the position 216 (Publication II). The alanine at this position is highly conserved among eukaryotes. Although this mutation has a severe phenotype in humans (Vithana et al., 2001), no degenerative phenotype in retina was

found in Prp31(A216P/+) heterozygot mouse (Bujakowska et al., 2009). However, several heterozygous mouse models with other genes mutated in retinitis pigmentosa had just a mild changes in retina, for example (Gao et al., 2002). Nevertheless, mouse with Prp31(A216P/A216P) genotype was embryonic lethal indicating that this mutation impairs substantially the function of Prp31 protein (Bujakowska et al., 2009). Previously it has been reported that AD29 mutation partially retains Prp31 protein in the cytoplasm (Deery et al., 2002) and enhances interaction of Prp31 with its binding partner in tri-snRNP, Prp6 (Wilkie et al., 2008). Why the mutation induces retinitis pigmentosa is not known. Although some of the mutations in Prp31, Prp3 and Prp8 cause changes in constitutive and alternative splicing (Tanackovic et al., 2011), processing of transcripts specifically important for retina function does not seem to be affected (Wilkie et al., 2008). Threfore the mechanism of disease causation is still unclear.

5. Alternative splicing increases protein complexity

In human cells, genes have approximately 9 exons on average (Lander et al., 2001). These exons are not recognized and spliced with the same efficiency – some of them called constitutive exons are always present in final mRNA, whereas the alternative exons can be present or missing. The process which decides about the exon appearence in mRNA is called alternative splicing. However, there are various other types of alternative splicing including usage of alternative splice sites (both 5´and 3´) or intron retention, which occurs predominantly in plants (see **Fig. 4**). Alternative splicing is extremely widespread in higher eukaryotes. For example, in human cells almost 95% of genes are alternatively spliced (Pan et al., 2008; Wang et al., 2008). What are rules for selection of alternative exons? Some of the signals are carried by pre-mRNA sequence itself: these signals are usually blocks of short sequences localized close to splice sites that can help or prevent correct recognition of splice sites, **Fig. 4** (Wang and Burge, 2008). These sequences are called splicing enhancers or splicing silencers and all together they form the „splicing code“ which determines alternative splicing outcome (Barash et al., 2010).

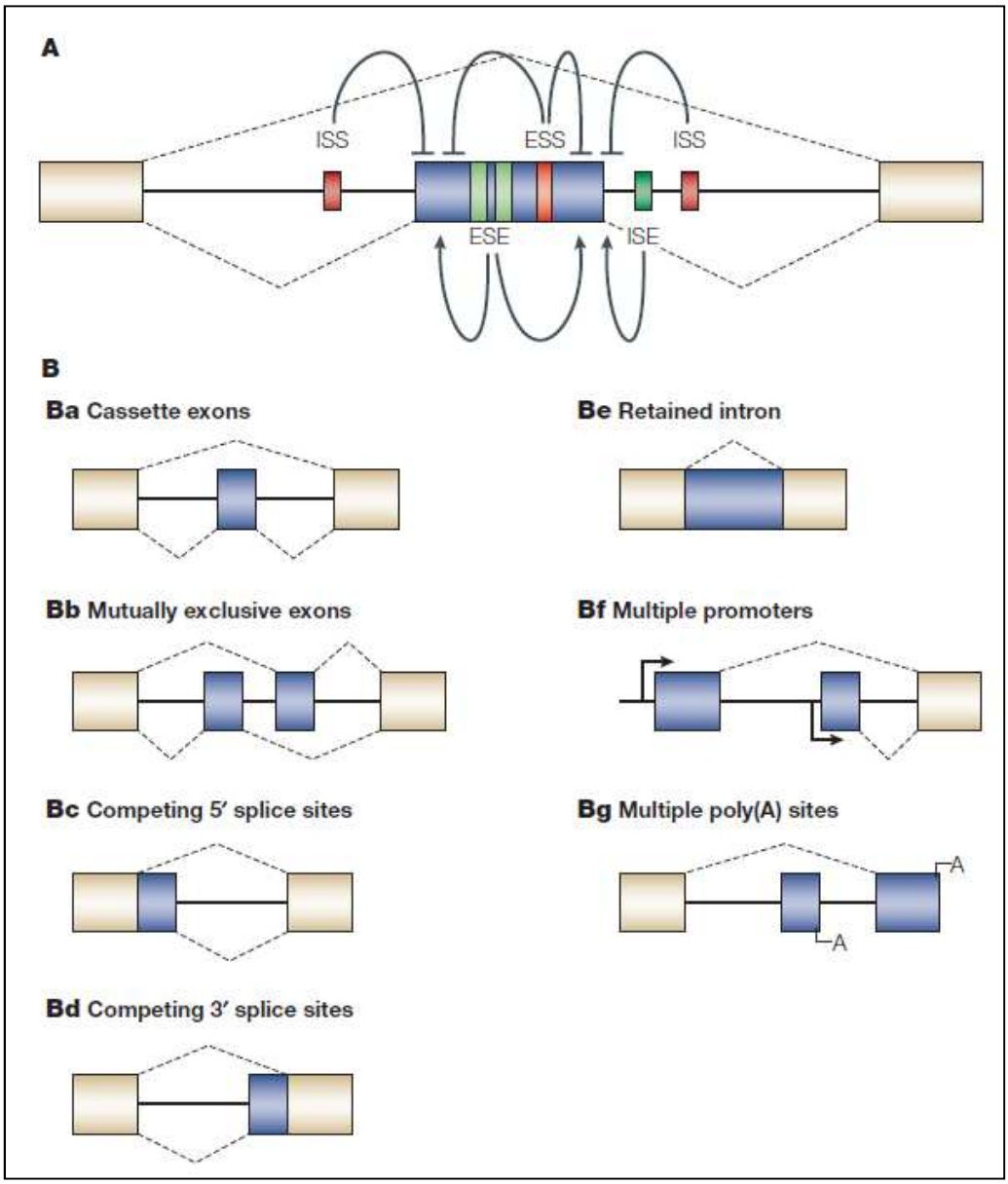

Fig. 4 Types of alternative splicing events and regulatory elements (Matlin et al., 2005).

(A) Intronic splicing (IS) or exonic splicing (ES) enhancers or silencers are short sequences in pre-mRNA that are bound by splicing factors which help to recruit spliceosome or block the recognition of 5´and 3´splice sites.

(B) Different alternative splicing events, the fibronectin EDB exon discussed in Publication III is spliced by cassette exon mechanism (Ba).

However, it seems that „splicing code“ cannot explain all alternative splicing events that occur in the cell. First, splicing silencers and enhancers are recognized by splicing factors and in many cell types or tissues with different alternative splicing patterns the concentration of these splicing factors is very similar. Second, the sequences identified by splicing factors are often very short, they can be found on many places in the pre-mRNA and there are examples that these sequences cannot solely explain the differential binding of splicing factors to dictinct mRNAs (Anko et al., 2010). Recently, evidences that alternative splicing can be regulated also by other mechanisms have appeared. These mechanisms are based on observations that many introns are spliced cotranscriptionally and splicing is coupled with transcription (these connections are discussed in Publication IV). Moreover, splicing seems to be at least in some genes regulated by chromatin. Several histone modifications have been reported to interact with spliceosomal proteins (detailly described in Publication IV). In Publication III we describe the effect of histone acetylation on alternative splicing on a model gene fibronectin.

6. Fibronectin: a model gene for alternative splicing studies

Fibronectin (FN1) is a large 250-kDa glycoprotein, which assembles into dimers that are connected by disulfide bonds at the C-termini. The protein is composed of three regions with repeated subunits that are called type I, II and III modules. The size of each structural module is 40-90 amino acid residues depending on the type. Each of these repeated modules is encoded by separate exon and very similar modules can be also found in other proteins (Pankov and Yamada, 2002). This lead to hypothesis that 75-kb fibronectin gene originally arose from exon shufling, which means that individual exons coding distict protein domains were gradually added and mixed during evolution (Patel et al., 1987). Fibronectin which has several alternatively spliced exons (White et al., 2008) was one of the first genes where alternative splicing had been detected (Kornblihtt et al., 1984; Schwarzbauer et al., 1983). Three alternatively spliced regions can be found in this gene: Two exons coding type III modules, EDA and EDB (called also ED-A and ED-B or EIIIA and EIIIB exons) are cassette exons

that can be either included or skipped in final mRNA. The fibronectin mRNA variability is further increased by alternative splicing of IIICS region near the end of the gene, which can give 5 different mRNA isoforms, thus in total fibronectin alternative splicing results in 20 different mRNA variants. Although it is not much known about the regulation of IIICS alternative splicing, the EDA and EDB exons have been extensively studied due to their relationship to human diseases. Both EDA and EDB exons served as model exons in experiments performed in Publication III in this thesis.

Fibronectin is a component of extracellular matrix. It binds to integrins, transmembrane proteins that connect extracellular matrix to actin cytoskeleton. Therefore fibronectin is important for cell adhesion, embryonic development and all processes connected with cell migration. Fibronectin is also needed during wound healing when the extracellular matrix must be renewed. Two types of fibronectin can be found in human body. The cellular type of fibronectin is expressed locally, it is assembled on the surface of the cells and contains low levels of EDA and EDB (Maurer et al., 2010). However, extracellular matrix fibronectin can also originated from deposition of plasma fibronectin (Moretti et al., 2007). Plasma type of fibronectin is soluble abundant protein in blood which participates in platelet coagulation and formation of blood clot as a ligand of platelet surface receptors. Plasma fibronectin is synthetised in livers and lacks completely EDA and EDB (White et al., 2008). It was shown that aberrant alternative splicing of EDA and EDB exons causes various disorders. Mouse strains constitutively expressing EDA exon (EDA+/+) in all fibronectin mRNAs develop thrombosis easily (Chauhan et al., 2008). The increase of EDA and EDB containing fibronectin in extracellular matrix of blood-vessels is associated with the development of artherosclerosis (Magnusson and Mosher, 1998). Fibronectin with high content of EDA and EBD seems to be essential for cardiovascular development, however not only during during embryogenesis, but also during tumorigenesis (Astrof and Hynes, 2009). Strong upregulation of EDA or EDB fibronectin correlates with tumor angiogenesis and these types of fibronectins are often observed in blood-vessels around tumors (Castellani et al., 1994). EDA and EDB fibronectin splice variants are even called “oncofetal fibronectin isoforms” which reflects their high expression in embryos and tumors

(Astrof and Hynes, 2009; Ruoslahti, 2002). Recently, antibodies recognizing specifically EDA or EDB domains of fibronectin have been developed and tested in patients (Pini et al., 1998; Villa et al., 2008). These antibodies were able to target tumors (Borsi et al., 2002; Santimaria et al., 2003). L19 against EDB domain conjugated with ^{131}I together with F8 (recognizing EDA) conjugated with Interleukin-10 are now in clinical trials for targeted pharmacodelivery of radionucleotides and cytokines and might be new therapeutic agents in the future. On the contrary, mice lacking completely EDA exon display abnormal skin wound healing (Muro et al., 2003). Mice without both EDA and EDB exons (EDA−/−/EDB−/−) are embryonic lethal (Astrof et al., 2007) and resemble knockout mice lacking the whole fibronectin gene (George et al., 1993) indicating that not only fibronectin itself, but also correct fibronectin splicing are necessary for proper development. However, although EDB exon is extremely conserved among vertebrates (White et al., 2008), the exact EDB function remains unclear. EDB−/− mouse strain develops normally, but EDB depleted fibroblast grow slowly compared to wild type cells for unknown reasons (Fukuda et al., 2002).

How is alternative splicing of these two alternative exons regulated? Both exons contain regulatory sequences, which are bound by SR proteins. SR proteins are RNA-binding proteins that contain RRM (RNA Recognition Motif) domain and RS domain rich in serine and arginine amino acids, which is important for interactions of SR proteins with spliceosome (**Fig. 1**). SR proteins mostly enhance the recognition of splice sites by promoting spliceosome assembly, however there are also some examples of SR protein induced exon skipping (Han et al., 2011; Lemaire et al., 1999). EDA exon contains exonic splicing enhancers that are bound by SF2/ASF and 9G8 proteins (members of the SR protein family). The binding of both SF2/ASF and 9G8 enhances recognition and inclusion of EDA exon (Cramer et al., 1999; de la Mata and Kornblihtt, 2006), however, it can be modulated by pre-mRNA secondary structure (Buratti et al., 2004). SF2/ASF effect on EDA splicing is also controlled by signaling pathways. Activation of the PI 3-kinase pathway and its downstream target Akt kinase by mitogenic signals such as growth factors causes SF2/ASF phosphorylation and EDA exon inclusion (Blaustein et al., 2004; Blaustein et al.,

2005). mTOR pathway was reported to regulate splicing of EDA exon presumably also through SF2/ASF (White et al., 2010). Interestingly, overexpression of Clk and SRPK kinases, two members of the SR protein kinase families that also phosphorylate SR proteins including SF2/ASF, has completely opposite effect and induces EDA exon skipping (Blaustein et al., 2005), which is really surprising. Another SR protein, SRp20 promotes EDA exon skipping, but only when the gene is transcribed by RNA polymerase II with complete carboxyterminal domain indicating that this type of regulation is coupled with transcription (de la Mata and Kornblihtt, 2006). EDA exon was one of the first exons whose splicing was shown to be dependent on transcription. The first experiments performed on minigenes 10 years ago showed that the promoter structure affects EDA alternative splicing (Kadener et al., 2002; Kadener et al., 2001; Nogues et al., 2002). Later on, partial explanation of this phenomenon came with the observations that the speed of RNA polymerase II during transcription elongation regulated EDA exon inclusion or skipping (de la Mata et al., 2003; Kadener et al., 2002; Nogues et al., 2003). This lead to the kinetic model of coupling between transcription and alternative splicing, which postulates that when the speed of transcription is high, splicing machinery does not have enough time to recognize weak splice sites of alternative exon, downstream constitutive exon with strong splice sites is used and alternative exon is skipped (see **Fig. 5**).

EDB exon splicing is regulated mainly by SR protein SRp40 (Du and Taub, 1997; Lim and Sharp, 1998). SRp40 increases EDB exon inclusion. A negative regulator of EDB exon recognition is PTB, which promotes EDB skipping (Norton and Hynes, 1993). In transfected minigenes, SRp40 regulation of EDB exon splicing can be also modulated by promoters (Monsalve et al., 2000). SRp40 interacts with PGC-1, transcription coactivator that regulates genes involved in energy metabolism. When PGC-1 is loaded on promoter, it inhibits SRp40 directed inclusion of EDB alterantive exon. However, when PGC-1 is not tethered to the promoter, it does not have any effect on EDB alternative splicing indictaing that transcription also influences EDB alternative splicing. In Publication III we studied association of SRp40 and a negative regulator PTB with EDB exon in a context of endogenous fibronectin gene.

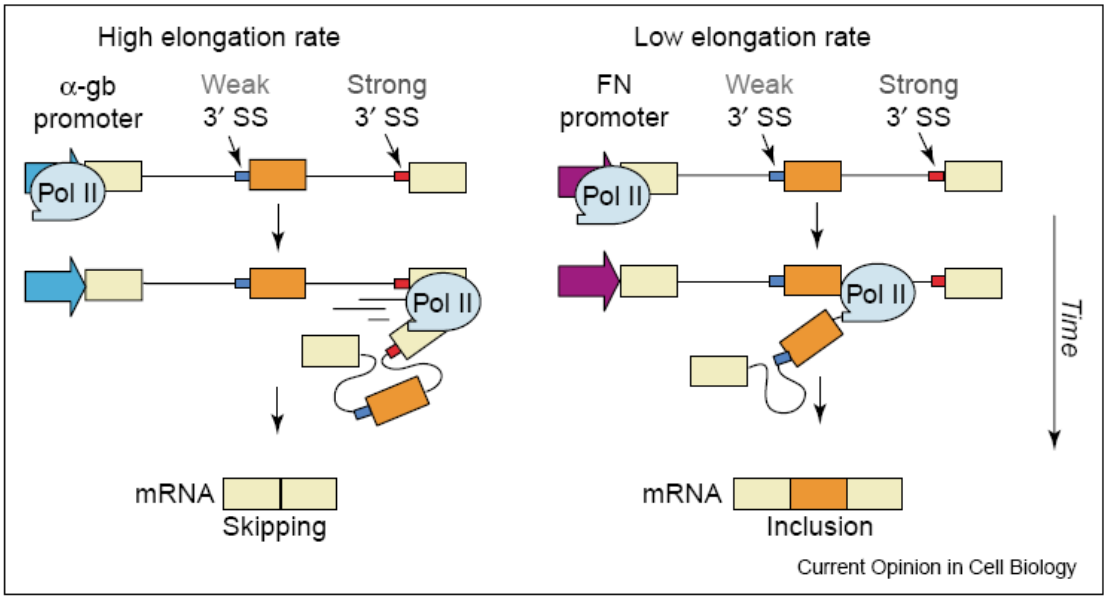

Fig. 5 The kinetic coupling model for regulation of alternative splicing

Slow transcription rate promotes inclusion of alternative exon, fast RNA polymerase II elongation induces alternative exon skipping (Kornblihtt, 2005).

7. Histone acetylation – dynamic chromatin modification

First studies describing histone modifications appeared in the early 60s (Allfrey et al., 1964). Since that many different types of histone posttranslational modifications have been identified. Histones can be acetylated, phosphorylated, methylated, ubiquitinylated, sumoylated, arginines and citrullines of histones can be deiminated, serine and threonine can be modified by single sugar β-N-acetylglucosamine, glutamate and arginine residues can be mono- and poly-ADP ribosylated, prolines are isomerated and finally, the whole histone tail can be clipped by proteolytic cleavage (Kouzarides, 2007). The histone acetylation is a dynamic modification regulated by histone acetyltransferases (HAT) and histone deacetylases (HDAC). Histone acetyltransferases add an acetyl group from acetyl CoA to the ε-amino group of lysines. There are two types of HAT in cells: so called B-HATs acetylate free histones in the cytoplasm (histones H4 have to be acetylated on lysine 5 and 12 before they are deposited on the DNA). More diverse A-HATs operate in the nucleus and includes GNAT, MYST and p300/CBP enzyme families (Hodawadekar and Marmorstein, 2007).

Histone acetylation neutralize positive charge of lysines. It is supposed that acetylation weakens the interactions between histones and DNA and promotes less compact chromatin structure. There are over 20 different lysine residues that can be acetylated in one nucleosome. This lead to hypothesis that acetylation might influence chromatin by cumulative mechanism independent of specific lysines that would have to be acetylated, e.g. (Dion et al., 2005). Nevetheless, acetylation of lysine 16 histone H4 was shown to affect chromatin state directly and independently of other acetylated lysines (Shogren-Knaak et al., 2006). H4K16ac modulates higher order chromatin structure – it inhibits the formation of compact 30 nm fiber. Acetylated histones are recognized by bromodomain-containing proteins and these proteins can also efficiently distinguish particular lysines (Sanchez and Zhou, 2009).

Histone deacetylases remove acetyl groups from lysines and although they are called „histone“ deacetylases, they act also on many other protein substrates in addition to histones (Peserico and Simone, 2010). Mammalian HDACs are divided into four classes based on their highly evolutionary conserved deacetylase domain. Interestingly, bacterial homologues of these domains have been also identified indicating the role of HDACs in deacetylation of non-histone proteins (Khochbin and Wolffe, 1997). Class III HDACs are homologous to the yeast-silencing protein Sir2 and they are called sirtuins. Sirtuins require nicotinamide adenine dinucleotide (NAD^+) for the deacetylation reaction. Three other classes (class I, II, IV) are zinc-dependent amidohydrolases related to the yeast Rpd3, Had1, and Hos3 proteins. Class I contains four mammalian HDACs: HDAC1, HDAC2, HDAC3 and HDAC8 (see **Fig. 6**). In contrast to other classes, class I HDACs have quite similar structure basically containing only deacetylase domain with short C-terminal extensions. Class I HDACs are expressed ubiquitinously in different tissues and cell types and they are localized in the nucleus (Haberland et al., 2009). On the contrary, HDACs from other classes can be localized also in the cytoplasm - cytoplasmatic HDAC6 deacetylates cytoskeletal proteins such as α-tubulin or transmembrane proteins (Hubbert et al., 2002; Matsuyama et al., 2002; Tang et al., 2007) or expression of these HDACs is restricted only to particular tissues – for example HDAC4 is expressed in brain and growing parts of skeleton (Vega et al., 2004).

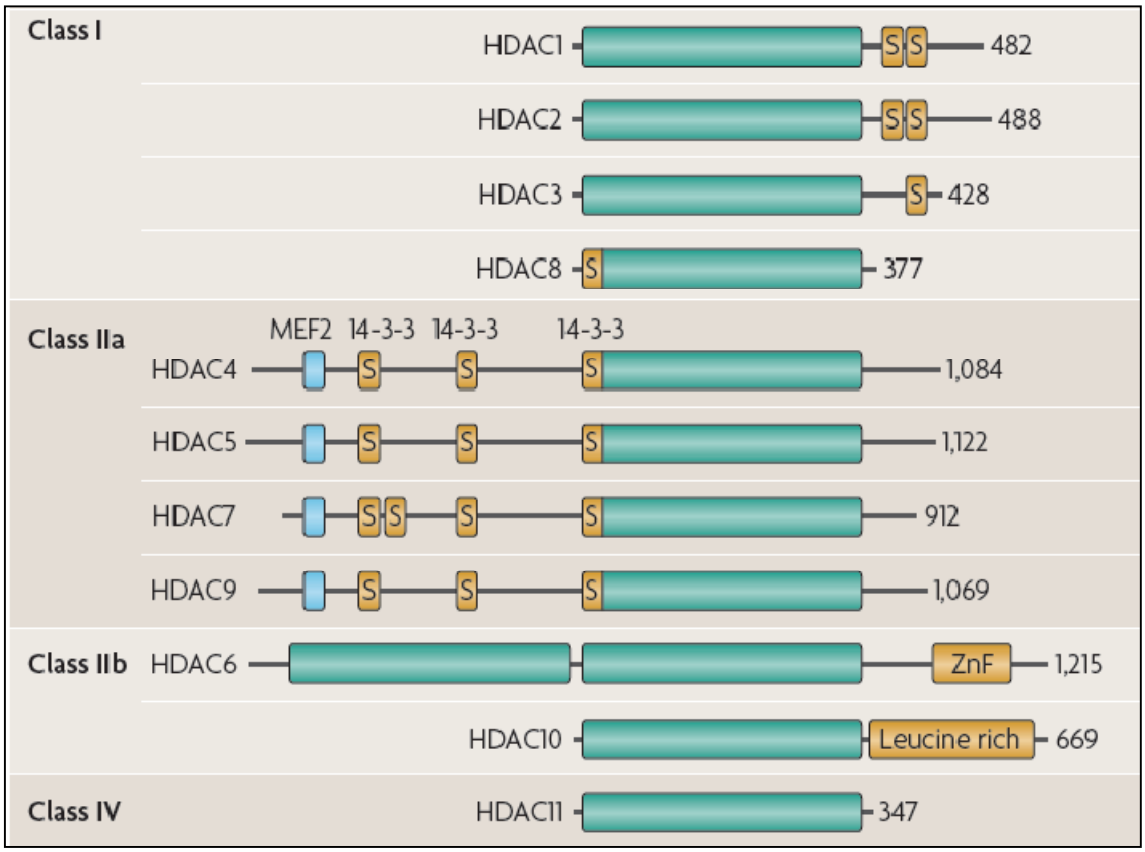

Fig. 6 HDAC protein family (Haberland et al., 2009)

All HDACs have conserved histone deacetylase domain (green rectangle). „S“ indicates serine phosphorylation sites, „ZnF“ zinc finger and „MEF2“ and „14-3-3“ are binding sites for these factors.
HDAC1 and HDAC2 were used in experiments in Publication III.

HDAC1 and HDAC2 are nearly identical - there is 82% amino acid identity between human HDAC1 and HDAC2 (Brunmeir et al., 2009). Not surprisingly considering their sequence homology, both HDAC1 and HDAC2 are often found in the same protein complexes. Several HDAC1/HDAC2-containing complexes exist in human cells: the SIN3 corepressor complex involved in transcriptional silencing (Grzenda et al., 2009); the nucleosome remodelling and deacetylase complex (NuRD) that is a large macromolecular complex coupling deacetylase and chromatin remodeling ATPase activity (Denslow and Wade, 2007); CoREST complex which plays an important role in regulating neuronal gene expression (Lakowski et al., 2006) and NODE (Nanog and Oct4 associated deacetylase) complex which is found in embryonic stem cells and represses

Oct4 and Nanog target genes (Liang et al., 2008). Recently, SHIP complex containing HDAC1 has been characterized in spermatocytes and it seems to be important for chromatin remodeling during spermatogenesis (Choi et al., 2008). Besides HDAC1/2 presence in large multiprotein complexes, both HDACs can also interact directly with transcription factors. HDAC1 associates with mammalian DNA methyltransferase DNMT1, Rb and E2F1 to repress transcription from promoters containing E2F-binding sites (Robertson et al., 2000). HDAC1/2 binds truncated isoform of transcription factor p73 which modulates neuronal differentiation (Zhang and Chen, 2007) or HDAC1 in complex with Groucho regulate Wnt signalling pathway by inhibition of TCF/LEF transcription factors (Chen et al., 1999). There is a plenty of various transcription factors that need HDAC1/2 for transcription repression: for example EKLF which regulates adult β-globin expression in erythroid cells (Chen and Bieker, 2001), GFI-1 regulating cell death and cell cycle in hematopoietic cells (Saleque et al., 2007) and Snail1 repressing E-cadherin during epithelial-mesenchymal transition in gastrulation but also during cancer development (Peinado et al., 2007; Peinado et al., 2004). Thus, HDAC1/2 that themselves do not contain any DNA binding domains, are targeted to chromatin by many transcription factors and protein complexes and these complexes then control and direct histone deacetylation.

Because of HDAC1/2 similarity it has been suggested that HDAC1 and HDAC2 might be redundant and interchangeable. However, knockout mice lacking any of class I HDACs are not viable (Haberland et al., 2009) implicating that HDAC1 cannot be compensated by HDAC2 and vice versa. HDAC1−/− mice die by embryonic day 10.5 (Lagger et al., 2002; Montgomery et al., 2007) and HDAC1 deficient cells show reduced proliferation rate (Lagger et al., 2002). In contast to HDAC1 knockout mouse, HDAC2−/− mice die after birth due to the severe cardiac malformations (Montgomery et al., 2007). In cardiomyocytes, HDAC2 interacts with transcription factor HOP, which regulates cardiomyocyte proliferation (Chen et al., 2002; Kook et al., 2003; Shin et al., 2002). In Publication III we examined the role of both HDAC1 and HDAC2 in regulation of alternative splicing.

8. HDAC inhibitors – therapeutic agens

Plenty of chemical substances have been reported to inhibit histone deacetylases (**Fig. 7**). Typically, HDAC inhibitors have a broad effect - they usually inhibit nonspecifically at least several different histone deacetylases and importantly, they are able to modify transcription. By altering gene expression, HDAC inhibitors can influence many processes in the cell, particularly proliferation, differentiation or apoptosis. While normal cells are quite resistant to HDAC inhibition, transformed cells treated with HDAC inhibitors activate antitumor pathways and undergo growth arrest, differentiation or apoptosis (Xu et al., 2007). Therefore dozens of HDAC inhibitors are currently in clinical trials as anti-cancer drugs (Wagner et al., 2010). Two of them have been approved recently: First drug approved by FDA in October 2006 was Vorinostat (Zolinza®, suberoylanilide hydroxamic acid, SAHA) currently used to treat patients with cutaneous T-cell lymphoma (CTCL). A second HDAC inhibitor, Romidepsin (Istodax®), has been approved recently for the treatment of the same disease. However, HDAC inhibitors are also widely used in psychiatry and neurology (Grayson et al., 2010). Vaplroic acid is an antiepileptic drugs (sold as Depakene® or Convulex®) and mood stabilizing drug used to treat bipolar disorder (manic-depressive disorder). Other HDAC inhibitors are now in clinical trials focused on neurodegenerative diseases (Morrison et al., 2007).

HDAC inhibitors have been divided into different groups based on their structure – see **Fig. 7** (de Ruijter et al., 2003). Above mentioned Vorinostat belongs together with Trichostatin A to the group of hydroxamid acids. Generally, hydroxamid acid based inhibitors are pan-HDAC inhibitors with high nanomolar potency. Trichostatin A is a natural compound isolated originally from *Streptomyces hygroscopicus* as an antifungal antibiotic in 1976 (Tsuji et al., 1976). Ten years later, TSA was shown to induce differentiation of murine erythroleukemia cells, to inhibit cell cycle (Yoshida et al., 1987) and to increase histone acetylation (Yoshida et al., 1990). This lead to the conclusion that the effect of HDAC inhibitors on cell proliferation is caused by modulation of gene expression.

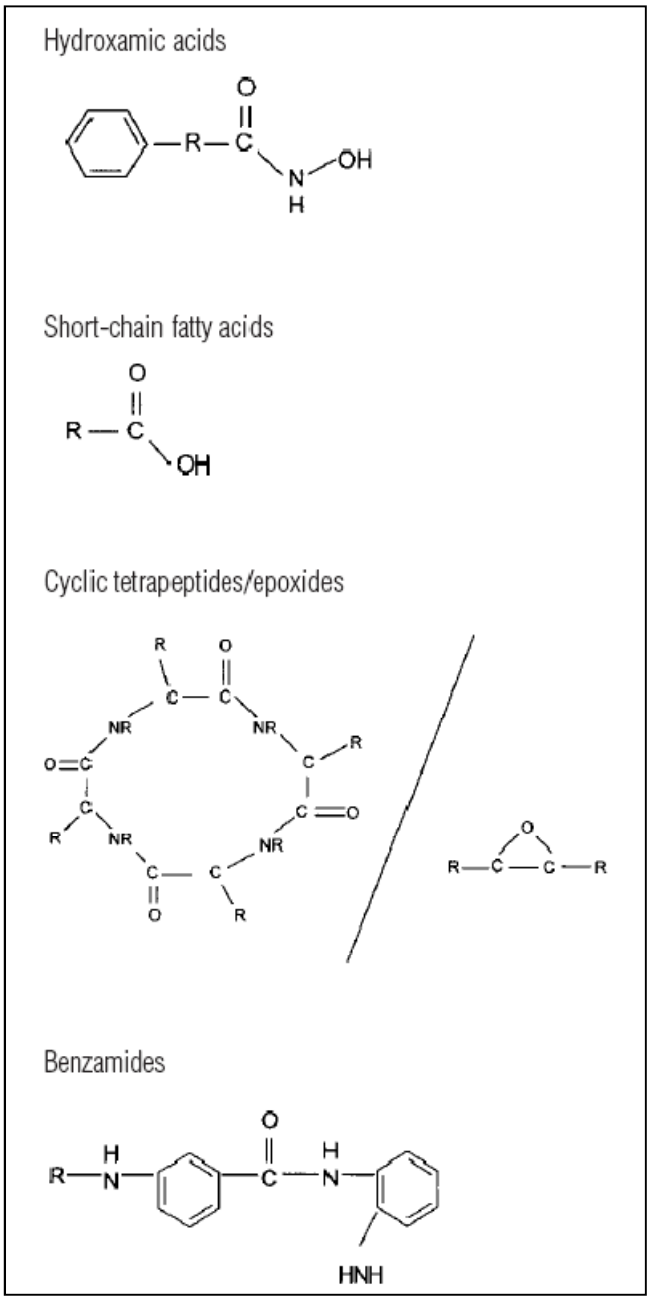

TSA (Trichostatin A)
SAHA (Vorinostat, suberoylanilide hydroxamic acid), CBHA (M-carboxycinnamic acid bishydroxamide), Scriptaid, Belinostat, Pyroxamide, Oxamflatin. Panobinostat

NaB (Sodium Butyrate)
Phenylbutyrate
VPA (Valproic acid)

Trapoxin, HC-toxin, Chlamydocin, Depudesin, Apicidine,
Depsipeptide (FK228, Romidepsin)

N-acetyldinaline (CI-994),
MS-275 (Entinostat), MGCD0103

Fig. 7 HDAC inhibitors (de Ruijter et al., 2003)

Four structurally distinct types of HDAC inhibitors. Red – HDAC inhibitors that have been already approved by FDA. Many others are in clinical trials (for example Belinostat, Parabinostat or Entinostat are in trials for hematologic malignancies), **bold** – HDAC inhibitors used in Publication III.

Short-chain fatty acid inhibitors include components with simple structure such as sodium butyrate or valproic acid. They are less potent working mostly in millimolar range for class I and IIa HDACs. Valproic acid (VPA) was first

derived in 1882 from valeric acid produced in plant *Valeriana officinalis* and almost one century it had been used as a solvent for organic compounds (Chateauvieux et al., 2010). During studies in 1960s where VPA was used as a molecular carrier of chemical compounds tested for anti-convulsive activity, it was observed that VPA itself prevents convulsions and has anti-epileptic properties (Lebreton et al., 1964). Although valproic acid has a weak inhibitory potential, it is broadly used in psychopharmacology (mentioned above). In brain, VPA affects excitation of neurons via modulation of the level of inhibitory neurotransmitter GABA (γ-Aminobutyric acid) and it also influences activity of several other voltage dependent channels (Mesdjian et al., 1982; VanDongen et al., 1986). Today, VPA is in several monotherapy clinical studies for neurological disorders such as autism, migraine or dependences (cocaine, alcohol). VPA is also in combination clinical trials including other diseases and cancer. For example, the combination of valproic acid and 5-azacytidine (Vidaza®) is tested as a therapeutic agens to treat myelodysplastic syndrome, disease causing loss of blood cells (Voso et al., 2009). The four-carbon fatty acid butyrate is a natural by-product of dietary fibre bacterial fermentation in the human colon. Butyrate was one of the first HDAC inhibitors described (Riggs et al., 1977). It has been even suggested that butyrate in the gut putatively suppresses colorectal cancer (Sengupta et al., 2006; Scharlau et al., 2009) and prevents infections (Fernandez-Rubio et al., 2009), for these reasons butyrate was introduced as feed additive in poultry farms. In addition, butyrate and its derivates are again in many clinical trials for human diseases. Although different HDAC inhibitors are utilized in variety of applications, the precise mechanism they operate in these diverse circumstances remains often unclear.

9. Alternative splicing and disease

Retinitis pigmentosa is not the only disease connected with splicing. Especially misregulaton of alternative splicing causes plenty of human diseases. One of the examples is upregulation of fibronectin EDB alternative exon during vascularization of tumors discussed previously. During cancer development, many genes change alternative splicing pattern (Srebrow and Kornblihtt, 2006).

One of these genes is CD44 cell surface glycoprotein that contains a region of nine alternative spliced exons. These exons are expressed only during development and T-cell activation and they are not present in CD44 molecules of healthy adult tissues (Faustino and Cooper, 2003). However, CD44 variants with included alternative exons were found also in several types of malignant tumors (Sneath and Mangham, 1998) and have been reported to induce metastatic potencial of cells (Klingbeil et al., 2009). Recently, the regulation pathway controlling alternative splicing of pyruvate kinase has been described (David et al., 2010). Pyruvate kinase has two alternatively spliced functionally distinct isoforms: PKM1, the adult isoform promotes oxidative phosphorylation, whereas PKM2 is expressed during embryonic development and promotes aerobic glycolysis. PKM2 is present in cancer cells where it alters their metabolism. PTB, hnRNP A1 and A2 are splicing factors that enhance expression of „cancer isoform“ PKM2 (Clower et al., 2010; David et al., 2010). In cancer cells, these splicing factors are upregulated by transcription factor c-Myc. Another splicing factor SF2/ASF, one of the SR proteins, is a well established proto-oncogene frequently elevated in tumors which affects alternative splicing of genes involved in apoptosis or cell motility (Ghigna et al., 2005; Karni et al., 2007). Other diaseases induced by incorrect alternative splicing are for example Spinal Muscular Atrophy causing loss of motor neurons, Myotonic Dystrophy leading to muscle wasting or FTDP-17 (Frontotemporal dementia and Parkinsonism linked to Chromosome 17). FTDP-17 is caused by aggregation of tau protein in neurons. Tau is microtubule-associated protein with several alternative spliced isoforms. Abnormal splicing which increases inclusion of exon 10 into tau mRNA leads to tau accumulation and aggregation in neurons of affected patients (Zhou et al., 2008). Tau was one of the genes changing alternative splicing after HDAC inhibition in Publication III.

10. Methods to study splicing

We used several methods that are able to monitor changes in alternative splicing pattern or differences in composition of snRNP complexes.

Experiments using exon microarrays (GeneChip® Human Exon 1.0 ST Array produced by Affymetrix) were performed in Publication III. Exon arrays measure the expression of every identified or predicted exon in genome separately. These arrays contain on average 4 probes for each particular exon. Labelled cDNA is hybridised to these probes and the mean of signal determines the expression of the exon which is then compared to expression of mRNA (calculated as an average of all exons). The expression of exons is compared between samples and exons with increased/decreased expression are identified.

To distinguish snRNP complexes, we separated them by the zonal glycerol gradient centrifugation. The sample – nuclear extract (Dignam et al., 1983) is loaded on a linear 10-30% preformed gradient which is made of a viscous component usually glycerol. Fractionation is achieved by ultracentrifugation for a defined time. The snRNP complexes sediment in the gradient due to differences in their sedimentation constant (Svedberg, S), which depends on their volume, weight, density and shape. U1 snRNPs peakes in fractions corresponding to a sedimentation coefficient of 10-12S, U2 snRNP sedimentation constant is 17S, free U5 has 20S, tri-snRNP sediments as 25S particle, activated spliceosome 45S and U5 snRNP retained in post-spliceosomal complex sediments at 35S (Makarov et al., 2002). This method was used in Publication I and II.

The association of splicing proteins with nascent RNAs in the cell nucleus can be measured by splicing factor ChIP (Listerman et al., 2006). This type of chromatin imunoprecipitation is performed with antibodies recognizing splicing factors which bind to the nascent RNA and will pull down only the genome regions to which they are attached via this nascent RNA (see **Fig. 8** on the next page). These ChIPs were performed in Publication III.

.

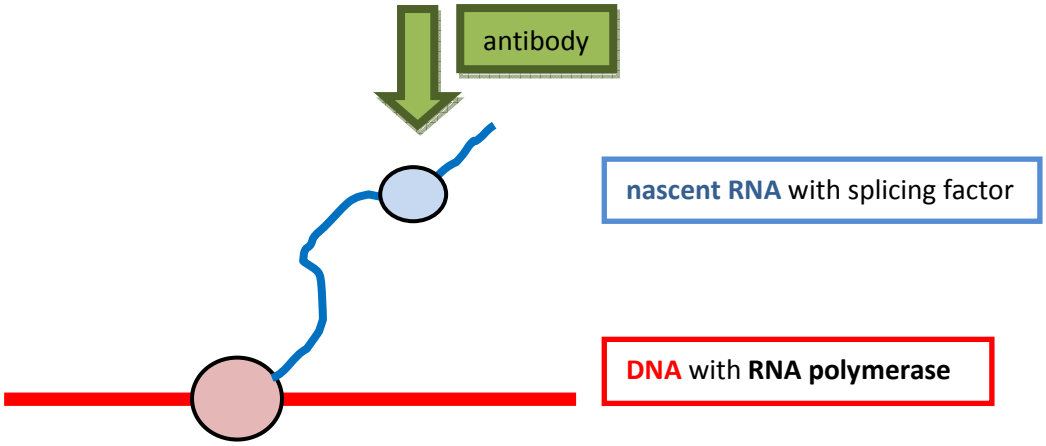

Fig. 8 Splicing factor ChIP

Antibody recognizing RNA-binding protein pulls down genome regions attached to this protein through nascent RNA. This method was used to examine cotransriptional binding of SRp40 with nascent fibronectin RNA (Publication III).

Aims

The aims of this thesis were to study the regulation of pre-mRNA splicing.

The main questions were:

1. How and where in the cell nucleus recycling of spliceosomal snRNPs occurs?
2. What is the role of AD29 mutation in spliceosomal snRNP assembly?
3. Does chromatin influence alternative splicing?

Commentary to the results

The first results are focused on assembly and recycling of splicing machinery, the second part of the thesis mainly discuss the regulation of alternative splicing.

In Publication I we show that Cajal bodies play a role in tri-snRNP metabolism. By microscopic techniques we verified that mature snRNPs repeatedly cycle through Cajal bodies. To elucidate whether tri-snRNP is recycled in Cajal bodies, we depleted by siRNA TFIP11 and hPrp22, two proteins necessary for disassembly of postspliceosomal complexes. After the depletion, U4/U6 snRNPs accumulated in Cajal bodies, but the level of U5 snRNP components in Cajal bodies decreased. We suggest that this decrease is caused by the lack of U5 snRNP in the nucleus because proteins from U5 snRNP cannot be efficiently released from postspliceosomal complexes. Supporting this hypothesis, we could partially see reduction of free U5 snRNP in TFIP11 or hPrp22 depleted cells. These data show that reassembly of the tri-snRNP occurs in Cajal bodies. I contributed to this project by performing biochemical experiments (isolation of nuclear extracts with spliceosomal complexes and optimalization of snRNP complexes separation in glycerol gradients by ultracentrifugation). These methods were used to show that the amount of free U5 snRNP was affected by knockdown of TFIP11 and hPrp22 proteins. I also validated the efficiency of siRNA knockdowns by Western blotting.

In Publication II we prepared a model cell line carrying AD29 mutation in hPrp31 protein. This is one of the mutations causing retinitis pigmentosa, the disease ending usually with complete blindness. Although the disease is rather common, the mechanism of induction of this illness is still unclear. hPrp31 is spliceosomal protein of U4/U6 snRNP important for association of U4/U6 snRNP with U5 snRNP (hPrp31 interacts with U5-specific protein hPrp6 and this interaction is necessary for tri-snRNP formation). We found that AD29 mutation decreases cell growth. Although AD29-hPrp31 is not inserted to U4/U6 snRNP, suprisingly it partially interacts with U5 snRNP proteins, especially it strongly binds to hPrp6. It seems that AD29-hPrp31 affects tri-snRNP by tethering of hPrp6, because when hPrp6 is added to mutation containing cells,

they start to grow normally. The AD29-hPrp31 is also unstable and degraded within 6 hours in the cells indicating again its toxic probably even in a limited amount – it can harm the cellular metabolism, although it is quite rapidly removed from the cells. These results indicate that the onset of retinitis pigmentosa can be caused by mixture of proposed models (these models are discussed in the introduction). The AD29 mutation is toxic, but it can also lead to haploinsufficiency in patients because it causes protein instability. In this project I performed glycerol gradient ultracentrifugation to analyze distribution of wild type and mutated hPrp31 among different snRNP complexes containing mutated and wild type hPrp31 and stability of different snRNP complexes.

Specific conclusions reflecting general snRNP metabolism are:

- Tri-snRNP is assembled in Cajal bodies and used repeatedly for splicing catalysis.
- The final steps of splicing reaction and spliceosome recycling are precisely regulated: the disassembly of spliceosome from intron depends on the presence of TFIP11 and hPrp22 and both proteins are required for recycling of spliceosome components.
- The imbalance in the level of tri-snRNP proteins can partially explain the cause of retinitis pigmentosa: AD29 mutation in hPrp31 leads to hPrp31 degradation, it slows down cell growth and also affects its binding partner hPrp6; the phenotype induced by AD29 can be rescued by addition of hPrp6.

Many human diseases are caused by aberrant alternative splicing. One of the examples is the form of dementia called FTDP-17 caused by aberrant splicing of Tau protein. We showed in Publication III that there might be a possibility to treat this disease by addition of HDAC inhibitors, which are able to repair alternative splicing of Tau mRNA. We used exon arrays to monitor alternative splicing changes and identified almost 700 genes with modified alternative splicing pattern after HDAC inhibition. One of them was fibronectin EDB exon, therefore we focused on this gene to reveal mechanism of HDAC inhibition effect on alternative splicing. We showed that increased histone acetylation

enhances RNA polymerase II processivity which subsequently diminishes binding of SRp40 - splicing regulator of EDB exon. This leads to skipping of this particular alternative exon. Skipping of EDB exon is also increased in HDAC1 depleted cells. Mouse HDAC1 can rescue EDB exon inclusion, however, mouse HDAC1 without deacetylase activity has no rescue effect. Thus, it seems that histone acetylation can modulate alternative splicing outcome. In this project I performed majority of experiments (including preparation of samples for exon arrays and RT PCR validation of resuls, DRB treatment, HDAC inhibition, HDAC1/2 knockdowns and RT PCR and quantitative PCR measurement of fibronectin alternative splicing, preparation of catalytically inactive mouse HDAC1 mutant and rescue experiments after human HDAC1 depletion, native chromatin immunoprecipitations (ChIP) with antibodies against modified histones, crosslinked ChIPs with antibodies recognizing different variants of RNA polymerase II, splicing factor ChIPs and control Western blots).

Specific conclusions regarding the role of histone acetylation in alternative splicing are:

- Sodium butyrate changes alternative splicing of 700 genes.
- HDAC1 deacetylase activity regulates alternative splicing of fibronectin.
- Histone acetylation affects cotranscriptional binding of splicing factors, probably thought the modulation of transcription.
- there is a potential to use HDAC inhibitors in therapy of splicing related disorders.

The idea that chromatin state regulates alternative splicing was further expanded in Publication IV, which is a review article summarizing known interaction between splicing machinery and histones. I prepared the figure and table and wrote vast majority of the manuscript.

Conclusion

For a long time pre-mRNA splicing has been studied as an isolated process which is rather independent on processes ocurring in the surrounding. A lot of important observations were made in experiments using *in vitro* splicing reactions. This fundamental assay enabled to identify individual steps of pre-mRNA splicing catalysis, but nowadays, it seems that it is necessary to extend this research to the cellular level and to study splicing in the context of the cell nucleus which can have a huge impact on the whole process. The results of this PhD thesis confirmed this assumption and showed that splicing is influenced by the cellular environment.

How can splicing in the nucleus be different than splicing in *in vitro* reactions? Splicing, formation and recycling of spliceosomal components in the cell are compartmentalized and the efficiency of both events depends on their locations inside the nucleus. This is highly functionally important, because the place can modify the event; for example, alternative splicing decisions can be affected by the vicinity of chromatin or RNA polymerase II. The influence of these factors is lost when pre-mRNA is detached from the site of transcription. Furthemore, recycling of tri-snRNP spliceosomal complex takes place in Cajal bodies where single subunits of this complex are captured. Another important factor that might play a significant role in pre-mRNA splicing is time. Introns in the pre-mRNA molecule are presented to the splicing machinery sequentially as they are transcribed and emerge from RNA polymerase II. Splicing proceeds differently if the whole pre-mRNA molecule appears immediately at once. The time influences the probability that particular sequence is recognized by splicing factor and we showed that at least for some genes, time delay during transcription can modulate splicing. Therefore it appears that it is needful to investigate pre-mRNA splicing in natural surroundings. Today, the research in this field is just at the beginning and it is valid to suppose that our current knowledge about this issue represents just the tip of the iceberg.

References

Akman, L., A. Yamashita, H. Watanabe, K. Oshima, T. Shiba, M. Hattori, and S. Aksoy, 2002. Genome sequence of the endocellular obligate symbiont of tsetse flies, Wigglesworthia glossinidia. Nat Genet 32: 402-7.

Allfrey, V.G., R. Faulkner, and A.E. Mirsky, 1964. Acetylation and Methylation of Histones and Their Possible Role in the Regulation of Rna Synthesis. Proc Natl Acad Sci U S A 51: 786-94.

Andrade, L.E., E.K. Chan, I. Raska, C.L. Peebles, G. Roos, and E.M. Tan, 1991. Human autoantibody to a novel protein of the nuclear coiled body: immunological characterization and cDNA cloning of p80-coilin. J Exp Med 173: 1407-19.

Anko, M.L., L. Morales, I. Henry, A. Beyer, and K.M. Neugebauer, 2010. Global analysis reveals SRp20- and SRp75-specific mRNPs in cycling and neural cells. Nat Struct Mol Biol 17: 962-70.

Arenas, J.E., and J.N. Abelson, 1997. Prp43: An RNA helicase-like factor involved in spliceosome disassembly. Proc Natl Acad Sci U S A 94: 11798-802.

Aronova, A., D. Bacikova, L.B. Crotti, D.S. Horowitz, and B. Schwer, 2007. Functional interactions between Prp8, Prp18, Slu7, and U5 snRNA during the second step of pre-mRNA splicing. RNA 13: 1437-44.

Astrof, S., and R.O. Hynes, 2009. Fibronectins in vascular morphogenesis. Angiogenesis 12: 165-75.

Astrof, S., D. Crowley, and R.O. Hynes, 2007. Multiple cardiovascular defects caused by the absence of alternatively spliced segments of fibronectin. Dev Biol 311: 11-24.

Barash, Y., J.A. Calarco, W. Gao, Q. Pan, X. Wang, O. Shai, B.J. Blencowe, and B.J. Frey, 2010. Deciphering the splicing code. Nature 465: 53-9.

Bell, M., S. Schreiner, A. Damianov, R. Reddy, and A. Bindereif, 2002. p110, a novel human U6 snRNP protein and U4/U6 snRNP recycling factor. EMBO J 21: 2724-35.

Berget, S.M., C. Moore, and P.A. Sharp, 1977. Spliced segments at the 5' terminus of adenovirus 2 late mRNA. Proc Natl Acad Sci U S A 74: 3171-5.

Blaustein, M., F. Pelisch, O.A. Coso, M.J. Bissell, A.R. Kornblihtt, and A. Srebrow, 2004. Mammary epithelial-mesenchymal interaction regulates fibronectin alternative splicing via phosphatidylinositol 3-kinase. J Biol Chem 279: 21029-37.

Blaustein, M., F. Pelisch, T. Tanos, M.J. Munoz, D. Wengier, L. Quadrana, J.R. Sanford, J.P. Muschietti, A.R. Kornblihtt, J.F. Caceres, O.A. Coso, and A. Srebrow, 2005. Concerted regulation of nuclear and cytoplasmic activities of SR proteins by AKT. Nat Struct Mol Biol 12: 1037-44.

Boon, K.L., T. Auchynnikava, G. Edwalds-Gilbert, J.D. Barrass, A.P. Droop, C. Dez, and J.D. Beggs, 2006. Yeast ntr1/spp382 mediates prp43 function in postspliceosomes. Mol Cell Biol 26: 6016-23.

Borsi, L., E. Balza, M. Bestagno, P. Castellani, B. Carnemolla, A. Biro, A. Leprini, J. Sepulveda, O. Burrone, D. Neri, and L. Zardi, 2002. Selective targeting of tumoral vasculature: comparison of different formats of an antibody (L19) to the ED-B domain of fibronectin. Int J Cancer 102: 75-85.

Brunmeir, R., S. Lagger, and C. Seiser, 2009. Histone deacetylase HDAC1/HDAC2-controlled embryonic development and cell differentiation. Int J Dev Biol 53: 275-89.

Bruzik, J.P., K. Van Doren, D. Hirsh, and J.A. Steitz, 1988. Trans splicing involves a novel form of small nuclear ribonucleoprotein particles. Nature 335: 559-62.

Bujakowska, K., C. Maubaret, C.F. Chakarova, N. Tanimoto, S.C. Beck, E. Fahl, M.M. Humphries, P.F. Kenna, E. Makarov, O. Makarova, F. Paquet-Durand, P.A.

Ekstrom, T. van Veen, T. Leveillard, P. Humphries, M.W. Seeliger, and S.S. Bhattacharya, 2009. Study of gene-targeted mouse models of splicing factor gene Prpf31 implicated in human autosomal dominant retinitis pigmentosa (RP). Invest Ophthalmol Vis Sci 50: 5927-33.

Buratti, E., A.F. Muro, M. Giombi, D. Gherbassi, A. Iaconcig, and F.E. Baralle, 2004. RNA folding affects the recruitment of SR proteins by mouse and human polypurinic enhancer elements in the fibronectin EDA exon. Mol Cell Biol 24: 1387-400.

Cajal, R.Y., 1903. Un sencillo metodo de coloracion seletiva del reticulo protoplasmatico y sus efectos en los diversos organos nerviosos de vertebrados e invertebrados. Trab Lab Investig Biol Univ Madr 2: 129–221.

Campbell, D.A., D.A. Thornton, and J.C. Boothroyd, 1984. Apparent discontinuous transcription of Trypanosoma brucei variant surface antigen genes. Nature 311: 350-5.

Cao, H., J. Wu, S. Lam, R. Duan, C. Newnham, R.S. Molday, J.J. Graziotto, E.A. Pierce, and J. Hu, 2011. Temporal and tissue specific regulation of RP-associated splicing factor genes PRPF3, PRPF31 and PRPC8--implications in the pathogenesis of RP. PLoS One 6: e15860.

Castellani, P., G. Viale, A. Dorcaratto, G. Nicolo, J. Kaczmarek, G. Querze, and L. Zardi, 1994. The fibronectin isoform containing the ED-B oncofetal domain: a marker of angiogenesis. Int J Cancer 59: 612-8.

Cech, T.R., 1986. The generality of self-splicing RNA: relationship to nuclear mRNA splicing. Cell 44: 207-10.

Clower, C.V., D. Chatterjee, Z. Wang, L.C. Cantley, M.G. Vander Heiden, and A.R. Krainer, 2010. The alternative splicing repressors hnRNP A1/A2 and PTB influence pyruvate kinase isoform expression and cell metabolism. Proc Natl Acad Sci U S A 107: 1894-9.

Collins, L., and D. Penny, 2005. Complex spliceosomal organization ancestral to extant eukaryotes. Mol Biol Evol 22: 1053-66.

Company, M., J. Arenas, and J. Abelson, 1991. Requirement of the RNA helicase-like protein PRP22 for release of messenger RNA from spliceosomes. Nature 349: 487-93.

Cramer, P., J.F. Caceres, D. Cazalla, S. Kadener, A.F. Muro, F.E. Baralle, and A.R. Kornblihtt, 1999. Coupling of transcription with alternative splicing: RNA pol II promoters modulate SF2/ASF and 9G8 effects on an exonic splicing enhancer. Mol Cell 4: 251-8.

Darzacq, X., B.E. Jady, C. Verheggen, A.M. Kiss, E. Bertrand, and T. Kiss, 2002. Cajal body-specific small nuclear RNAs: a novel class of 2'-O-methylation and pseudouridylation guide RNAs. EMBO J 21: 2746-56.

David, C.J., M. Chen, M. Assanah, P. Canoll, and J.L. Manley, 2010. HnRNP proteins controlled by c-Myc deregulate pyruvate kinase mRNA splicing in cancer. Nature 463: 364-8.

de la Mata, M., and A.R. Kornblihtt, 2006. RNA polymerase II C-terminal domain mediates regulation of alternative splicing by SRp20. Nat Struct Mol Biol 13: 973-80.

de la Mata, M., C.R. Alonso, S. Kadener, J.P. Fededa, M. Blaustein, F. Pelisch, P. Cramer, D. Bentley, and A.R. Kornblihtt, 2003. A slow RNA polymerase II affects alternative splicing in vivo. Mol Cell 12: 525-32.

de Ruijter, A.J., A.H. van Gennip, H.N. Caron, S. Kemp, and A.B. van Kuilenburg, 2003. Histone deacetylases (HDACs): characterization of the classical HDAC family. Biochem J 370: 737-49.

Deery, E.C., E.N. Vithana, R.J. Newbold, V.A. Gallon, S.S. Bhattacharya, M.J. Warren, D.M. Hunt, and S.E. Wilkie, 2002. Disease mechanism for retinitis pigmentosa (RP11) caused by mutations in the splicing factor gene PRPF31. Hum Mol Genet 11: 3209-19.

Denslow, S.A., and P.A. Wade, 2007. The human Mi-2/NuRD complex and gene regulation. Oncogene 26: 5433-8.
Dignam, J.D., R.M. Lebovitz, and R.G. Roeder, 1983. Accurate transcription initiation by RNA polymerase II in a soluble extract from isolated mammalian nuclei. Nucleic Acids Res 11: 1475-89.
Dion, M.F., S.J. Altschuler, L.F. Wu, and O.J. Rando, 2005. Genomic characterization reveals a simple histone H4 acetylation code. Proc Natl Acad Sci U S A 102: 5501-6.
Dryja, T.P., T.L. McGee, E. Reichel, L.B. Hahn, G.S. Cowley, D.W. Yandell, M.A. Sandberg, and E.L. Berson, 1990. A point mutation of the rhodopsin gene in one form of retinitis pigmentosa. Nature 343: 364-6.
Du, K., and R. Taub, 1997. Alternative splicing and structure of the human and mouse SFRS5/HRS/SRp40 genes. Gene 204: 243-9.
Faustino, N.A., and T.A. Cooper, 2003. Pre-mRNA splicing and human disease. Genes Dev 17: 419-37.
Fernandez-Rubio, C., C. Ordonez, J. Abad-Gonzalez, A. Garcia-Gallego, M.P. Honrubia, J.J. Mallo, and R. Balana-Fouce, 2009. Butyric acid-based feed additives help protect broiler chickens from Salmonella Enteritidis infection. Poult Sci 88: 943-8.
Fukuda, T., N. Yoshida, Y. Kataoka, R. Manabe, Y. Mizuno-Horikawa, M. Sato, K. Kuriyama, N. Yasui, and K. Sekiguchi, 2002. Mice lacking the EDB segment of fibronectin develop normally but exhibit reduced cell growth and fibronectin matrix assembly in vitro. Cancer Res 62: 5603-10.
Gahura, O., K. Abrhamova, M. Skruzny, A. Valentova, V. Munzarova, P. Folk, and F. Puta, 2009. Prp45 affects Prp22 partition in spliceosomal complexes and splicing efficiency of non-consensus substrates. J Cell Biochem 106: 139-51.
Gao, J., K. Cheon, S. Nusinowitz, Q. Liu, D. Bei, K. Atkins, A. Azimi, S.P. Daiger, D.B. Farber, J.R. Heckenlively, E.A. Pierce, L.S. Sullivan, and J. Zuo, 2002. Progressive photoreceptor degeneration, outer segment dysplasia, and rhodopsin mislocalization in mice with targeted disruption of the retinitis pigmentosa-1 (Rp1) gene. Proc Natl Acad Sci U S A 99: 5698-703.
George, E.L., E.N. Georges-Labouesse, R.S. Patel-King, H. Rayburn, and R.O. Hynes, 1993. Defects in mesoderm, neural tube and vascular development in mouse embryos lacking fibronectin. Development 119: 1079-91.
Ghetti, A., M. Company, and J. Abelson, 1995. Specificity of Prp24 binding to RNA: a role for Prp24 in the dynamic interaction of U4 and U6 snRNAs. RNA 1: 132-45.
Ghigna, C., S. Giordano, H. Shen, F. Benvenuto, F. Castiglioni, P.M. Comoglio, M.R. Green, S. Riva, and G. Biamonti, 2005. Cell motility is controlled by SF2/ASF through alternative splicing of the Ron protooncogene. Mol Cell 20: 881-90.
Grayson, D.R., M. Kundakovic, and R.P. Sharma, 2010. Is there a future for histone deacetylase inhibitors in the pharmacotherapy of psychiatric disorders? Mol Pharmacol 77: 126-35.
Graziotto, J.J., C.F. Inglehearn, M.A. Pack, and E.A. Pierce, 2008. Decreased levels of the RNA splicing factor Prpf3 in mice and zebrafish do not cause photoreceptor degeneration. Invest Ophthalmol Vis Sci 49: 3830-8.
Grzenda, A., G. Lomberk, J.S. Zhang, and R. Urrutia, 2009. Sin3: master scaffold and transcriptional corepressor. Biochim Biophys Acta 1789: 443-50.
Haberland, M., R.L. Montgomery, and E.N. Olson, 2009. The many roles of histone deacetylases in development and physiology: implications for disease and therapy. Nat Rev Genet 10: 32-42.
Hall, S.L., and R.A. Padgett, 1996. Requirement of U12 snRNA for in vivo splicing of a minor class of eukaryotic nuclear pre-mRNA introns. Science 271: 1716-8.
Hamel, C., 2006. Retinitis pigmentosa. Orphanet J Rare Dis 1: 40.

Han, J., J.H. Ding, C.W. Byeon, J.H. Kim, K.J. Hertel, S. Jeong, and X.D. Fu, 2011. SR proteins induce alternative exon skipping through their activities on the flanking constitutive exons. Mol Cell Biol 31: 793-802.

Haugen, P., D.M. Simon, and D. Bhattacharya, 2005. The natural history of group I introns. Trends Genet 21: 111-9.

Hodawadekar, S.C., and R. Marmorstein, 2007. Chemistry of acetyl transfer by histone modifying enzymes: structure, mechanism and implications for effector design. Oncogene 26: 5528-40.

Hubbert, C., A. Guardiola, R. Shao, Y. Kawaguchi, A. Ito, A. Nixon, M. Yoshida, X.F. Wang, and T.P. Yao, 2002. HDAC6 is a microtubule-associated deacetylase. Nature 417: 455-8.

Huranova, M., I. Ivani, A. Benda, I. Poser, Y. Brody, M. Hof, Y. Shav-Tal, K.M. Neugebauer, and D. Stanek, 2010. The differential interaction of snRNPs with pre-mRNA reveals splicing kinetics in living cells. J Cell Biol 191: 75-86.

Chakarova, C.F., M.M. Hims, H. Bolz, L. Abu-Safieh, R.J. Patel, M.G. Papaioannou, C.F. Inglehearn, T.J. Keen, C. Willis, A.T. Moore, T. Rosenberg, A.R. Webster, A.C. Bird, A. Gal, D. Hunt, E.N. Vithana, and S.S. Bhattacharya, 2002. Mutations in HPRP3, a third member of pre-mRNA splicing factor genes, implicated in autosomal dominant retinitis pigmentosa. Hum Mol Genet 11: 87-92.

Chapman, K.B., and J.D. Boeke, 1991. Isolation and characterization of the gene encoding yeast debranching enzyme. Cell 65: 483-92.

Chateauvieux, S., F. Morceau, M. Dicato, and M. Diederich, 2010. Molecular and therapeutic potential and toxicity of valproic acid. J Biomed Biotechnol 2010.

Chauhan, A.K., J. Kisucka, M.R. Cozzi, M.T. Walsh, F.A. Moretti, M. Battiston, M. Mazzucato, L. De Marco, F.E. Baralle, D.D. Wagner, and A.F. Muro, 2008. Prothrombotic effects of fibronectin isoforms containing the EDA domain. Arterioscler Thromb Vasc Biol 28: 296-301.

Chen, F., H. Kook, R. Milewski, A.D. Gitler, M.M. Lu, J. Li, R. Nazarian, R. Schnepp, K. Jen, C. Biben, G. Runke, J.P. Mackay, J. Novotny, R.J. Schwartz, R.P. Harvey, M.C. Mullins, and J.A. Epstein, 2002. Hop is an unusual homeobox gene that modulates cardiac development. Cell 110: 713-23.

Chen, G., J. Fernandez, S. Mische, and A.J. Courey, 1999. A functional interaction between the histone deacetylase Rpd3 and the corepressor groucho in Drosophila development. Genes Dev 13: 2218-30.

Chen, X., and J.J. Bieker, 2001. Unanticipated repression function linked to erythroid Kruppel-like factor. Mol Cell Biol 21: 3118-25.

Choi, E., C. Han, I. Park, B. Lee, S. Jin, H. Choi, H. Kim do, Z.Y. Park, E.M. Eddy, and C. Cho, 2008. A novel germ cell-specific protein, SHIP1, forms a complex with chromatin remodeling activity during spermatogenesis. J Biol Chem 283: 35283-94.

Chow, L.T., R.E. Gelinas, T.R. Broker, and R.J. Roberts, 1977. An amazing sequence arrangement at the 5' ends of adenovirus 2 messenger RNA. Cell 12: 1-8.

Jady, B.E., X. Darzacq, K.E. Tucker, A.G. Matera, E. Bertrand, and T. Kiss, 2003. Modification of Sm small nuclear RNAs occurs in the nucleoplasmic Cajal body following import from the cytoplasm. EMBO J 22: 1878-88.

Jurica, M.S., and M.J. Moore, 2003. Pre-mRNA splicing: awash in a sea of proteins. Mol Cell 12: 5-14.

Kadener, S., J.P. Fededa, M. Rosbash, and A.R. Kornblihtt, 2002. Regulation of alternative splicing by a transcriptional enhancer through RNA pol II elongation. Proc Natl Acad Sci U S A 99: 8185-90.

Kadener, S., P. Cramer, G. Nogues, D. Cazalla, M. de la Mata, J.P. Fededa, S.E. Werbajh, A. Srebrow, and A.R. Kornblihtt, 2001. Antagonistic effects of T-Ag and VP16 reveal a role for RNA pol II elongation on alternative splicing. EMBO J 20: 5759-68.

Karijolich, J., and Y.T. Yu, 2010. Spliceosomal snRNA modifications and their function. RNA Biol 7: 192-204.

Karni, R., E. de Stanchina, S.W. Lowe, R. Sinha, D. Mu, and A.R. Krainer, 2007. The gene encoding the splicing factor SF2/ASF is a proto-oncogene. Nat Struct Mol Biol 14: 185-93.

Khochbin, S., and A.P. Wolffe, 1997. The origin and utility of histone deacetylases. FEBS Lett 419: 157-60.

Kiss, A.M., B.E. Jady, X. Darzacq, C. Verheggen, E. Bertrand, and T. Kiss, 2002. A Cajal body-specific pseudouridylation guide RNA is composed of two box H/ACA snoRNA-like domains. Nucleic Acids Res 30: 4643-9.

Klingauf, M., D. Stanek, and K.M. Neugebauer, 2006. Enhancement of U4/U6 small nuclear ribonucleoprotein particle association in Cajal bodies predicted by mathematical modeling. Mol Biol Cell 17: 4972-81.

Klingbeil, P., R. Marhaba, T. Jung, R. Kirmse, T. Ludwig, and M. Zoller, 2009. CD44 variant isoforms promote metastasis formation by a tumor cell-matrix cross-talk that supports adhesion and apoptosis resistance. Mol Cancer Res 7: 168-79.

Kook, H., J.J. Lepore, A.D. Gitler, M.M. Lu, W. Wing-Man Yung, J. Mackay, R. Zhou, V. Ferrari, P. Gruber, and J.A. Epstein, 2003. Cardiac hypertrophy and histone deacetylase-dependent transcriptional repression mediated by the atypical homeodomain protein Hop. J Clin Invest 112: 863-71.

Kornblihtt, A.R., 2005. Promoter usage and alternative splicing. Curr Opin Cell Biol 17: 262-8.

Kornblihtt, A.R., K. Vibe-Pedersen, and F.E. Baralle, 1984. Human fibronectin: molecular cloning evidence for two mRNA species differing by an internal segment coding for a structural domain. EMBO J 3: 221-6.

Kouzarides, T., 2007. Chromatin modifications and their function. Cell 128: 693-705.

Krause, M., and D. Hirsh, 1987. A trans-spliced leader sequence on actin mRNA in C. elegans. Cell 49: 753-61.

Lagger, G., D. O'Carroll, M. Rembold, H. Khier, J. Tischler, G. Weitzer, B. Schuettengruber, C. Hauser, R. Brunmeir, T. Jenuwein, and C. Seiser, 2002. Essential function of histone deacetylase 1 in proliferation control and CDK inhibitor repression. EMBO J 21: 2672-81.

Lakowski, B., I. Roelens, and S. Jacob, 2006. CoREST-like complexes regulate chromatin modification and neuronal gene expression. J Mol Neurosci 29: 227-39.

Lambowitz, A.M., and S. Zimmerly, 2010. Group II Introns: Mobile Ribozymes that Invade DNA. Cold Spring Harb Perspect Biol.

Lander, E.S., L.M. Linton, B. Birren, C. Nusbaum, M.C. Zody, J. Baldwin, K. Devon, K. Dewar, M. Doyle, W. FitzHugh, R. Funke, D. Gage, K. Harris, A. Heaford, J. Howland, L. Kann, J. Lehoczky, R. LeVine, P. McEwan, K. McKernan, J. Meldrim, J.P. Mesirov, C. Miranda, W. Morris, J. Naylor, C. Raymond, M. Rosetti, R. Santos, A. Sheridan, C. Sougnez, N. Stange-Thomann, N. Stojanovic, A. Subramanian, D. Wyman, J. Rogers, J. Sulston, R. Ainscough, S. Beck, D. Bentley, J. Burton, C. Clee, N. Carter, A. Coulson, R. Deadman, P. Deloukas, A. Dunham, I. Dunham, R. Durbin, L. French, D. Grafham, S. Gregory, T. Hubbard, S. Humphray, A. Hunt, M. Jones, C. Lloyd, A. McMurray, L. Matthews, S. Mercer, S. Milne, J.C. Mullikin, A. Mungall, R. Plumb, M. Ross, R. Shownkeen, S. Sims, R.H. Waterston, R.K. Wilson, L.W. Hillier, J.D. McPherson, M.A. Marra, E.R. Mardis, L.A. Fulton, A.T. Chinwalla, K.H. Pepin, W.R. Gish, S.L. Chissoe, M.C. Wendl, K.D. Delehaunty, T.L. Miner, A. Delehaunty, J.B. Kramer, L.L. Cook, R.S. Fulton, D.L. Johnson, P.J. Minx, S.W. Clifton, T. Hawkins, E. Branscomb, P. Predki, P. Richardson, S. Wenning, T. Slezak, N. Doggett, J.F. Cheng, A. Olsen, S. Lucas, C. Elkin, E. Uberbacher, M. Frazier*, et al.*, 2001. Initial sequencing and analysis of the human genome. Nature 409: 860-921.

Lebreton, S., G. Carraz, H. Meunier, and H. Beriel, 1964. [Pharmacodynamic Properties of 2,2-Dipropylacetic Acid. 2d Report on Its Anti-Epileptic Properties]. Therapie 19: 451-6.

Lemaire, R., A. Winne, M. Sarkissian, and R. Lafyatis, 1999. SF2 and SRp55 regulation of CD45 exon 4 skipping during T cell activation. Eur J Immunol 29: 823-37.

Liang, J., M. Wan, Y. Zhang, P. Gu, H. Xin, S.Y. Jung, J. Qin, J. Wong, A.J. Cooney, D. Liu, and Z. Songyang, 2008. Nanog and Oct4 associate with unique transcriptional repression complexes in embryonic stem cells. Nat Cell Biol 10: 731-9.

Lim, L.P., and P.A. Sharp, 1998. Alternative splicing of the fibronectin EIIIB exon depends on specific TGCATG repeats. Mol Cell Biol 18: 3900-6.

Linder, B., H. Dill, A. Hirmer, J. Brocher, G.P. Lee, S. Mathavan, H.J. Bolz, C. Winkler, B. Laggerbauer, and U. Fischer, 2011. Systemic splicing factor deficiency causes tissue-specific defects: a zebrafish model for retinitis pigmentosa. Hum Mol Genet 20: 368-77.

Listerman, I., A.K. Sapra, and K.M. Neugebauer, 2006. Cotranscriptional coupling of splicing factor recruitment and precursor messenger RNA splicing in mammalian cells. Nat Struct Mol Biol 13: 815-22.

Liu, S., R. Rauhut, H.P. Vornlocher, and R. Luhrmann, 2006. The network of protein-protein interactions within the human U4/U6.U5 tri-snRNP. RNA 12: 1418-30.

Magnusson, M.K., and D.F. Mosher, 1998. Fibronectin: structure, assembly, and cardiovascular implications. Arterioscler Thromb Vasc Biol 18: 1363-70.

Makarov, E.M., O.V. Makarova, H. Urlaub, M. Gentzel, C.L. Will, M. Wilm, and R. Luhrmann, 2002. Small nuclear ribonucleoprotein remodeling during catalytic activation of the spliceosome. Science 298: 2205-8.

Makarova, O.V., E.M. Makarov, S. Liu, H.P. Vornlocher, and R. Luhrmann, 2002. Protein 61K, encoded by a gene (PRPF31) linked to autosomal dominant retinitis pigmentosa, is required for U4/U6*U5 tri-snRNP formation and pre-mRNA splicing. EMBO J 21: 1148-57.

Martin, A., S. Schneider, and B. Schwer, 2002. Prp43 is an essential RNA-dependent ATPase required for release of lariat-intron from the spliceosome. J Biol Chem 277: 17743-50.

Matlin, A.J., F. Clark, and C.W. Smith, 2005. Understanding alternative splicing: towards a cellular code. Nat Rev Mol Cell Biol 6: 386-98.

Matsuyama, A., T. Shimazu, Y. Sumida, A. Saito, Y. Yoshimatsu, D. Seigneurin-Berny, H. Osada, Y. Komatsu, N. Nishino, S. Khochbin, S. Horinouchi, and M. Yoshida, 2002. In vivo destabilization of dynamic microtubules by HDAC6-mediated deacetylation. EMBO J 21: 6820-31.

Maurer, L.M., B.R. Tomasini-Johansson, and D.F. Mosher, 2010. Emerging roles of fibronectin in thrombosis. Thromb Res 125: 287-91.

Mayas, R.M., H. Maita, and J.P. Staley, 2006. Exon ligation is proofread by the DExD/H-box ATPase Prp22p. Nat Struct Mol Biol 13: 482-90.

McKie, A.B., J.C. McHale, T.J. Keen, E.E. Tarttelin, R. Goliath, J.J. van Lith-Verhoeven, J. Greenberg, R.S. Ramesar, C.B. Hoyng, F.P. Cremers, D.A. Mackey, S.S. Bhattacharya, A.C. Bird, A.F. Markham, and C.F. Inglehearn, 2001. Mutations in the pre-mRNA splicing factor gene PRPC8 in autosomal dominant retinitis pigmentosa (RP13). Hum Mol Genet 10: 1555-62.

McManus, C.J., and B.R. Graveley, 2008. Getting the message out. Mol Cell 31: 4-6.

Mesdjian, E., L. Ciesielski, M. Valli, B. Bruguerolle, G. Jadot, P. Bouyard, and P. Mandel, 1982. Sodium valproate: kinetic profile and effects on GABA levels in various brain areas of the rat. Prog Neuropsychopharmacol Biol Psychiatry 6: 223-33.

Monsalve, M., Z. Wu, G. Adelmant, P. Puigserver, M. Fan, and B.M. Spiegelman, 2000. Direct coupling of transcription and mRNA processing through the thermogenic coactivator PGC-1. Mol Cell 6: 307-16.

Montgomery, R.L., C.A. Davis, M.J. Potthoff, M. Haberland, J. Fielitz, X. Qi, J.A. Hill, J.A. Richardson, and E.N. Olson, 2007. Histone deacetylases 1 and 2 redundantly regulate cardiac morphogenesis, growth, and contractility. Genes Dev 21: 1790-802.

Mordes, D., X. Luo, A. Kar, D. Kuo, L. Xu, K. Fushimi, G. Yu, P. Sternberg, Jr., and J.Y. Wu, 2006. Pre-mRNA splicing and retinitis pigmentosa. Mol Vis 12: 1259-71.

Moretti, F.A., A.K. Chauhan, A. Iaconcig, F. Porro, F.E. Baralle, and A.F. Muro, 2007. A major fraction of fibronectin present in the extracellular matrix of tissues is plasma-derived. J Biol Chem 282: 28057-62.

Morrison, B.E., N. Majdzadeh, and S.R. D'Mello, 2007. Histone deacetylases: focus on the nervous system. Cell Mol Life Sci 64: 2258-69.

Muro, A.F., A.K. Chauhan, S. Gajovic, A. Iaconcig, F. Porro, G. Stanta, and F.E. Baralle, 2003. Regulated splicing of the fibronectin EDA exon is essential for proper skin wound healing and normal lifespan. J Cell Biol 162: 149-60.

Nissen, P., J. Hansen, N. Ban, P.B. Moore, and T.A. Steitz, 2000. The structural basis of ribosome activity in peptide bond synthesis. Science 289: 920-30.

Nogues, G., M.J. Munoz, and A.R. Kornblihtt, 2003. Influence of polymerase II processivity on alternative splicing depends on splice site strength. J Biol Chem 278: 52166-71.

Nogues, G., S. Kadener, P. Cramer, D. Bentley, and A.R. Kornblihtt, 2002. Transcriptional activators differ in their abilities to control alternative splicing. J Biol Chem 277: 43110-4.

Norton, P.A., and R.O. Hynes, 1993. Characterization of HeLa nuclear factors which interact with a conditionally processed rat fibronectin pre-mRNA. Biochem Biophys Res Commun 195: 215-21.

Nottrott, S., H. Urlaub, and R. Luhrmann, 2002. Hierarchical, clustered protein interactions with U4/U6 snRNA: a biochemical role for U4/U6 proteins. EMBO J 21: 5527-38.

Nottrott, S., K. Hartmuth, P. Fabrizio, H. Urlaub, I. Vidovic, R. Ficner, and R. Luhrmann, 1999. Functional interaction of a novel 15.5kD [U4/U6.U5] tri-snRNP protein with the 5' stem-loop of U4 snRNA. EMBO J 18: 6119-33.

Novotny, I., M. Blazikova, D. Stanek, P. Herman, and J. Malinsky, 2011. In vivo kinetics of U4/U6.U5 tri-snRNP formation in Cajal bodies. Mol Biol Cell 22: 513-23.

Ohno, M., and Y. Shimura, 1996. A human RNA helicase-like protein, HRH1, facilitates nuclear export of spliced mRNA by releasing the RNA from the spliceosome. Genes Dev 10: 997-1007.

Pan, Q., O. Shai, L.J. Lee, B.J. Frey, and B.J. Blencowe, 2008. Deep surveying of alternative splicing complexity in the human transcriptome by high-throughput sequencing. Nat Genet 40: 1413-5.

Pankov, R., and K.M. Yamada, 2002. Fibronectin at a glance. J Cell Sci 115: 3861-3.

Patel, R.S., E. Odermatt, J.E. Schwarzbauer, and R.O. Hynes, 1987. Organization of the fibronectin gene provides evidence for exon shuffling during evolution. EMBO J 6: 2565-72.

Peinado, H., D. Olmeda, and A. Cano, 2007. Snail, Zeb and bHLH factors in tumour progression: an alliance against the epithelial phenotype? Nat Rev Cancer 7: 415-28.

Peinado, H., E. Ballestar, M. Esteller, and A. Cano, 2004. Snail mediates E-cadherin repression by the recruitment of the Sin3A/histone deacetylase 1 (HDAC1)/HDAC2 complex. Mol Cell Biol 24: 306-19.

Peserico, A., and C. Simone, 2010. Physical and functional HAT/HDAC interplay regulates protein acetylation balance. J Biomed Biotechnol 2011: 371832.

Pini, A., F. Viti, A. Santucci, B. Carnemolla, L. Zardi, P. Neri, and D. Neri, 1998. Design and use of a phage display library. Human antibodies with subnanomolar affinity against a marker of angiogenesis eluted from a two-dimensional gel. J Biol Chem 273: 21769-76.

Poole, A.M., D.C. Jeffares, and D. Penny, 1998. The path from the RNA world. J Mol Evol 46: 1-17.

Raghunathan, P.L., and C. Guthrie, 1998. A spliceosomal recycling factor that reanneals U4 and U6 small nuclear ribonucleoprotein particles. Science 279: 857-60.

Raska, I., L.E. Andrade, R.L. Ochs, E.K. Chan, C.M. Chang, G. Roos, and E.M. Tan, 1991. Immunological and ultrastructural studies of the nuclear coiled body with autoimmune antibodies. Exp Cell Res 195: 27-37.

Ray, P., X. Luo, E.J. Rao, A. Basha, E.A. Woodruff, 3rd, and J.Y. Wu, 2010. The splicing factor Prp31 is essential for photoreceptor development in Drosophila. Protein Cell 1: 267-74.

Riggs, M.G., R.G. Whittaker, J.R. Neumann, and V.M. Ingram, 1977. n-Butyrate causes histone modification in HeLa and Friend erythroleukaemia cells. Nature 268: 462-4.

Robertson, K.D., S. Ait-Si-Ali, T. Yokochi, P.A. Wade, P.L. Jones, and A.P. Wolffe, 2000. DNMT1 forms a complex with Rb, E2F1 and HDAC1 and represses transcription from E2F-responsive promoters. Nat Genet 25: 338-42.

Rodriguez-Trelles, F., R. Tarrio, and F.J. Ayala, 2006. Origins and evolution of spliceosomal introns. Annu Rev Genet 40: 47-76.

Ruoslahti, E., 2002. Specialization of tumour vasculature. Nat Rev Cancer 2: 83-90.

Saleque, S., J. Kim, H.M. Rooke, and S.H. Orkin, 2007. Epigenetic regulation of hematopoietic differentiation by Gfi-1 and Gfi-1b is mediated by the cofactors CoREST and LSD1. Mol Cell 27: 562-72.

Sanchez, R., and M.M. Zhou, 2009. The role of human bromodomains in chromatin biology and gene transcription. Curr Opin Drug Discov Devel 12: 659-65.

Santimaria, M., G. Moscatelli, G.L. Viale, L. Giovannoni, G. Neri, F. Viti, A. Leprini, L. Borsi, P. Castellani, L. Zardi, D. Neri, and P. Riva, 2003. Immunoscintigraphic detection of the ED-B domain of fibronectin, a marker of angiogenesis, in patients with cancer. Clin Cancer Res 9: 571-9.

Sengupta, S., J.G. Muir, and P.R. Gibson, 2006. Does butyrate protect from colorectal cancer? J Gastroenterol Hepatol 21: 209-18.

Sharp, P.A., 1985. On the origin of RNA splicing and introns. Cell 42: 397-400.

Shin, C.H., Z.P. Liu, R. Passier, C.L. Zhang, D.Z. Wang, T.M. Harris, H. Yamagishi, J.A. Richardson, G. Childs, and E.N. Olson, 2002. Modulation of cardiac growth and development by HOP, an unusual homeodomain protein. Cell 110: 725-35.

Shogren-Knaak, M., H. Ishii, J.M. Sun, M.J. Pazin, J.R. Davie, and C.L. Peterson, 2006. Histone H4-K16 acetylation controls chromatin structure and protein interactions. Science 311: 844-7.

Schaffert, N., M. Hossbach, R. Heintzmann, T. Achsel, and R. Luhrmann, 2004. RNAi knockdown of hPrp31 leads to an accumulation of U4/U6 di-snRNPs in Cajal bodies. EMBO J 23: 3000-9.

Scharlau, D., A. Borowicki, N. Habermann, T. Hofmann, S. Klenow, C. Miene, U. Munjal, K. Stein, and M. Glei, 2009. Mechanisms of primary cancer prevention by butyrate and other products formed during gut flora-mediated fermentation of dietary fibre. Mutat Res 682: 39-53.

Scherer, S., 2008. A short guide to the human genome Cold Spring Harbor Laboratory Press, Cold Spring Harbor, N.Y.

Schwarzbauer, J.E., J.W. Tamkun, I.R. Lemischka, and R.O. Hynes, 1983. Three different fibronectin mRNAs arise by alternative splicing within the coding region. Cell 35: 421-31.

Schwer, B., and C.H. Gross, 1998. Prp22, a DExH-box RNA helicase, plays two distinct roles in yeast pre-mRNA splicing. EMBO J 17: 2086-94.
Simpson, A.G., E.K. MacQuarrie, and A.J. Roger, 2002. Eukaryotic evolution: early origin of canonical introns. Nature 419: 270.
Sneath, R.J., and D.C. Mangham, 1998. The normal structure and function of CD44 and its role in neoplasia. Mol Pathol 51: 191-200.
Song, E.J., S.L. Werner, J. Neubauer, F. Stegmeier, J. Aspden, D. Rio, J.W. Harper, S.J. Elledge, M.W. Kirschner, and M. Rape, 2010. The Prp19 complex and the Usp4Sart3 deubiquitinating enzyme control reversible ubiquitination at the spliceosome. Genes Dev 24: 1434-47.
Srebrow, A., and A.R. Kornblihtt, 2006. The connection between splicing and cancer. J Cell Sci 119: 2635-41.
Stanek, D., and K.M. Neugebauer, 2004. Detection of snRNP assembly intermediates in Cajal bodies by fluorescence resonance energy transfer. J Cell Biol 166: 1015-25.
Stanek, D., and K.M. Neugebauer, 2006. The Cajal body: a meeting place for spliceosomal snRNPs in the nuclear maze. Chromosoma 115: 343-54.
Strzelecka, M., S. Trowitzsch, G. Weber, R. Luhrmann, A.C. Oates, and K.M. Neugebauer, 2010. Coilin-dependent snRNP assembly is essential for zebrafish embryogenesis. Nat Struct Mol Biol 17: 403-9.
Tanackovic, G., A. Ransijn, P. Thibault, S. Abou Elela, R. Klinck, E.L. Berson, B. Chabot, and C. Rivolta, 2011. PRPF mutations are associated with generalized defects in spliceosome formation and pre-mRNA splicing in patients with retinitis pigmentosa. Hum Mol Genet.
Tanaka, N., A. Aronova, and B. Schwer, 2007. Ntr1 activates the Prp43 helicase to trigger release of lariat-intron from the spliceosome. Genes Dev 21: 2312-25.
Tang, X., J.S. Gao, Y.J. Guan, K.E. McLane, Z.L. Yuan, B. Ramratnam, and Y.E. Chin, 2007. Acetylation-dependent signal transduction for type I interferon receptor. Cell 131: 93-105.
Tarn, W.Y., and J.A. Steitz, 1996. A novel spliceosome containing U11, U12, and U5 snRNPs excises a minor class (AT-AC) intron in vitro. Cell 84: 801-11.
Tsai, R.T., R.H. Fu, F.L. Yeh, C.K. Tseng, Y.C. Lin, Y.H. Huang, and S.C. Cheng, 2005. Spliceosome disassembly catalyzed by Prp43 and its associated components Ntr1 and Ntr2. Genes Dev 19: 2991-3003.
Tsai, R.T., C.K. Tseng, P.J. Lee, H.C. Chen, R.H. Fu, K.J. Chang, F.L. Yeh, and S.C. Cheng, 2007. Dynamic interactions of Ntr1-Ntr2 with Prp43 and with U5 govern the recruitment of Prp43 to mediate spliceosome disassembly. Mol Cell Biol 27: 8027-37.
Tseng, C.K., and S.C. Cheng, 2008. Both catalytic steps of nuclear pre-mRNA splicing are reversible. Science 320: 1782-4.
Tsuji, N., M. Kobayashi, K. Nagashima, Y. Wakisaka, and K. Koizumi, 1976. A new antifungal antibiotic, trichostatin. J Antibiot (Tokyo) 29: 1-6.
Tuma, R.S., J.A. Stolk, and M.B. Roth, 1993. Identification and characterization of a sphere organelle protein. J Cell Biol 122: 767-73.
Valadkhan, S., and J.L. Manley, 2001. Splicing-related catalysis by protein-free snRNAs. Nature 413: 701-7.
Van Doren, K., and D. Hirsh, 1988. Trans-spliced leader RNA exists as small nuclear ribonucleoprotein particles in Caenorhabditis elegans. Nature 335: 556-9.
Vanacova, S., W. Yan, J.M. Carlton, and P.J. Johnson, 2005. Spliceosomal introns in the deep-branching eukaryote Trichomonas vaginalis. Proc Natl Acad Sci U S A 102: 4430-5.
Vandenberghe, A.E., T.H. Meedel, and K.E. Hastings, 2001. mRNA 5'-leader trans-splicing in the chordates. Genes Dev 15: 294-303.

VanDongen, A.M., M.G. VanErp, and R.A. Voskuyl, 1986. Valproate reduces excitability by blockage of sodium and potassium conductance. Epilepsia 27: 177-82.

Vega, R.B., K. Matsuda, J. Oh, A.C. Barbosa, X. Yang, E. Meadows, J. McAnally, C. Pomajzl, J.M. Shelton, J.A. Richardson, G. Karsenty, and E.N. Olson, 2004. Histone deacetylase 4 controls chondrocyte hypertrophy during skeletogenesis. Cell 119: 555-66.

Villa, A., E. Trachsel, M. Kaspar, C. Schliemann, R. Sommavilla, J.N. Rybak, C. Rosli, L. Borsi, and D. Neri, 2008. A high-affinity human monoclonal antibody specific to the alternatively spliced EDA domain of fibronectin efficiently targets tumor neo-vasculature in vivo. Int J Cancer 122: 2405-13.

Vithana, E.N., L. Abu-Safieh, L. Pelosini, E. Winchester, D. Hornan, A.C. Bird, D.M. Hunt, S.A. Bustin, and S.S. Bhattacharya, 2003. Expression of PRPF31 mRNA in patients with autosomal dominant retinitis pigmentosa: a molecular clue for incomplete penetrance? Invest Ophthalmol Vis Sci 44: 4204-9.

Vithana, E.N., L. Abu-Safieh, M.J. Allen, A. Carey, M. Papaioannou, C. Chakarova, M. Al-Maghtheh, N.D. Ebenezer, C. Willis, A.T. Moore, A.C. Bird, D.M. Hunt, and S.S. Bhattacharya, 2001. A human homolog of yeast pre-mRNA splicing gene, PRP31, underlies autosomal dominant retinitis pigmentosa on chromosome 19q13.4 (RP11). Mol Cell 8: 375-81.

Voso, M.T., V. Santini, C. Finelli, P. Musto, E. Pogliani, E. Angelucci, G. Fioritoni, G. Alimena, L. Maurillo, A. Cortelezzi, F. Buccisano, M. Gobbi, L. Borin, A. Di Tucci, G. Zini, M.C. Petti, G. Martinelli, E. Fabiani, P. Fazi, M. Vignetti, A. Piciocchi, V. Liso, S. Amadori, and G. Leone, 2009. Valproic acid at therapeutic plasma levels may increase 5-azacytidine efficacy in higher risk myelodysplastic syndromes. Clin Cancer Res 15: 5002-7.

Wagner, J.D., E. Jankowsky, M. Company, A.M. Pyle, and J.N. Abelson, 1998. The DEAH-box protein PRP22 is an ATPase that mediates ATP-dependent mRNA release from the spliceosome and unwinds RNA duplexes. EMBO J 17: 2926-37.

Wagner, J.M., B. Hackanson, M. Lubbert, and M. Jung, 2010. Histone deacetylase (HDAC) inhibitors in recent clinical trials for cancer therapy. Clin Epigenetics 1: 117-136.

Wahl, M.C., C.L. Will, and R. Luhrmann, 2009. The spliceosome: design principles of a dynamic RNP machine. Cell 136: 701-18.

Wang, E.T., R. Sandberg, S. Luo, I. Khrebtukova, L. Zhang, C. Mayr, S.F. Kingsmore, G.P. Schroth, and C.B. Burge, 2008. Alternative isoform regulation in human tissue transcriptomes. Nature 456: 470-6.

Wang, Z., and C.B. Burge, 2008. Splicing regulation: from a parts list of regulatory elements to an integrated splicing code. RNA 14: 802-13.

White, E.S., F.E. Baralle, and A.F. Muro, 2008. New insights into form and function of fibronectin splice variants. J Pathol 216: 1-14.

White, E.S., R.L. Sagana, A.J. Booth, M. Yan, A.M. Cornett, C.A. Bloomheart, J.L. Tsui, C.A. Wilke, B.B. Moore, J.D. Ritzenthaler, J. Roman, and A.F. Muro, 2010. Control of fibroblast fibronectin expression and alternative splicing via the PI3K/Akt/mTOR pathway. Exp Cell Res 316: 2644-53.

Wilihoeft, U., E. Campos-Gongora, S. Touzni, I. Bruchhaus, and E. Tannich, 2001. Introns of Entamoeba histolytica and Entamoeba dispar. Protist 152: 149-56.

Wilkie, S.E., V. Vaclavik, H. Wu, K. Bujakowska, C.F. Chakarova, S.S. Bhattacharya, M.J. Warren, and D.M. Hunt, 2008. Disease mechanism for retinitis pigmentosa (RP11) caused by missense mutations in the splicing factor gene PRPF31. Mol Vis 14: 683-90.

Xu, W.S., R.B. Parmigiani, and P.A. Marks, 2007. Histone deacetylase inhibitors: molecular mechanisms of action. Oncogene 26: 5541-52.

Yoshida, M., S. Nomura, and T. Beppu, 1987. Effects of trichostatins on differentiation of murine erythroleukemia cells. Cancer Res 47: 3688-91.
Yoshida, M., M. Kijima, M. Akita, and T. Beppu, 1990. Potent and specific inhibition of mammalian histone deacetylase both in vivo and in vitro by trichostatin A. J Biol Chem 265: 17174-9.
Yoshimoto, R., N. Kataoka, K. Okawa, and M. Ohno, 2009. Isolation and characterization of post-splicing lariat-intron complexes. Nucleic Acids Res 37: 891-902.
Yuan, L., M. Kawada, N. Havlioglu, H. Tang, and J.Y. Wu, 2005. Mutations in PRPF31 inhibit pre-mRNA splicing of rhodopsin gene and cause apoptosis of retinal cells. J Neurosci 25: 748-57.
Zhang, J., and X. Chen, 2007. DeltaNp73 modulates nerve growth factor-mediated neuronal differentiation through repression of TrkA. Mol Cell Biol 27: 3868-80.
Zhou, J., Q. Yu, and T. Zou, 2008. Alternative splicing of exon 10 in the tau gene as a target for treatment of tauopathies. BMC Neurosci 9 Suppl 2: S10.

Publications

Research paper I

Stanek D., Pridalová-Hnilicová J., Novotný I., Huranová M., Blazíková M., Wen X,. Sapra A.K., Neugebauer K.M.: Spliceosomal small nuclear ribonucleoprotein particles repeatedly cycle through Cajal bodies.
Mol Biol Cell. 2008 Jun;19(6):2534-43.

Research paper II

Huranová M.*, Hnilicová J.*, Fleischer B., Cvacková Z., Stanek D.: A mutation linked to retinitis pigmentosa in HPRP31 causes protein instability and impairs its interactions with spliceosomal snRNPs.
Hum Mol Genet. 2009 Jun 1;18(11):2014-23.

* shared first co-authorship

Research Paper III

Hnilicová J., Hozeifi S., Dušková E., Icha J., Tománková T., Staněk D.: Histone deacetylase activity modulates alternative splicing.
PLoS One. 2011 Feb2;6(2):e16727.

Review Paper IV

Hnilicová J., Staněk D.: Where splicing joins chromatin.
Nucleus, in press

Molecular Biology of the Cell
Vol. 19, 2534–2543, June 2008

Spliceosomal Small Nuclear Ribonucleoprotein Particles Repeatedly Cycle through Cajal Bodies

David Staněk,* Jarmila Přidalová-Hnilicová,* Ivan Novotný,* Martina Huranová,* Michaela Blažíková,† Xin Wen,‡ Aparna K. Sapra,§ and Karla M. Neugebauer§

*Institute of Molecular Genetics and †Institute of Experimental Medicine, Academy of Sciences of the Czech Republic, 142 20 Prague 4, Czech Republic; ‡Center for Craniofacial Molecular Biology, School of Dentistry, University of Southern California, Los Angeles, CA 90033; and §Max Planck Institute of Molecular Cell Biology and Genetics, 01307 Dresden, Germany

Submitted December 18, 2007; Revised March 10, 2008; Accepted March 13, 2008
Monitoring Editor: Wendy Bickmore

The Cajal body (CB) is a nuclear structure closely associated with import and biogenesis of small nuclear ribonucleoprotein particles (snRNPs). Here, we tested whether CBs also contain mature snRNPs and whether CB integrity depends on the ongoing snRNP splicing cycle. Sm proteins tagged with photoactivatable and color-maturing variants of fluorescent proteins were used to monitor snRNP behavior in living cells over time; mature snRNPs accumulated in CBs, traveled from one CB to another, and they were not preferentially replaced by newly imported snRNPs. To test whether CB integrity depends on the snRNP splicing cycle, two human orthologues of yeast proteins involved in distinct steps in spliceosome disassembly after splicing, hPrp22 and hNtr1, were depleted by small interfering RNA treatment. Surprisingly, depletion of either protein led to the accumulation of U4/U6 snRNPs in CBs, suggesting that reassembly of the U4/U6·U5 tri-snRNP was delayed. Accordingly, a relative decrease in U5 snRNPs compared with U4/U6 snRNPs was observed in CBs, as well as in nuclear extracts of treated cells. Together, the data show that particular phases of the spliceosome cycle are compartmentalized in living cells, with reassembly of the tri-snRNP occurring in CBs.

INTRODUCTION

Pre-mRNA splicing is a two-step transesterification reaction catalyzed by the spliceosome, a large complex assembled from preformed subcomplexes, called spliceosomal small nuclear ribonucleoprotein particles (snRNPs) and hundreds of additional proteins (Jurica and Moore, 2003). In turn, the five major spliceosomal snRNPs, U1, U2, U4, U5, and U6, each consist of a single small nuclear RNA (snRNA) and specific set of proteins. Among the shared protein components of snRNPs are the seven Sm proteins, which are assembled as a stable, heteroheptameric ring on the RNA polymerase II-transcribed snRNAs: U1, U2, U4, and U5. After transcription, these snRNAs are transported to the cytoplasm, where the Sm ring is assembled on snRNAs by the SMN complex. Subsequently, the 5′ ends of the snRNAs are hypermethylated to generate the trimethyl-guanosine cap, which together with SMN, promotes snRNP nuclear import (reviewed in Will and Luhrmann, 2001; Matera and Shpargel, 2006; Tycowski *et al*., 2006). Because snRNPs do not shuttle between the nucleus and cytoplasm (Änkö and Neugebauer, unpublished data), Sm ring assembly seems to occur early and only once in the lifetime of each snRNP. A related heteroheptameric ring, consisting of seven "like-Sm" (LSm) proteins, is assembled on U6, an RNA polymerase III transcript, which is thought to remain in the nucleus for all assembly steps (Achsel *et al*., 1999; Mayes *et al*., 1999; Kiss, 2004; Listerman *et al*., 2007).

Once back in the cell nucleus, snRNPs first accumulate in CBs before distributing throughout the nucleoplasm, where splicing occurs (Sleeman and Lamond, 1999; Sleeman *et al*., 2001; Neugebauer, 2002). This suggests a role for CBs in nuclear steps of snRNP maturation, a prediction borne out by the following set of observations. First, posttranscriptional modifications of the snRNAs themselves occur in CBs after snRNP reimport from the cytoplasm (Darzacq *et al*., 2002; Kiss, 2002; Jady *et al*., 2003). These modifications, including pseudouridinylation and 2′-*O*-methylation, are guided by small Cajal body-specific RNAs. Second, CBs are the site of complex assembly steps that involve RNA–RNA annealing and the sequential addition of proteins. For example, the U4/U6 snRNP is formed when the U4 and U6 snRNAs anneal, a step catalyzed by U6-specific LSm proteins and SART3 (also named hPrp24 or p110) (Ghetti *et al*., 1995; Raghunathan and Guthrie, 1998; Achsel *et al*., 1999; Bell *et al*., 2002). Subsequently, the U4/U6·U5 tri-snRNP assembles when U5 snRNP associates by protein–protein interactions with the U4/U6 snRNP (Makarova *et al*., 2002; Schaffert *et al*., 2004). Both U4/U6 and U4/U6·U5 tri-snRNP assembly occur in CBs (Schaffert *et al*., 2004; Stanek and Neugebauer, 2004). Recently, mathematical modeling of U4/U6 snRNP formation in the cell nucleus revealed that accumulation of U4 and U6 snRNPs in CBs should greatly increase the efficiency of U4/U6 assembly (Klingauf *et al*., 2006). An additional role of CBs in U2 snRNP formation (Nesic *et al*., 2004) further points to CBs as the key site of nuclear steps in snRNP assembly. The observation that depletion of coilin, a protein required for snRNP concen-

This article was published online ahead of print in *MBC in Press* (http://www.molbiolcell.org/cgi/doi/10.1091/mbc.E07–12–1259) on March 26, 2008.

Address correspondence to: David Staněk (stanek@img.cas.cz).

Abbreviations used: CB, Cajal body; snRNA, small nuclear RNA; snRNP, small nuclear ribonucleoprotein particle.

tration in CBs, impairs cell proliferation (Lemm *et al*., 2006) is consistent with the proposal that snRNP assembly is inefficient in the absence of CBs.

snRNPs must not only assemble de novo but also may regenerate after splicing to complete the so-called spliceosome cycle. During spliceosome assembly and activation, snRNPs undergo structural rearrangements, including U4/U6 snRNA unwinding and release of the U4 snRNP from the spliceosome (Staley and Guthrie, 1998). After splicing, mRNA is released from the spliceosome by the DEAH-box helicase hPrp22/HRH1 and snRNPs remain associated with the excised intron lariat (Company *et al*., 1991; Ohno and Shimura, 1996). In *Saccharomyces cerevisiae*, a complex of three proteins (Prp43/Ntr1/Ntr2) was shown to be essential for release of individual snRNPs from the lariat (Arenas and Abelson, 1997; Martin *et al*., 2002; Tsai *et al*., 2005; Boon *et al*., 2006; Tanaka *et al*., 2007; Tsai *et al*., 2007). If these released snRNPs are to participate in subsequent rounds of splicing, they have to be reassembled into the active U4/U6·U5 tri-snRNP. Several studies provide genetic and biochemical evidence for snRNP reassembly (Raghunathan and Guthrie, 1998; Bell *et al*., 2002; Verdone *et al*., 2004; Chen *et al*., 2006). Although snRNPs are highly expressed, the long half-lives of snRNAs suggests that they likely recycle and function again (Yu *et al*., 1999).

In the present study, we address the hypothesis that snRNPs cycle more than once through CBs. We show in living cells that CBs contain mostly mature snRNPs, which are capable of exchanging with nucleoplasm and visiting multiple CBs. Targeted knockdown of proteins involved in spliceosome recycling, hPrp22, and the human homologue of the recently identified yeast Ntr1, led to a dramatic accumulation of the U4/U6 snRNP in CBs. These data demonstrate that the CB is a vital way station in the spliceosomal cycle.

MATERIALS AND METHODS

Cells and Antibodies

HeLa cells were cultured in DMEM supplemented with 10% fetal calf serum, penicillin, and streptomycin (Invitrogen, Carlsbad, CA). To create a stable HeLa cell line expressing human Prp8 tagged with green fluorescent protein (GFP) at the C terminus and expressed under the control of its own promoter, a bacterial artificial chromosome (BAC) harboring the human Prp8 gene was obtained from the BACPAC Resources Center (http://bacpac.chori.org). Neo/Kanr-dsRed and EGFP-IRES-Neo cassettes were polymerase chain reaction (PCR) amplified with primers carrying 50 nucleotides of homology to the targeting sequence. Recombineering of the BACs was performed as described previously (Zhang *et al*., 2000) (Gene Bridges, Dresden, Germany); and after transduction, neo-resistant cells were sorted by fluorescence-activated cell sorting (FACS) to obtain single colonies. Immunoprecipitation using anti-GFP antibodies showed that hPrp8-GFP is properly incorporated into the U5 snRNP and the tri-snRNP (data not shown).

The following antibodies were used: rabbit anti-SART3/p110 antibodies (Stanek *et al*., 2003); monoclonal antibody (mAb) anti-coilin (5P10) (Almeida *et al*., 1998), kindly provided by M. Carmo-Fonseca (Institute of Molecular Medicine, Lisbon, Portugal); rabbit antibodies against LSm4 (Achsel *et al*., 1999); hPrp31 (U4/U6–61K) (Makarova *et al*., 2002); hPrp4 (U4/U6–60K) (Lauber *et al*., 1997); and hSnu114 (U5–116K) (Fabrizio *et al*., 1997), kindly provided by R. Lührmann (Max Planck Institute, Göttingen, Germany). Monoclonal antibodies against U2B′′ and U1-70K were purchased from Progen (Heidelberg, Germany). Rabbit anti-mouse Ntr1 was raised against a peptide, LQNEFNPNRQRHWQ (amino acids 32–45; Zymed Laboratories, South San Francisco, CA), and was provided by Michael Paine (University of Southern California, Los Angeles, CA).

Protein Tagging

SART3-cyan fluorescent protein (CFP), coilin-CFP, and hPrp31-CFP were described previously (Stanek and Neugebauer, 2004). SMN-yellow fluorescent protein (YFP) was kindly provided by M. Dundr (Chicago Medical School, North Chicago, IL; Dundr *et al*., 2004) and SmB-YFP and SmD1-GFP by A. Lamond (University of Dundee, United Kingdom; Sleeman and Lamond, 1999). SmB was subcloned into ECFP-C1 (Clontech, Mountain View, CA), photoactivatable (PA)-GFP-C1 (Patterson and Lippincott-Schwartz, 2004) and E5-red fluorescent protein (RFP)-C1 by using HindIII/KpnI sites. SmD1 was recloned into ECFP-C1, PA-GFP-C1, and E5-RFP-C1 by using BamHI/PstI sites. E5-RFP-C1 vector was created by replacing GFP sequence in GFP-C1 plasmid (Clontech) with E5-RFP sequence from pTimer-1 plasmid (Clontech) by using AgeI/BglII restriction sites. SART3-HcDiRed construct was created by cloning SART3 sequence into the HcDiRed-N1 vector, which originated from the H2B-HcDiRed-N1 plasmid obtained from J. Ellenberg (European Molecular Biology Laboratory, Heidelberg, Germany; Gerlich *et al*., 2003).

Live Cell Imaging

Cells were plated on glass bottomed Petri dishes (MatTek, Ashland, MA), and after 20–24 h, they were transfected with appropriate DNA constructs by using FuGENE 6 (Roche Diagnostics, Mannheim, Germany). The cells were imaged 22–24 h after transfection by using either a Zeiss 510 microscope equipped with water immersion objective (63× 1.2 numerical aperture [NA]) or a Leica SP2 confocal microscope equipped with water immersion objective (63× 1.2 NA) and an environmental chamber controlling CO_2 level and temperature. PA-GFP was activated by short pulses of 405-nm laser line, and images of activated PA-GFP (excitation with 488-nm laser line) and either CFP (excitation with 458-nm laser line) or HcDiRed (excitation with 594-nm laser line) were acquired at 15-s intervals in activation of one CB or every 2 min in activation of the whole nucleus. The raw images were analyzed using ImageJ software (http://rsb.info.nih.gov/ij/). For publication, fluorescent levels were linearly adjusted using Adobe Photoshop (Adobe Systems, Mountain View, CA).

For E5-RFP experiments, cells were transfected with SmB-E5-RFP or SmD1-E5-RFP, fixed at different times after transfection with 4% paraformaldehyde/piperazine-*N*,*N*′-bis(2-ethanesulfonic acid) (PIPES) and embedded in glycerol containing 4′,6-diamidino-2-phenylindole and 2.5% 1,4-diazabicyclo[2.2.2]octane (DABCO; Sigma Chemie, Deisenhofen, Germany) as an anti-fade reagent. Alternatively, cells were treated for 2 h before fixation with 30 ng/ml leptomycin B (LC Laboratories Woburn, MA). Images were collected using the DeltaVision microscope system (Applied Precision, Issaquah, WA) coupled with Olympus IX70 microscope equipped with oil immersion objective (60× 1.4 NA) by using the same settings for each sample. Stacks of 25 z-sections with 200-nm z-step were collected per sample and subjected to mathematical deconvolution by using measured point spread function (SoftWorx; Applied Precision). Mean intensities in green and red channel were quantified using SoftWorx.

Fluorescence Resonance Energy Transfer (FRET) Measurement

Cells were transfected with fluorescent protein-tagged constructs using FuGENE 6, grown for 24–26 h, and fixed in 4% paraformaldehyde/PIPES (Sigma-Aldrich) for 10 min at room temperature. After rinsing with Mg-phosphate-buffered saline (PBS) (PBS supplemented with 10 mM Mg^{2+}) and water, cells were embedded in glycerol containing DABCO. FRET was measured by acceptor photobleaching method as described previously (Stanek and Neugebauer, 2004) by using the Leica SP2 confocal microscope. Intensities of CFP (excited by 405-nm laser set to 5–10% of maximum power) and YFP (excited by 514-nm laser line set to 2% of maximum power) were measured. Then, YFP was bleached in a region of interest by three to five intensive (30% maximum power) pulses of 514-nm laser line and CFP and YFP fluorescence measured again. Apparent FRET efficiency calculated according to the equation $FRET_{efficiency}[\%] = (CFP_{after} - CFP_{before}) \times 100/CFP_{after}$. Unbleached regions of the same cell were used as a negative control. Ten cells were measured per each FRET pair, and average and SE were calculated.

Small Interfering RNA (siRNA) Transfection

Preannealed siRNA duplexes were obtained either from Ambion (Austin, TX) or QIAGEN (Hilden, Germany). Three independent siRNA duplexes were used against hNtr1, and five duplexes were used to target hPrp22. The sequences of sense siRNAs were as follows: from Ambion: hNtr1-27-5′-CCUGUUAAGCAGGACGACUtt, hNtr1-28-5′-GCAGGACGACUUUCCUAAGtt, hNtr1-29-5′-GGAUUAGCAAGAAGCUCACtt; hPrp22-55-5′-GCUUUAAUGCCCAGCGCAGtt; hPrp22-56-5′-GGAAUAAAGUGAAGUCUAGtt; and hPrp22-57-5′-CCCAAAUAGACGGCGAAAUtt; from Qiagen: hPrp22-3-5′-GGGACAGGACAAAGAAGAAtt and hPrp22-4-5′-CAGAGAAGUGGGAGAUCAAtt.

The negative control 1 siRNA from Ambion was used as a negative control. Oligofectamine (Invitrogen) was used for siRNA transfection. Cells were incubated 48 h before further treatment. Within this incubation period we did not observe any extensive cell death with respect to the treatment with the negative control siRNA.

Reverse Transcription (RT)-PCR

Total RNA was isolated 48 h after siRNA transfection by using TRIzol reagent (Invitrogen). cDNA was synthesized using a gene-specific reverse primer and SuperScript III (Invitrogen). Taq polymerase was used to amplify cDNA (25

cycles). Controls without RT reaction were performed to verify that there was no residual DNA contamination. The following primers were used for RT-PCR and quantitative PCR: hPrp22-For, CAAGAGGTGGGCTACACCAT; hPrp22-Rev, 5′-TGATCGCGTACTGAGTGAGG; hNtr1-For, 5′-TGTCTTCACTCCTG-GCTCCT; hNtr1-Rev, 5′-AAGCCACTTGGGGAAGAAGT; 18S-For, 5′-TTGTT-GGTTTTCGGAACTGAG; 18S-Rev, 5′-GCAAATGCTTCGGCTCTGGTC; c-myc-mRNA-For, 5′-GCGACTCTGAGGAGGAACAAGAAG; c-myc-mRNA-Rev, 5′-ACTCTGACCTTTTGCCAGGAGC; c-myc-pre-mRNA-For, 5′-TGCTCCCT-TTATTCCCCCAC; c-myc-pre-mRNA-Rev, 5′-GGTCATAGTTCCTGTTGGT-GAAGC; LDHA mRNA-For, 5′-AGAACACCAAAGATTGTCTCTGGC; LDHA mRNA-Rev, 5′-TTTCCCCCATCAGGTAACGG; LDHA pre-mRNA-For, 5′-CCTTTCAACTCTCTTTTGGCAACC; LDHA pre-mRNA-Rev, 5′-AATCTTAT-TCTGGGGGGTCTGTTC; Tubulin mRNA-For, 5′-GCTGCTTTGTGGAGTG-GATTCC; Tubulin mRNA-Rev, 5′-CCGTGTTGTTGCCAATGAAGG; Tubulin pre-mRNA-For, 5′-GACCTTCCTCCTGCTTTCAGTTC; and Tubulin pre-mRNA-Rev, 5′-TCTGCTTGTGTTCCCAGTTGC.

Quantitative PCR was done as described previously (Listerman *et al*., 2006), and ratio of pre-mRNA to mRNA was calculated for each siRNA treatment according to $R_{siRNA} = 2^{(Ctpre\text{-}mRNA - CtmRNA)}$, normalized to NC siRNA treated cells ($R_n = R_{siRNA}/R_{ncsiRNA}$), and plotted.

Glycerol Gradient Ultracentrifugation

Nuclear extracts were prepared according to Dignam *et al*. (1983), diluted in gradient buffer (20 mM HEPES/KOH, pH 8.0, 150 mM NaCl, 1.5 mM $MgCl_2$, and 0.5 mM dithiothreitol), and fractionated in a linear 10–30% glycerol gradient by centrifugation at 32,000 rpm for 17 h by using the SW-41 rotor (Beckman Coulter, Fullerton, CA). Individual fractions (700 μl) were collected, and RNA was extracted from each fraction with phenol:chloroform: isoamylalcohol, separated on 10% urea-polyacrylamide gel electrophoresis (PAGE), and silver stained. In parallel, proteins were precipitated from the phenol phase by acetone, dissolved in SDS-PAGE sample buffer, and analyzed by immunoblotting.

Indirect Immunofluorescence

Forty-eight hours after the siRNA transfection the cells were fixed in 4% paraformaldehyde/PIPES for 10 min, permeabilized for 5 min with 0.2% Triton X-100 (Sigma Chemie), and incubated with appropriate primary antibodies. Secondary anti-rabbit antibodies conjugated with fluorescein isothiocyanate (FITC) and anti-mouse antibodies conjugated with tetramethylrhodamine B isothiocyanate (TRITC) (Jackson ImmunoResearch Laboratories, West Grove, PA) were used. Images were collected using a DeltaVision microscope system and subjected to mathematical deconvolution as described above. Mean fluorescence intensities in CBs and the nucleoplasm were determined in individual optical sections by using ImageJ as described previously (Stanek and Neugebauer, 2004).

In Situ Hybridization

Digoxigenin-labeled DNA probes directed against human U2, U4, and U5 snRNAs were obtained by PCR as described previously (Bell *et al*., 2002) by using pSP65U2H, pSPU4b, pSP64U5 (Black and Pinto, 1989) as templates. Forty-eight hours after siRNA transfection cells were fixed in 4% paraformaldehyde/PIPES for 10 min, permeabilized with 0.5% Triton X-100 for 5 min, and incubated with anti-SART3 antibodies as a marker of CBs followed by incubation with secondary antibody conjugated with FITC (Jackson ImmunoResearch Laboratories). Cells were again fixed in 4% paraformaldehyde/PIPES for 5 min, quenched for 5 min in 0.1 M glycine/0.2 M Tris, pH 7.4, and incubated with digoxigenin-labeled probe in 2× SSC/50% formamide/10% dextran sulfate/1% BSA for 60 min at 37°C. After washing in 2× SSC/50% formamide, 2× SSC and 1× SSC, the probe was detected by mouse anti-digoxigenin antibody (Roche Diagnostics) followed by incubation with goat anti-mouse antibody coupled with TRITC (Jackson ImmunoResearch Laboratories). Images were collected using a DeltaVision microscope system, and fluorescence intensities in CBs and the nucleoplasm were determined as describe above.

RESULTS

Accumulation of Mature snRNPs in Cajal Bodies

It is not known whether the pool of snRNPs in CBs consists of only newly imported and incompletely assembled snRNPs, or whether mature snRNPs that have already participated in splicing accumulate in CBs as well. We probed the relative "age" of snRNPs in CBs, by tagging SmB and SmD1 proteins with a "fluorescent timer," a mutant of red fluorescent protein drFP583 (E5-RFP) that changes its fluorescence emission properties during maturation, converting from green-to-red emission within the course of 3 h (Terskikh *et al*., 2000). Changes in the red-to-green ratio over time are therefore indicative of relative shifts in the age of the molecules present in a given subcellular location. Because there is no evidence of Sm protein exchange once the Sm ring has been assembled on snRNA (Wang and Meier, 2004; Shpargel and Matera, 2005), we assume that Sm proteins remain stably associated with nuclear snRNPs after assembly and import; thus, Sm protein dynamics likely reflect those of mature snRNPs. In addition, fluorescently tagged Sm proteins efficiently incorporate into snRNP particles, and their expression is comparable with endogenous Sm proteins (Supplemental Figure 1). HeLa cells expressing SmB- or SmD1-E5-RFP were fixed at different times after transfection, and E5-RFP fluorescence intensities in the green and red spectra were measured (Figure 1A). Note that both Sm-E5-RFP constructs localized properly in CBs. Surprisingly, both green and red forms of E5-RFP were clearly present in CBs at the earliest time point (11 h) that CBs were detectable, indicating that a portion of E5-RFP had already matured to the red form before fluorescence reached the detection threshold. Absolute intensities of green fluorescence did not change over the time, indicating a constant influx of new snRNPs that must reside for a consistent

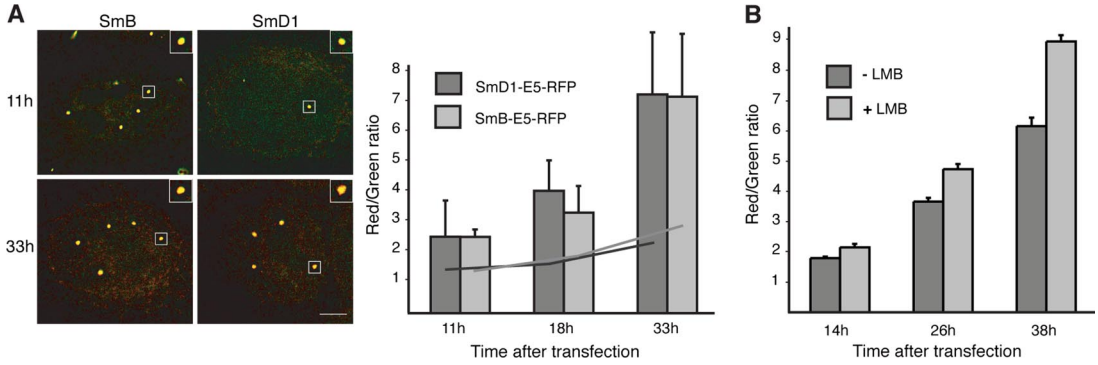

Figure 1. Mature snRNPs accumulate in Cajal bodies. To determine the age of snRNPs in CBs, SmB and SmD1 proteins that are stable components of snRNPs were tagged with E5-RFP. During maturation, E5-RFP changes its fluorescence from green to red in a time course of a couple hours. (A) HeLa cells were transfected with SmB-E5-RFP or SmD1-E5-RFP and fixed at different times after transfection. Ratio of red to green was measured in CBs (bars are SD) and in the nucleoplasm (lines). Red fluorescence in CBs increased ~3 times over 22 h, indicating that mature snRNPs accumulate in CBs. (B) Cells were transiently transfected with SmB-E5-RFP, and 2 h before fixation they were treated with leptomycin B (LMB) that inhibits biogenesis of new snRNPs by blocking export of new snRNA from the nucleus. A 45% increase of red-to-green ratio after 38 h indicates import inhibition of the green (new) variant of SmB-E5-RFP. Bars are SE.

period in the CB. An increase in red fluorescence and the red-to-green fluorescence ratio was observed, and over the period of 22 h it increased ~2 times in the nucleoplasm and 3 times in CBs. If CBs selectively recruited only newly imported snRNPs, we would have expected the red-to-green ratio to remain the same or even decrease in CBs, despite the fact that more of the red variant accumulates in the nucleus.

To test whether Sm-E5-RFP proteins are imported to the cell nucleus within snRNP particles, cells were treated for 2 h before fixation with leptomycin B that efficiently inhibits export of newly synthesized snRNAs to the cytoplasm and consequently also import of newly formed snRNPs. A 45% increase in the red-to-green ratio observed 38 h after transfection (Figure 1B) indicates impairment of green SmB-E5-RFP import, indicating that SmB-E5-RFP is indeed imported together with snRNAs beginning the biogenesis pathway in the cytoplasm. The finding that CBs accumulate more old snRNPs in CBs compared with the nucleoplasm indicates that the pool of snRNPs concentrated in CB contains not only fresh snRNPs but also relatively older, presumably mature snRNPs.

A complementary experiment was suggested by the fact that, although they are highly concentrated in CBs, snRNPs exchange rapidly with the surrounding nucleoplasm and only reside in CBs for few seconds on average (Dundr *et al.*, 2004; Sleeman, 2007). We tagged Sm proteins with PA-GFP to determine whether the snRNPs that exit CBs at any given moment are replaced by new or old snRNPs. SmB- or SmD1-PA-GFP was expressed and the entire nucleus was photoactivated (Figure 2). If CBs contain exclusively new (nonactivated) snRNPs imported from the cytoplasm, fluorescence would be lost from these CBs over time. On the contrary, SmB-GFP fluorescence CBs remained high 20 min after photoactivation (Figure 2), 100 times longer than the residence time of snRNPs in CBs. Measurement of fluorescence intensities in CBs and nucleoplasm revealed a 0–25% decrease (average 6%) in fluorescence intensity in CBs relative to nucleoplasm. These data show that the exchanging population of snRNPs in CBs consists largely of "older" nuclear snRNPs.

To further examine the assembly status of snRNPs in CBs and in the cytoplasm, we probed snRNP interactions with the SMN protein, which is localized both in the cytoplasm and in CBs. The SMN protein is a part of the SMN complex,

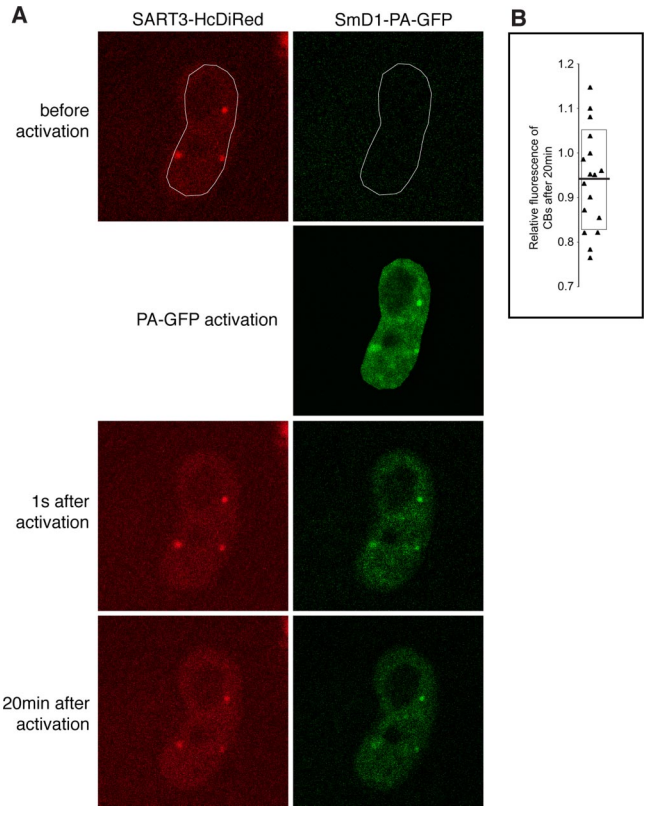

Figure 2. snRNPs newly imported from the cytoplasm represent only a minor fraction in CBs. (A) The SmD1 protein was tagged with PA-GFP and coexpressed in HeLa cells with SART3-HcDiRed as a marker of CBs. To distinguish between nuclear and cytoplasmic pool of snRNPs, nuclear snRNPs were specifically activated by short pulse of 405-nm laser line. Images were taken every 2 min for total 20 min. (B) Quantification of CB fluorescence. To avoid photobleaching effects, the ratio of fluorescent signals CB:nucleoplasm were determined immediately after activation and 20 min later. Values for individual CBs are plotted. Mean value is indicated by a solid line SD by a box. A small decrease in CB fluorescence indicates that within 20 min, snRNPs imported from the cytoplasm represent only small fraction of snRNPs in CBs.

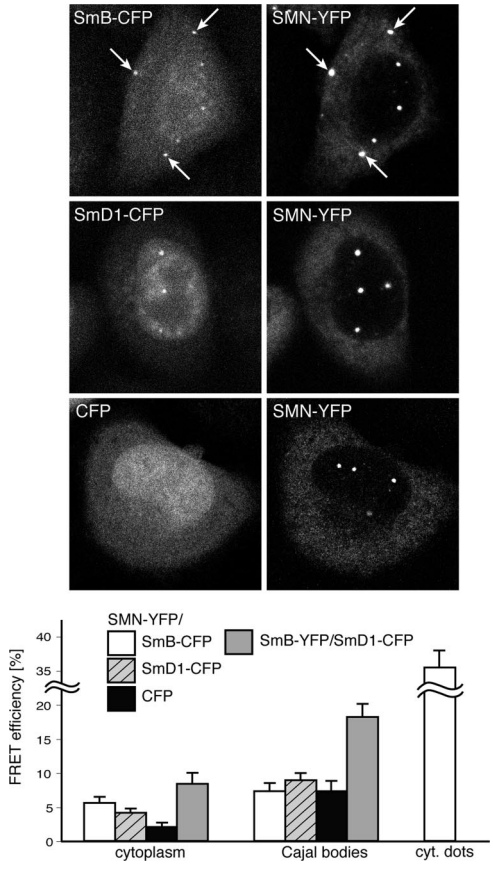

Figure 3. The SMN protein interacts with Sm proteins in the cytoplasm. To compare SMN–snRNP complexes in CBs and the cytoplasm, SMN-YFP was coexpressed with SmD1-CFP, SmB-CFP, or CFP alone as a negative control, and FRET was measured in the cytoplasm and in CBs by acceptor photobleaching method. The SMN-Sm FRET signal was two- to threefold higher over negative control in the cytoplasm but not in CBs. The SmB–SmD1 pair used as a positive control exhibited high FRET signal both in the cytoplasm and in CBs. In some cells, we observed cytoplasmic accumulation of SmB and SMN proteins (arrows) and high FRET signal was measured in these cytoplasmic inclusions. Ten measurements for each pair are averaged and are shown in the graph with SE bars.

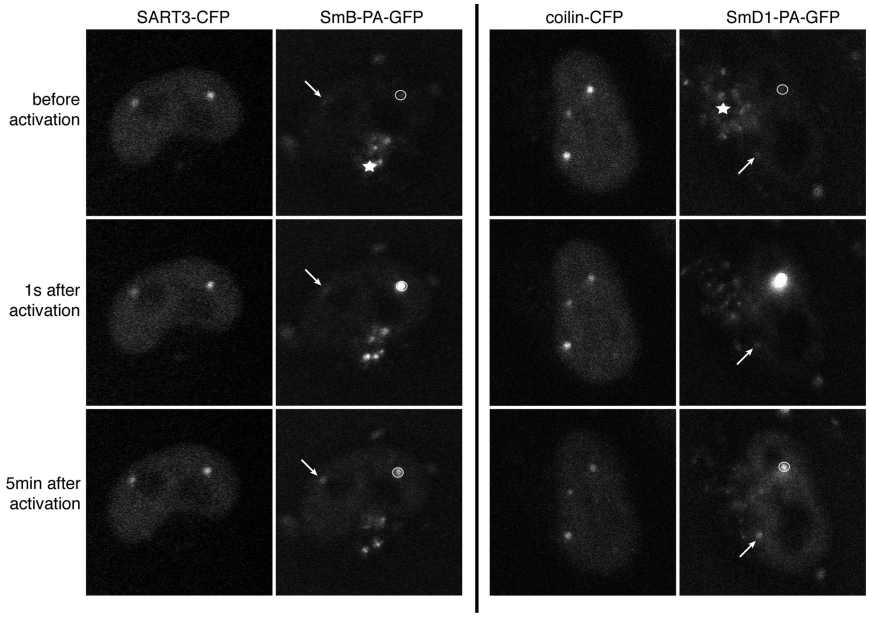

Figure 4. snRNPs cycle between CBs. To observe movement of snRNPs between CBs and the nucleoplasm, SmB-PA-GFP was coexpressed with SART3-CFP and SmD1-PA-GFP with coilin-CFP. Sm-PA-GFPs were specifically activated in one CB (circle) by short pulse of 405-nm laser, and movement of activated molecules was observed for 5 min (also see Supplemental Videos). Activated molecules moved throughout the whole nucleoplasm and accumulated in other CBs in the same nucleus (arrows). The detection system was adjusted to detect very low signals of PA-GFP, but by using this setup we also detected cell autofluorescence in the cytoplasm (stars).

which ensures proper assembly of Sm rings on snRNPs in the cytoplasm (Terns and Terns, 2001; Meister *et al*., 2002; Paushkin *et al*., 2002; Matera and Shpargel, 2006). The significance of SMN accumulation in CBs is not known. Because SMN is required for the import of newly assembled snRNPs (Narayanan *et al*., 2002, 2004), it is hypothesized that SMN is coimported into CBs with new snRNPs (Matera and Shpargel, 2006). Interactions between snRNPs and the SMN protein were measured by FRET. Because Sm proteins and SMN are present in the cytoplasm and in CBs, a FRET signal could indicate the presence of snRNP–SMN complexes, changes in their structure and composition in the different cellular compartments, or both. SmD1-CFP or SmB-CFP were coexpressed with SMN-YFP in HeLa cells, and FRET was measured by the acceptor photobleaching method in the cytoplasm and CBs of the same cell (Figure 3). As a negative control, SMN-YFP was coexpressed with CFP only. As expected, FRET between SMN and the Sm proteins was detected in the cytoplasm, but no FRET signal above the negative control was observed in CBs. Overall higher FRET values in CBs are likely caused by local accumulation of SMN. In some cells, Sm proteins and SMN accumulated in cytoplasmic bodies, presumably due to coexpression of exogenous SMN and Sm proteins (Shpargel *et al*., 2003); these aggregates resembled recently identified U bodies (Liu and Gall, 2007) and contained similar amounts of fluorescent proteins as nuclear CBs. High FRET signals detected in these cytoplasmic inclusions indicate accumulation of SmB–SMN complexes. In addition, FRET between SmB-YFP and SmD1-CFP were robust in the cytoplasm as well as in CBs. Preassembled Sm subcomplexes are used during assembly of the Sm-ring; SmB and SmD1 proteins are not part of the same Sm subcomplexes, but they lay next to each other in the ring (Raker *et al*., 1996; Kambach *et al*., 1999). Thus, detection of FRET between these two components represents a good marker for Sm-ring assembly and further indicates that fluorescently tagged Sm proteins are correctly incorporated into mature snRNPs. These results show that snRNPs in CBs differ from snRNPs localized in the cytoplasm; snRNPs in CBs either do not interact with SMN or snRNP-SMN com-

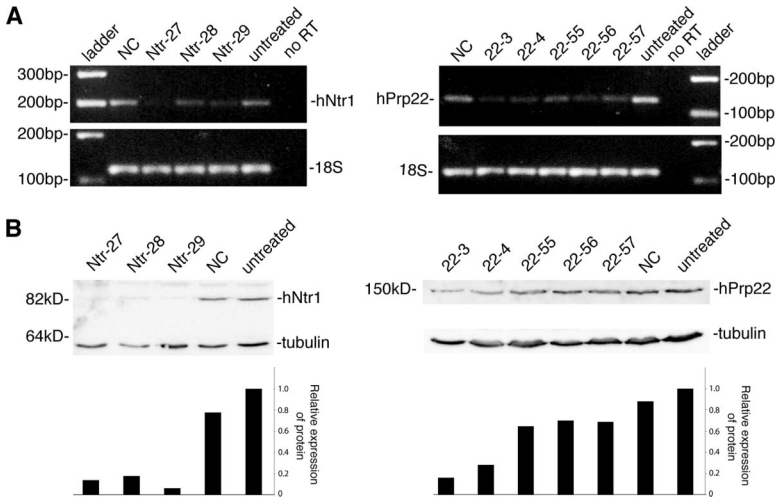

Figure 5. siRNA targeted depletion of hPrp22 and hNtr1. (A) Five different siRNAs against hPrp22 and three against hNtr1 protein were used. Cells were treated with siRNAs for 48 h, and mRNA levels of hPrp22 and hNtr1 were determined by RT-PCR. RT-PCR of 18S rRNA served as a loading control. (B) Extract from cells treated for 48 h with siRNAs was loaded on gel, and hNtr1 and hPrp22 protein levels were determined. Anti-tubulin antibody used as a loading control.

plexes in CBs have an altered structure that does not support FRET detection.

Cycling of snRNPs between CBs

Because Sm proteins exchange rapidly between CBs and the nucleoplasm (Dundr *et al*., 2004; Sleeman, 2007), our finding that CBs contain predominantly mature snRNPs implies that snRNPs cycle constantly between CBs and the nucleoplasm, visiting CBs repeatedly. To test this directly, SmD1 or SmB proteins tagged with PA-GFP were coexpressed with CFP-tagged markers of CBs (SART3, coilin). The Sm-PA-GFP proteins were activated by a short pulse of 405 nm laser in one CB and the movement of activated molecules monitored every 15 s over a 5-min time period (Figure 4, Supplemental Videos). Activated SmB- and SmD1-PA-GFP proteins moved from the activated CB, diffused throughout the nucleoplasm and accumulated in another (nonactivated) CB within the time course of the experiment. This behavior was not affected by coexpression of any of the CB markers used and no movement of activated molecules was observed in fixed cells (Supplemental Figure 2). These data show directly that snRNPs repeatedly visit CBs.

Accumulation of U4/U6 snRNPs in CBs after Inhibition of Spliceosome Disassembly

Previous reports showed that ongoing snRNP biogenesis is necessary for structural integrity of CBs (Shpargel and Matera, 2005; Girard *et al*., 2006; Lemm *et al*., 2006). However, our data show that the CB contains mainly mature snRNPs. We therefore aimed to test whether an ongoing supply of mature snRNPs is important for maintaining the CB structure as well. Two proteins implicated in spliceosome disassembly were depleted, with the expectation that inhibition of snRNP recycling after splicing would reduce the supply of mature snRNPs. Three different siRNA duplexes were used to target the human homologue of Ntr1 (also named TFIP11; Wen *et al*., 2005) and five duplexes for hPrp22. After 48 h, total RNA and proteins were isolated and mRNA and protein levels tested (Figure 5).

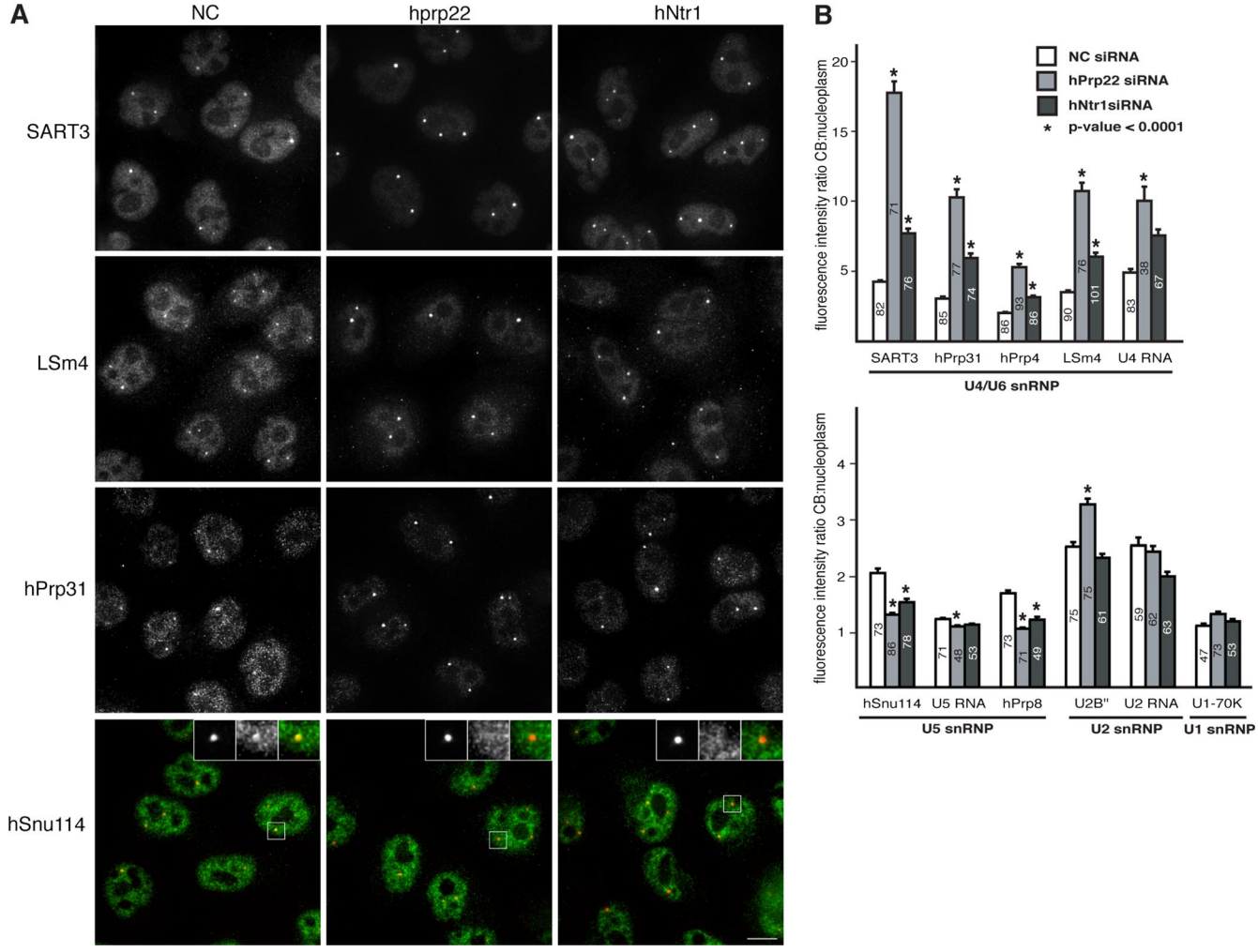

Figure 6. U4/U6-specific markers accumulate in CBs after hPrp22 and hNtr1 knockdown. (A) Cells treated with siRNA against hPrp22 (22–3) and hNtr1 (Ntr-27) for 48 h were fixed, and localization of snRNP-specific proteins was determined by antibody staining. To avoid distortion of CB morphology due to changes in intensity, the intensities of the images shown were adjusted to an equal maximum. This results in apparent fluorescent reduction in the nucleoplasm after siRNA treatments, which was not observed at raw images. NC, negative control siRNA. hSnu114, green; coilin, red. (B) Quantification of fluorescence is shown in the graph. Fluorescence ratio CB:nucleoplasm was calculated for each CB, and average with SE bars is shown (number of measured CBs indicated inside bars). *$p < 0.0001$ as determined by Student's *t* test with respect to cells treated with control siRNA.

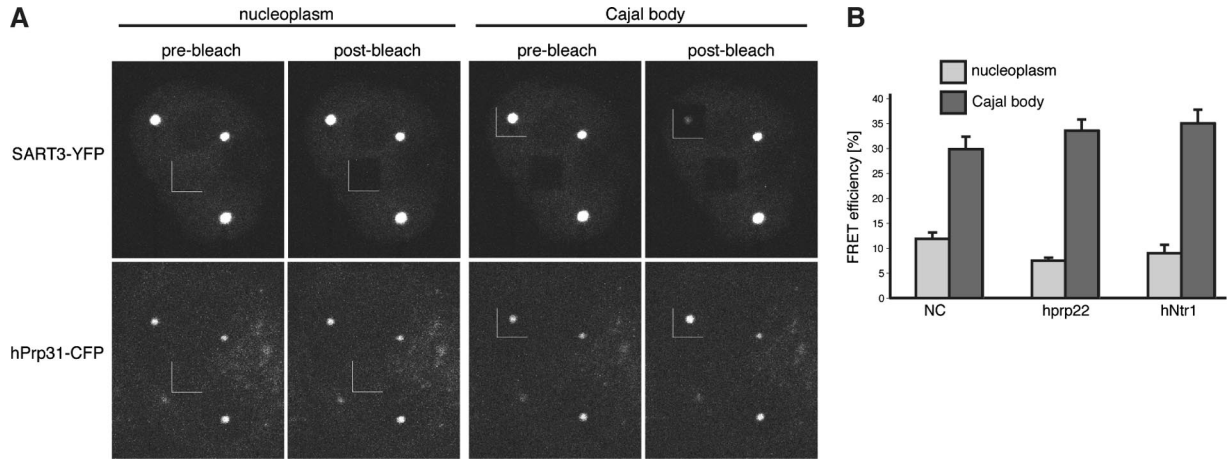

Figure 7. Assembled U4/U6 snRNP accumulates in Cajal bodies after hPrp22 and hNtr1 knockdown. (A) Cells treated with siRNA against hPrp22 (22-3) were transfected with SART3-YFP and hPrp31-CFP, and FRET was measured by acceptor photobleaching in the nucleoplasm and CBs. (B) Quantification of SART3-YFP/hPrp31-CFP FRET measurements in cells treated with control (NC), hPrp22-3, or hNtr1-27 siRNAs. Average values of 10 measurements with SE bars are shown.

To address the effects of hNtr1 and hPrp22 knockdown on CB structure, CBs were immunodetected after the siRNA treatment with anti-coilin and anti-SART3 antibodies. Coilin is a universal marker of CBs; SART3 interacts with the U4/U6 snRNP and its presence in the CB is sensitive to transcription/splicing inhibition (Stanek *et al*., 2003). Surprisingly, CBs remained intact and accumulated SART3 after either treatment (Figure 6A; data not shown). In fact, the detection of SART3 fluorescent signal in CBs was enhanced by treatment, and an elevated accumulation in CBs of other U4/U6 snRNP components was also observed upon depletion of hPrp22 or hNtr1 (Figure 6B). The CB accumulation of U4/U6-specific markers was not due to a decrease in nucleoplasmic fluorescence, which remained mostly unaffected by the siRNA treatment. Partial effects on the U2-specific U2B″ protein were observed after hPrp22 but not hNtr1 knockdown, and no significant changes in CB localization of the U2 snRNA or the U1-specific U1–70K protein were detected. In contrast, CB localization of the three tested U5 snRNP components—hSnu114, hPrp8-GFP, and the U5 snRNA—decreased after siRNA treatment. The hPrp8-GFP protein was expressed from a human BAC under the control of the endogenous promoter and was properly incorporated into the U5 and tri-snRNPs (data not shown).

Depletion of hPrp22 or hNtr1 caused the dramatic and specific accumulation of U4/U6 snRNP components in CBs. To determine whether bona fide U4/U6 snRNP particles had formed in CBs, we used FRET to measure interactions that are specific for the SART3·U4/U6 complex, a transient intermediate en route to tri-snRNP formation that was previously localized to CBs (Stanek and Neugebauer, 2004). Cells were incubated for 24h with the indicated siRNA, cotransfected with hPrp31-CFP and SART3-YFP, incubated additional 24 h and fixed. FRET was measured as described previously in the nucleoplasm and CBs by acceptor photobleaching (Stanek and Neugebauer, 2004). No significant changes were observed in CBs after treatment with anti-hPrp22 or anti-hNtr1 siRNAs (Figure 7), showing that U4/U6 components accumulating in CBs are assembled into the U4/U6 snRNP. These data indicate that inhibition of spliceosome recycling leads to specific accumulation of the U4/U6 snRNPs in CBs. To test whether U4/U6 snRNP accumulation in CBs resulted from an inhibition of splicing, three different genes (c-myc, LDHA, and tubulin) were tested for splicing efficiency by RT-quantitative PCR. Partial increases in pre-mRNA-to-mRNA ratios were detected after treatment with anti-hPrp22 siRNAs, but no substantial inhibition of splicing was observed after hNtr1 depletion (Supplemental Figure 3) indicating that U4/U6 snRNP concentration in CBs is not likely a general result of splicing inhibition and a lack of expression of necessary snRNP components.

Enhanced accumulation of the U4/U6 snRNPs in CBs had been previously observed after inhibition of U4/U6·U5 snRNP assembly (Schaffert *et al*., 2004). If depletion of hNtr1 and hPrp22 inhibits spliceosome recycling and thus reduces the amount of the free U5 snRNP, assembly of the functional tri-snRNP might be delayed. To assess the influence of hPrp22 or hNtr1 knockdown on snRNP assembly and recycling, nuclear extract was prepared from cells treated for 48 h with anti-hPrp22–3 or anti-hNtr1–27 siRNAs and snRNPs analyzed by glycerol gradient ultracentrifugation. RNA and proteins were isolated from individual fractions and U5-specific hSnu114 and U4/U6-associated hPrp4 proteins detected by immunoblotting (Figure 8). To determine the position of individual snRNP complexes in the gradient snRNAs from each fraction were resolved on denaturing gels and silver stained (data not shown). hPrp4 sedimented in two distinct peaks that reflect U4/U6 snRNPs (fractions 6–8) and U4/U6·U5 tri-snRNPs (fractions 11–13). The U5 marker hSnu114 fractionated with the tri-snRNP and with the mono-U5 snRNP (fractions 8–10). In addition to the mono-U5 and the tri-snRNP, hSnu114 accumulated in faster sedimenting complexes (fractions 15 and 16) in anti-hPrp22 siRNA treated cells, which might correspond to post-spliceosomal complexes (Makarov *et al*., 2002) that were not recycled properly after hPrp22 knockdown. Importantly, decreases in the mono-U5 snRNP relative to the U5 in the tri-snRNP fractions were observed in both hPrp22 and hNtr1 siRNA-treated cells, consistent with the reduced U5 snRNP concentration in CBs after both knockdowns (Figure 6).

DISCUSSION

It was previously shown that U2, U4/U6, and U4/U6·U5 tri-snRNP assembly steps occur in CBs (Nesic *et al*., 2004; Schaffert *et al*., 2004; Stanek and Neugebauer, 2004); how-

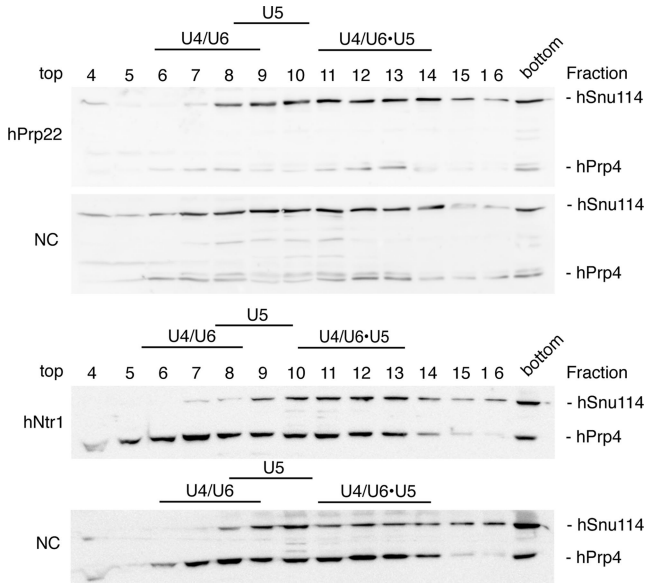

Figure 8. Mono-U5 snRNP is reduced after hPrp22 and hNtr1 knockdowns. HeLa cells were treated with 22-3 or Ntr-27 siRNA for 48 h, and nuclear extracts were centrifuged on 10–30% glycerol gradients. Parallel RNA gels were used for determination of snRNP complexes position in gradients. Proteins from individual fractions were isolated, and hSnu114 (marker of the U5 snRNP) and hPrp4 (marker of the U4/U6 snRNP) were detected. In siRNA-treated cells, the level of the free U5 snRNP decreased (fractions 8–10).

ever, it was not known whether the assembly events reflected de novo snRNP assembly or reassembly after splicing. In this study, we present data showing that in addition to de novo snRNP assembly, CBs could serve as the snRNP recycling center. These conclusions are based on three independent lines of evidence. First, we show by several experimental means, that the snRNPs concentrated in CBs include a substantial "mature" snRNP pool. Second, we show directly that snRNPs visit multiple CBs within the same nucleus and do so frequently; thus, there is no reason to suspect that CBs preferentially contain newly imported snRNPs. Third, targeted depletion of two factors required for spliceosome disassembly and snRNP release, hPrp22 and hNtr1, leads to an accumulation of U4/U6 snRNPs in CBs. We argue below that this accumulation likely reflects a failure of U5 snRNP recovery from spliceosomes; in the absence of sufficient U5 snRNP flux through CBs, tri-snRNP formation is blocked. These observations provide novel insights into how phases of the spliceosome cycle are compartmentalized in living cells.

Experiments establishing the relative maturity of snRNPs in CBs relied on three different fluorescence microscopy techniques. The E5-RFP fluorescent protein tag, which changes emission spectra from green to red as it matures, and PA-GFP were both used to tag Sm proteins (B and D1; see Figures 1 and 2) and to monitor snRNP movements. Both approaches proved that the snRNP pool in CBs largely consists of mature snRNPs that have visited CBs already multiple times. In agreement with these data, snRNP movements between CBs were observed, in which snRNPs photoactivated in one CB reappeared within a time course of minutes in another distant CB. A similar movement of snRNPs between CBs was described recently (Sleeman, 2007).

In the third approach, we sought to compare snRNPs in CBs and in the cytoplasm by measuring FRET signals between Sm proteins and SMN, which plays a role in the cytoplasmic phase of snRNP biogenesis. SMN is coimported with new snRNPs to the nucleus, and it is highly concentrated in CBs; because SMN binds coilin, it has been proposed that SMN delivers the newly imported snRNPs to CBs (Stanek and Neugebauer, 2006). However, although we detected SMN-snRNP interactions in the cytoplasm, we did not observe any significant interaction in CBs. This indicates that either 1) the SMN–snRNP complex falls apart immediately after the import of snRNPs, 2) that a conformational change occurs within the CB that is unfavorable for FRET, or 3) newly imported snRNP–SMN complexes form only a small fraction of snRNPs and SMN in CBs, and these are below the detection limit of the FRET assay. At present, we cannot distinguish among these possibilities; if snRNP–SMN complexes are present in CBs, they must differ at least conformationally from the complexes found in the cytoplasm. Perhaps SMN protein accumulates in the CB as a result of binding coilin after snRNP import and dissociation in the CB. Presumably, SMN eventually returns to the cytoplasm for further rounds of Sm ring assembly.

The conclusion that CBs contain not only new snRNPs imported from the cytoplasm but also mature snRNPs agrees with findings that the concentration of snRNPs in CBs is transcription dependent (Carmo-Fonseca *et al*., 1992; Blencowe *et al*., 1993; Stanek *et al*., 2003); in the absence of new intron-containing transcripts (i.e., under conditions of transcriptional blockade), the splicing process provides fewer "used" snRNPs for recycling. This highlights a paradox emerging in the field, because it has been proposed that snRNP biogenesis and import from the cytoplasm is required for snRNP accumulation in CBs and for integrity of CBs themselves (Carvalho *et al*., 1999; Shpargel and Matera, 2005; Girard *et al*., 2006; Lemm *et al*., 2006). If only a small proportion of snRNPs in CBs are newly imported, how can this fraction be required for CB integrity? The simplest explanation is that experimental reduction of snRNP biogenesis at various stages has long-term effects on the overall concentration of snRNPs in the nucleus, not just an acute effect on import. A reasonable proposal stemming from our present study and consistent with prior work of others is that CB integrity depends on the cellular level of splicing activity and the absolute concentration of nuclear snRNPs (Carmo-Fonseca *et al*., 1992; Blencowe *et al*., 1993; Sleeman *et al*., 2001; Stanek *et al*., 2003).

Our data show that mature snRNPs repeatedly visit CBs. To test whether this cycling through CBs correlates with snRNP regeneration after splicing, proteins involved in spliceosome disassembly were depleted, and localization of distinct snRNPs in CBs was examined. Surprisingly, depletion of two tested proteins involved in spliceosome disassembly resulted in accumulation of U4/U6 snRNPs in CBs. Because transcription/splicing inhibition by α-amanitin leads to opposite effects—the snRNPs and SART3 leave CBs (Carmo-Fonseca *et al*., 1992; Blencowe *et al*., 1993; Sleeman *et al*., 2001; Stanek *et al*., 2003)—it seems unlikely that U4/U6 snRNP accumulates in CBs as a result of splicing inhibition. In addition, splicing of c-fos and c-myc pre-mRNAs was only slightly reduced after siRNA treatment (Supplemental Figure 3). Instead, the phenotype more closely resembles the situation after inhibition of U4/U6·U5 snRNP formation, when accumulation of U4/U6 snRNPs in CBs was also observed (Schaffert *et al*., 2004). Why does inhibition of spliceosome disassembly and inhibition of tri-snRNP assembly have the same phenotype? According to current models of spliceosome recycling, inhibition of this process should trap U5 and U6 snRNPs in the late spliceosome (Will and Luhr-

mann, 2006) and thus decrease levels of free U5 and U6 snRNPs in the nucleoplasm. In contrast, the U4 snRNP leaves the spliceosome at an earlier step, just as the tri-snRNP joins the assembling spliceosome (Makarov *et al*., 2002; Chan *et al*., 2003). Thus, the level of free U4 mono-snRNP in the nucleoplasm should be unaffected by Prp22 or Ntr1 depletion. Early studies showed that there is two- to threefold excess of the U6 snRNP over the U5 and U4 snRNPs (Tycowski *et al*., 2006), making it unlikely that U6 snRNP levels are limiting. In contrast to U4 and U6; however, levels of free U5 snRNP are likely decreased and formation of the U4/U6·U5 tri-snRNP inhibited, as was shown after Ntr1 depletion in yeast (Boon *et al*., 2006). Consistent with this, we observed a decrease in U5 snRNP levels both in CBs and nuclear extracts after knockdown. Thus, inhibition of spliceosome disassembly leads to a similar situation as inhibition of tri-snRNP assembly—accumulation of the U4/U6 snRNPs in CBs. Apparently, the supply of new U5 snRNPs from the cytoplasm is not sufficient to keep up with tri-snRNP assembly, underscoring the importance of the recycled U5 snRNP for assembly and regeneration of tri-snRNPs.

Together, these observations suggest that snRNP reassembly after splicing may obey similar rules to de novo snRNP assembly, even though the assembly of new snRNPs includes additional steps that need not be repeated (e.g., post-transcriptional RNA modification). This implies that snRNP assembly in CBs at any stage of their life cycle must be independent of snRNA posttranscriptional modifications or any other steps in snRNP biogenesis. Finally, it has been shown by mathematical modeling that CBs increase the rate of U4/U6 snRNP assembly, by providing a local environment with elevated snRNP concentrations (Klingauf *et al*., 2006). Thus, the localization of snRNPs to CBs likely promotes the assembly of new as well as regenerating snRNPs by the same mechanism, because snRNPs from either source will meet elevated concentrations of their potential partners in the CB.

ACKNOWLEDGMENTS

We are grateful to Reinhard Lührmann, Marc Schneider (Max Planck Institute, Göttingen, Germany), Maria Carmo-Fonseca, Angus Lamond, Jan Ellenberg, Michael Paine (University of Southern California, Los Angeles, CA), Petr Draber (Institute of Molecular Genetics, Academy of Sciences of the Czech Republic), and Miroslav Dundr for gifts of reagents. We thank Angus Lamond, Jason Swedlow, and Jean Beggs for helpful suggestions and Magdalena Strzelecka, Marta Pabis, and Arnold Kiss for comments on the manuscript. We are grateful to Jason Swedlow, Sam Swift, Jan Peychl, and Ondrej Sebesta for help with live cell imaging and Christian Merz and Reinhard Lührmann for help with the gradient centrifugation. This work was supported by the Max Planck Society and a grant from the DFG (to K.N.), a Partner group grant from the Max Planck Gesellschaft, the Grant Agency of the Czech Republic (301/05/0601), and the institutional project AV0Z50520514 awarded by the Academy of Sciences of the Czech republic (to D.S.). M.B. was supported by the grant GACR 204/07/0133.

REFERENCES

Achsel, T., Brahms, H., Kastner, B., Bachi, A., Wilm, M., and Luhrmann, R. (1999). A doughnut-shaped heteromer of human Sm-like proteins binds to the 3′-end of U6 snRNA, thereby facilitating U4/U6 duplex formation in vitro. EMBO J. *18*, 5789–5802.

Almeida, F., Saffrich, R., Ansorge, W., and Carmo-Fonseca, M. (1998). Microinjection of anti-coilin antibodies affects the structure of coiled bodies. J. Cell Biol. *142*, 899–912.

Arenas, J. E., and Abelson, J. N. (1997). Prp 43: an RNA helicase-like factor involved in spliceosome disassembly. Proc. Natl. Acad. Sci. USA *94*, 11798–11802.

Bell, M., Schreiner, S., Damianov, A., Reddy, R., and Bindereif, A. (2002). p110, a novel human U6 snRNP protein and U4/U6 snRNP recycling factor. EMBO J. *21*, 2724–2735.

Black, D. L., and Pinto, A. L. (1989). U5 small nuclear ribonucleoprotein: RNA structure analysis and ATP-dependent interaction with U4/U6. Mol. Cell. Biol. *9*, 3350–3359.

Blencowe, B. J., Carmo-Fonseca, M., Behrens, S. E., Luhrmann, R., and Lamond, A. I. (1993). Interaction of the human autoantigen p150 with splicing snRNPs. J. Cell Sci. *105*, 685–697.

Boon, K. L., Auchynnikava, T., Edwalds-Gilbert, G., Barrass, J. D., Droop, A. P., Dez, C., and Beggs, J. D. (2006). Yeast ntr1/spp382 mediates prp43 function in postspliceosomes. Mol. Cell. Biol. *26*, 6016–6023.

Carmo-Fonseca, M., Pepperkok, R., Carvalho, M. T., and Lamond, A. I. (1992). Transcription-dependent colocalization of the U1, U2, U4/U6, and U5 snRNPs in coiled bodies. J. Cell Biol. *117*, 1–14.

Carvalho, T., Almeida, F., Calapez, A., Lafarga, M., Berciano, M. T., and Carmo-Fonseca, M. (1999). The spinal muscular atrophy disease gene product, SMN: a link between snRNP biogenesis and the Cajal (coiled) body. J. Cell Biol. *147*, 715–728.

Chan, S. P., Kao, D. I., Tsai, W. Y., and Cheng, S. C. (2003). The Prp19p-associated complex in spliceosome activation. Science *302*, 279–282.

Chen, C. H., Kao, D. I., Chan, S. P., Kao, T. C., Lin, J. Y., and Cheng, S. C. (2006). Functional links between the Prp19-associated complex, U4/U6 biogenesis, and spliceosome recycling. RNA *12*, 765–774.

Company, M., Arenas, J., and Abelson, J. (1991). Requirement of the RNA helicase-like protein PRP22 for release of messenger RNA from spliceosomes. Nature *349*, 487–493.

Darzacq, X., Jady, B. E., Verheggen, C., Kiss, A. M., Bertrand, E., and Kiss, T. (2002). Cajal body-specific small nuclear RNAs: a novel class of 2′-O-methylation and pseudouridylation guide RNAs. EMBO J. *21*, 2746–2756.

Dignam, J. D., Lebovitz, R. M., and Roeder, R. G. (1983). Accurate transcription initiation by RNA polymerase II in a soluble extract from isolated mammalian nuclei. Nucleic Acids Res. *11*, 1475–1489.

Dundr, M., Hebert, M. D., Karpova, T. S., Stanek, D., Xu, H., Shpargel, K. B., Meier, U. T., Neugebauer, K. M., Matera, A. G., and Misteli, T. (2004). In vivo kinetics of Cajal body components. J. Cell Biol. *164*, 831–842.

Fabrizio, P., Laggerbauer, B., Lauber, J., Lane, W. S., and Luhrmann, R. (1997). An evolutionarily conserved U5 snRNP-specific protein is a GTP-binding factor closely related to the ribosomal translocase EF-2. EMBO J. *16*, 4092–4106.

Gerlich, D., Beaudouin, J., Kalbfuss, B., Daigle, N., Eils, R., and Ellenberg, J. (2003). Global chromosome positions are transmitted through mitosis in mammalian cells. Cell *112*, 751–764.

Ghetti, A., Company, M., and Abelson, J. (1995). Specificity of Prp24 binding to RNA: a role for Prp24 in the dynamic interaction of U4 and U6 snRNAs. RNA *1*, 132–145.

Girard, C., Neel, H., Bertrand, E., and Bordonne, R. (2006). Depletion of SMN by RNA interference in HeLa cells induces defects in Cajal body formation. Nucleic Acids Res. *34*, 2925–2932.

Jady, B. E., Darzacq, X., Tucker, K. E., Matera, A. G., Bertrand, E., and Kiss, T. (2003). Modification of Sm small nuclear RNAs occurs in the nucleoplasmic Cajal body following import from the cytoplasm. EMBO J. *22*, 1878–1888.

Jurica, M. S., and Moore, M. J. (2003). Pre-mRNA splicing: awash in a sea of proteins. Mol Cell *12*, 5–14.

Kambach, C., Walke, S., Young, R., Avis, J. M., de la Fortelle, E., Raker, V. A., Luhrmann, R., Li, J., and Nagai, K. (1999). Crystal structures of two Sm protein complexes and their implications for the assembly of the spliceosomal snRNPs. Cell *96*, 375–387.

Kiss, T. (2002). Small nucleolar RNAs: an abundant group of noncoding RNAs with diverse cellular functions. Cell *109*, 145–148.

Kiss, T. (2004). Biogenesis of small nuclear RNPs. J. Cell Sci. *117*, 5949–5951.

Klingauf, M., Stanek, D., and Neugebauer, K. M. (2006). Enhancement of U4/U6 small nuclear ribonucleoprotein particle association in Cajal bodies predicted by mathematical modeling. Mol. Biol. Cell *17*, 4972–4981.

Lauber, J., Plessel, G., Prehn, S., Will, C. L., Fabrizio, P., Groning, K., Lane, W. S., and Luhrmann, R. (1997). The human U4/U6 snRNP contains 60 and 90kD proteins that are structurally homologous to the yeast splicing factors Prp4p and Prp3p. RNA *3*, 926–941.

Lemm, I., Girard, C., Kuhn, A. N., Watkins, N. J., Schneider, M., Bordonne, R., and Luhrmann, R. (2006). Ongoing U snRNP Biogenesis Is Required for the Integrity of Cajal Bodies. Mol. Biol. Cell *17*, 3221–3231.

Listerman, I., Bledau, A. S., Grishina, I., and Neugebauer, K. M. (2007). Extragenic accumulation of RNA polymerase II enhances transcription by RNA polymerase III. PLoS Genet. *3*, e212.

Listerman, I., Sapra, A. K., and Neugebauer, K. M. (2006). Cotranscriptional coupling of splicing factor recruitment and precursor messenger RNA splicing in mammalian cells. Nat. Struct. Mol. Biol. *13*, 815–822.

Liu, J. L., and Gall, J. G. (2007). U bodies are cytoplasmic structures that contain uridine-rich small nuclear ribonucleoproteins and associate with P bodies. Proc. Natl. Acad. Sci. USA *104*, 11655–11659.

Makarov, E. M., Makarova, O. V., Urlaub, H., Gentzel, M., Will, C. L., Wilm, M., and Luhrmann, R. (2002). Small nuclear ribonucleoprotein remodeling during catalytic activation of the spliceosome. Science *298*, 2205–2208.

Makarova, O. V., Makarov, E. M., Liu, S., Vornlocher, H. P., and Luhrmann, R. (2002). Protein 61K, encoded by a gene (PRPF31) linked to autosomal dominant retinitis pigmentosa, is required for U4/U6center dotU5 tri-snRNP formation and pre-mRNA splicing. EMBO J. *21*, 1148–1157.

Martin, A., Schneider, S., and Schwer, B. (2002). Prp43 is an essential RNA-dependent ATPase required for release of lariat-intron from the spliceosome. J. Biol. Chem. *277*, 17743–17750.

Matera, A. G., and Shpargel, K. B. (2006). Pumping RNA: nuclear bodybuilding along the RNP pipeline. Curr. Opin. Cell Biol. *18*, 317–324.

Mayes, A. E., Verdone, L., Legrain, P., and Beggs, J. D. (1999). Characterization of Sm-like proteins in yeast and their association with U6 snRNA. EMBO J. *18*, 4321–4331.

Meister, G., Eggert, C., and Fischer, U. (2002). SMN-mediated assembly of RNPs: a complex story. Trends Cell Biol. *12*, 472–478.

Narayanan, U., Achsel, T., Luhrmann, R., and Matera, A. G. (2004). Coupled in vitro import of U snRNPs and SMN, the spinal muscular atrophy protein. Mol. Cell *16*, 223–234.

Narayanan, U., Ospina, J. K., Frey, M. R., Hebert, M. D., and Matera, A. G. (2002). SMN, the spinal muscular atrophy protein, forms a pre-import snRNP complex with snurportin1 and importin beta. Hum. Mol. Genet. *11*, 1785–1795.

Nesic, D., Tanackovic, G., and Kramer, A. (2004). A role for Cajal bodies in the final steps of U2 snRNP biogenesis. J. Cell Sci. *117*, 4423–4433.

Neugebauer, K. M. (2002). On the importance of being co-transcriptional. J. Cell Sci. *115*, 3865–3871.

Ohno, M., and Shimura, Y. (1996). A human RNA helicase-like protein, HRH1, facilitates nuclear export of spliced mRNA by releasing the RNA from the spliceosome. Genes Dev. *10*, 997–1007.

Patterson, G. H., and Lippincott-Schwartz, J. (2004). Selective photolabeling of proteins using photoactivatable GFP. Methods *32*, 445–450.

Paushkin, S., Gubitz, A. K., Massenet, S., and Dreyfuss, G. (2002). The SMN complex, an assemblyosome of ribonucleoproteins. Curr. Opin. Cell Biol. *14*, 305–312.

Raghunathan, P. L., and Guthrie, C. (1998). A spliceosomal recycling factor that reanneals U4 and U6 small nuclear ribonucleoprotein particles. Science *279*, 857–860.

Raker, V. A., Plessel, G., and Luhrmann, R. (1996). The snRNP core assembly pathway: identification of stable core protein heteromeric complexes and an snRNP subcore particle in vitro. EMBO J. *15*, 2256–2269.

Schaffert, N., Hossbach, M., Heintzmann, R., Achsel, T., and Luhrmann, R. (2004). RNAi knockdown of hPrp31 leads to an accumulation of U4/U6 di-snRNPs in Cajal bodies. EMBO J. *23*, 3000–3009.

Shpargel, K. B., and Matera, A. G. (2005). Gemin proteins are required for efficient assembly of Sm-class ribonucleoproteins. Proc. Natl. Acad. Sci. USA *102*, 17372–17377.

Shpargel, K. B., Ospina, J. K., Tucker, K. E., Matera, A. G., and Hebert, M. D. (2003). Control of Cajal body number is mediated by the coilin C-terminus. J. Cell Sci. *116*, 303–312.

Sleeman, J. (2007). A regulatory role for CRM1 in the multi-directional trafficking of splicing snRNPs in the mammalian nucleus. J. Cell Sci. *120*, 1540–1550.

Sleeman, J. E., Ajuh, P., and Lamond, A. I. (2001). snRNP protein expression enhances the formation of Cajal bodies containing p80-coilin and SMN. J. Cell Sci. *114*, 4407–4419.

Sleeman, J. E., and Lamond, A. I. (1999). Newly assembled snRNPs associate with coiled bodies before speckles, suggesting a nuclear snRNP maturation pathway. Curr. Biol. *9*, 1065–1074.

Staley, J. P., and Guthrie, C. (1998). Mechanical devices of the spliceosome: motors, clocks, springs, and things. Cell *92*, 315–326.

Stanek, D., and Neugebauer, K. M. (2004). Detection of snRNP assembly intermediates in Cajal bodies by fluorescence resonance energy transfer. J. Cell Biol. *166*, 1015–1025.

Stanek, D., and Neugebauer, K. M. (2006). The Cajal body: a meeting place for spliceosomal snRNPs in the nuclear maze. Chromosoma *115*, 343–354.

Stanek, D., Rader, S. D., Klingauf, M., and Neugebauer, K. M. (2003). Targeting of U4/U6 small nuclear RNP assembly factor SART3/p110 to Cajal bodies. J. Cell Biol. *160*, 505–516.

Tanaka, N., Aronova, A., and Schwer, B. (2007). Ntr1 activates the Prp43 helicase to trigger release of lariat-intron from the spliceosome. Genes Dev. *21*, 2312–2325.

Terns, M. P., and Terns, R. M. (2001). Macromolecular complexes: SMN–the master assembler. Curr. Biol. *11*, R862–R864.

Terskikh, A. *et al*. (2000). "Fluorescent timer": protein that changes color with time. Science *290*, 1585–1588.

Tsai, R. T., Fu, R. H., Yeh, F. L., Tseng, C. K., Lin, Y. C., Huang, Y. H., and Cheng, S. C. (2005). Spliceosome disassembly catalyzed by Prp43 and its associated components Ntr1 and Ntr2. Genes Dev. *19*, 2991–3003.

Tsai, R. T., Tseng, C. K., Lee, P. J., Chen, H. C., Fu, R. H., Chang, K. J., Yeh, F. L., and Cheng, S. C. (2007). Dynamic interactions of Ntr1-Ntr2 with Prp43 and with U5 govern the recruitment of Prp43 to mediate spliceosome disassembly. Mol. Cell. Biol. *27*, 8027–8037.

Tycowski, K. T., Kolev, N. G., Conrad, N. K., Fok, V., and Steitz, J. A. (2006). The ever-growing world of small nuclear ribonucleoproteins. In: The RNA world, ed. R. F. Gesteland, T. R. Cech, and J. F. Atkins, Cold Spring Harbor, NY: Cold Spring Harbor Laboratory Press, 327–368.

Verdone, L., Galardi, S., Page, D., and Beggs, J. D. (2004). Lsm proteins promote regeneration of pre-mRNA splicing activity. Curr. Biol. *14*, 1487–1491.

Wang, C., and Meier, U. T. (2004). Architecture and assembly of mammalian H/ACA small nucleolar and telomerase ribonucleoproteins. EMBO J. *23*, 1857–1867.

Wen, X., Lei, Y. P., Zhou, Y. L., Okamoto, C. T., Snead, M. L., and Paine, M. L. (2005). Structural organization and cellular localization of tuftelin-interacting protein 11 (TFIP11). Cell Mol. Life Sci. *62*, 1038–1046.

Will, C. L., and Luhrmann, R. (2001). Spliceosomal UsnRNP biogenesis, structure and function. Curr. Opin. Cell Biol. *13*, 290–301.

Will, C. L., and Luhrmann, R. (2006). Spliceosome structure and function. In: The RNA world, ed. R. F. Gesteland, T. R. Cech, and J. F. Atkins, Cold Spring Harbor, NY: Cold Spring Harbor Laboratory Press, 369–400.

Yu, Y. T., Sharl, E. C., Smith, C. M., and Steitz, J. A. (1999). The growing world of small nuclear ribonucleoproteins. In: The RNA world, ed. C. Gesteland and Atkins, Cold Spring Harbor, NY: Cold Spring Harbor Laboratory Press, 487–524.

Zhang, Y., Muyrers, J. P., Testa, G., and Stewart, A. F. (2000). DNA cloning by homologous recombination in *Escherichia coli*. Nat. Biotechnol. *18*, 1314–1317.

Human Molecular Genetics, 2009, Vol. 18, No. 11 **2014–2023**
doi:10.1093/hmg/ddp125
Advance Access published on March 17, 2009

A mutation linked to retinitis pigmentosa in HPRP31 causes protein instability and impairs its interactions with spliceosomal snRNPs

Martina Huranová†, Jarmila Hnilicová†, Branislav Fleischer, Zuzana Cvačková and David Staněk*

Department of RNA Biology, Institute of Molecular Genetics, Academy of Sciences of the Czech Republic, Vídeňská 1083, 142 20 Prague, Czech Republic

Received January 2, 2009; Revised February 27, 2009; Accepted March 13, 2009

The AD29 mutation in HPRP31 belongs to a series of mutations that were initially linked with the autosomal dominant disorder retinitis pigmentosa (RP) type 11. The HPRP31 gene encodes the hPrp31 protein that specifically associates with spliceosomal small nuclear ribonucleoprotein particles (snRNPs). Despite intensive research, it is still unclear how the AD29 (Ala216Pro) mutation causes RP. In this study, we report that the expression of this mutant protein affects cell proliferation and alters the structure of nuclear Cajal bodies that are connected with snRNP metabolism. Interestingly, these effects can be reversed by the overexpression of the hPrp6 protein, a binding partner of hPrp31. Although Ala216 is not contained within the U4 or U5 snRNP interacting domains, we present several lines of evidence that demonstrate that the association between the AD29 mutant and snRNPs in the cell nucleus is significantly reduced. Finally, we show that the stability of the AD29 mutant is severely affected resulting in its rapid degradation. Taken together, our results indicate that the Ala216Pro mutation destabilizes the hPrp31 protein structure in turn reducing its interaction with snRNP binding partners and leading to its rapid degradation. These findings significantly impact our understanding of the molecular mechanisms underlying RP and suggest that the insufficiency of the functional hPrp31 protein combined with the potential cytotoxicity associated with the expression the AD29 mutant are at least partially causative of the RP phenotype.

INTRODUCTION

Retinitis pigmentosa (RP) is the common name used to describe a group of inherited diseases characterized by the gradual degeneration of retina cells that lead to night blindness and visual field loss. Mutations within a variety of genes have been connected with RP, most of which are specifically expressed in photoreceptor cells. Surprisingly, mutations in three genes directly involved in pre-mRNA splicing have also been linked to autosomal dominant forms of RP. Products of these genes are well-characterized components of the spliceosomal small nuclear ribonucleoproteins (snRNP) (1–3; reviewed in 4). Of these proteins, hPrp8 is a key protein of the U5 snRNP that lies within the catalytic center of the spliceosome (5,6). hPrp3 and hPrp31 (also known as 61K) are components of the U4/U6 snRNP involved in the formation and stability of U4/U6 and U4/U6•U5 tri-snRNPs (7). In addition, a mutation in a tentative splicing factor PAP-1 has also been linked to RP (8).

Initially, the hPrp31 protein directly binds both the U4 snRNA and the U4 snRNP protein 15.5K to create the core of the U4 snRNP (9,10). This interaction is followed by U4 and U6 snRNAs annealing to form the U4/U6 snRNP. Finally, the key interaction for the formation of the U4/U6•U5 tri-snRNP is the interaction of hPrp31 with the U5 snRNP-specific protein hPrp6 (11). During the splicing reaction, the tri-snRNP undergoes dramatic rearrangements that result in disintegration of the tri-snRNP into individual snRNP components. In a process called the spliceosomal cycle, tri-snRNPs are re-assembled in a step-wise manner similar to *de novo* formation described above (7). U4/U6 and U4/U6•U5 snRNP formation

*To whom correspondence should be addressed. Tel: +420 296443118; Fax: +420 224310955; Email: stanek@img.cas.cz
†The authors wish it to be known that, in their opinion, the first two authors should be regarded as joint First Authors.

and recycling occur primarily in the nuclear inclusion called the Cajal body that accelerates the snRNP assembly reaction (12–16; reviewed in 17). The Cajal body is a dynamic structure whose integrity depends on transcription/splicing activity as well as snRNP biogenesis (14,16,18–20).

It is largely unknown why mutations in snRNP-specific proteins cause RP symptoms. It was reported that the expression of hPrp31 mutants in retina cells negatively influences splicing of retina-specific genes (21,22). However, most mutations in the HPRP31 gene result in the destabilization of hPrp31 mRNA that leads to a decrease in the synthesis of functional protein (23). Moreover, RP-affected families with large deletions of the HPRP31 gene have been identified (24,25). Together, these observations suggest a haploinsufficiency model that predicts that there is a critical concentration of snRNP protein necessary to support retina cell survival (23,26,27). Therefore, the expression from only one allele may not be sufficient to achieve this critical level of expression in retina cells. This model, however, does not apply to all snRNP mutations, as depletion of one HPRP3 allele does not trigger RP in mouse or zebrafish (28). In addition, it was shown that RP-associated mutations in yeast Prp8 and hPrp3 influence snRNP assembly (29,30) and thus might trigger the death program in sensitive cells.

In this study, we have concentrated on the hPpr31 point mutant, AD29, which contains an Ala216Pro substitution that does not apparently trigger a nonsense-mediated decay. It was recently shown that the expression of the AD29 mutant, while affecting the splicing of mini-gene reporter plasmids, had no effect on the splicing of a full-length gene derived reporter (31). Here, we have investigated whether the expression of the AD29 mutant has any effect on cell proliferation and snRNP assembly. Further, we have used co-immunoprecipitation, glycerol gradient ultracentrifugation and Förster resonance energy transfer (FRET) to map the interaction of this mutant protein with other snRNP proteins. Finally, we have probed the stability of the mutant protein and tested whether overexpression of hPrp31s major interacting partner in the tri-snRNP, hPrp6, can reverse phenotypes generated by AD29 expression.

RESULTS

Cells expressing the AD29 mutant exhibit slower proliferation

It has been shown that RP linked mutations in the splicing factor Prp8 cause disruption of U5 snRNP biogenesis in yeast (30). In a human cell line, a mutation in hPrp3 has been shown to have a negative effect on snRNP assembly (29). In this study, we decided to analyze the effects of expression of an hPrp31 mutant on cell growth and snRNP assembly in human cells. To achieve this, we established two stable cell lines that expressed either YFP tagged wild-type hPrp31 (WT31 cells) or mutant AD29 tagged with YFP (AD29 cells) (Fig. 1). Similar to endogenous protein (data not shown; 12,16), the wild-type hPrp31-YFP (WT31-YFP) localized to the cell nucleus and accumulated in Cajal bodies and splicing factor compartments (Fig. 1A). The localization pattern of the AD29-YFP mutant (AD29-YFP) was more diverse (Fig. 1B). In most cells analyzed, AD29-YFP localized to the cell nucleus and the cytoplasm; however, cells displaying a mostly cytoplasmic or nuclear accumulation were also presented. In comparison with the localization of WT31-YFP, AD29-YFP exhibited a more diffuse nuclear staining pattern and weak accumulation in Cajal bodies. A similar localization pattern has previously been observed in cells transiently expressing an AD29-GFP mutant (32). Of note, nucleolar accumulation was observed in cells highly expressing either of the YFP tagged proteins.

In order to test the effects of AD29 mutant expression on cell proliferation, AD29 cells were observed for 24 h and their growth compared with WT31 cells (Fig. 1C). Cells expressing the mutant protein divided 10% slower than cells expressing the wild-type protein. As both stable cell lines expressed the same amounts of endogenous hPrp31 and the expression of WT31-YFP and AD29-YFP was comparable (see below Fig. 3), these data indicate that the AD29 expression has a dominant negative effect on cell proliferation.

During live-cell imaging, we noticed that the localization of AD29-YFP changes during cell cycle. At early G1 phase, AD29-YFP was found mainly in the cytoplasm and only gradually accumulated in the nucleus during interphase. This observation explains the diverse localization of AD29 in an unsynchronized cell population. In contrast, WT31-YFP accumulated in the cell nucleus as soon as the nuclear membrane was formed after mitosis.

The AD29 mutant disrupts formation of Cajal bodies

As described above, our data indicate that the expression of AD29-YFP has a negative effect on cell growth (Fig. 1C). Given that hPrp31 is necessary for tri-snRNP formation, we decided to investigate snRNP metabolism in cells expressing the mutant protein. First, we analyzed cells for the presence of Cajal bodies because these bodies facilitate certain steps in tri-snRNP assembly (17) and their integrity depends on ongoing snRNP biogenesis and/or splicing (18,19). Staining cells with the Cajal body marker coilin revealed that the expression of AD29-YFP altered the structure of Cajal bodies (Fig. 2). Further, a significant fraction of AD29-YFP expressing cells did not have apparent Cajal bodies (Fig. 2C), and if Cajal bodies were present, they were often smaller than in WT31 cells. In the population of AD29 cells that did contained Cajal bodies, we analyzed the localization of snRNP-specific proteins within Cajal bodies. Interestingly, we observed in AD29 cells that accumulation of SART3, a marker of U4/U6 snRNP is reduced while the localization of the U5-specific protein hSnu114 and the U2-specific U2B″ were not significantly altered (Fig. 2D). Cajal body integrity is sensitive to snRNP metabolism and splicing. Therefore our data indicate that the expression of the AD29 mutant impacts upon snRNP metabolism and/or splicing.

Interaction between AD29 and snRNPs is significantly reduced

To analyze AD29 association with snRNP-specific proteins, we first employed the technique of FRET to detect protein complexes *in situ*. Either AD29-CFP or WT31-CFP was co-expressed with the YFP-tagged snRNP-specific protein

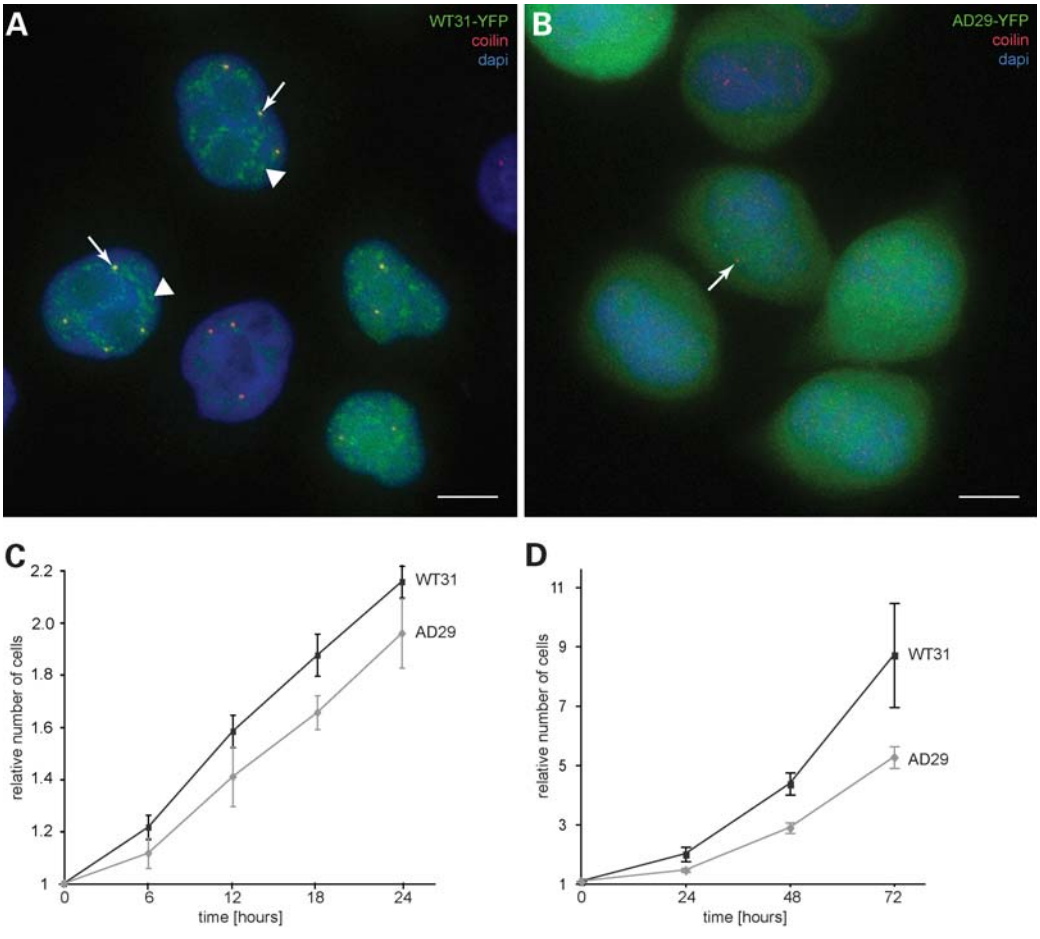

Figure 1. The AD29 mutant is aberrantly localized in the cytoplasm and inhibits cell growth. Stable cell lines expressing either the AD29-YFP mutant or wild-type hPrp31-YFP (WT31-YFP) were created from parental HeLa cells. (**A**) WT31-YFP was localized in the nucleus within splicing factor compartments (arrowheads) and Cajal bodies (arrows). (**B**) The AD29-YFP mutant was found abnormally localized within both the nucleus and cytoplasm. In the cell nucleus, AD29-YFP exhibited a more diffuse staining than wild-type protein and was only weakly accumulated in Cajal bodies (arrows). Cajal bodies were visualized by immunodetection of coilin (shown in red) that preferentially accumulates in Cajal bodies. DNA is visualized by dapi staining (blue). Bars represent 10 μm. (**C** and **D**) Proliferation of WT31 and AD29. (C) WT31 and AD29 cell growth was monitored on the microscope for 24 h and their proliferation graphically represented. (D) WT31 and AD29 cells were plated to the same density and their number calculated every 24 h for 3 days. The average of two experiments and SEM are shown.

SART3, hPrp4 or hPrp6 (Fig. 3A) and FRET was measured by acceptor photobleaching (Fig. 3B). We analyzed these snRNP proteins because they mark different stages of tri-snRNP formation: SART3 is specifically found in the U4/U6 snRNP intermediate, hPrp4 is a component of the U4/U6 snRNP and the tri-snRNP while hPrp6 is the U5-specific protein that interacts with hPrp31 to facilitate U4/U6•U5 tri-snRNP assembly. Cells co-expressing WT31-CFP and SART3-YFP exhibited a high FRET signal specifically within Cajal bodies that is consistent with previously published data that demonstrated that the U4/U6 snRNP is highly concentrated in Cajal bodies (13). A high FRET signal between hPrp6-YFP and WT31-CFP in the nucleoplasm indicates that there is a higher concentration of tri-snRNPs in the nucleoplasm than in Cajal bodies. Finally, the FRET signal between WT31-CFP and hPrp4-YFP was similar in the Cajal body and the nucleoplasm reflecting the localization of both U4/U6 and U4/U6•U5 snRNPs. Notably, the association between the AD29 mutant and U4/U6 snRNP proteins SART3 and hPrp4 (as measured by FRET) was reduced by approximately 40–50%. In contrast, the interaction between AD29 and hPrp6 was lowered only in the nucleoplasm, while this interaction in Cajal bodies was similar to wild-type hPrp31. These data indicate that the mutant protein is still able to partially integrate into snRNPs but its association with snRNPs is compromised.

To further test the interaction between AD29 and snRNPs, immunoprecipitation assays were carried out on WT31 or AD29 cells. As a negative control, the parental cell line was used. WT31 and AD29 cell lines expressed a similar amount of YFP-tagged proteins and their levels were lower than the level of endogenous hPrp31 (Fig. 3C). Co-precipitated proteins were analyzed by western blotting. Both hPrp3 and hPrp4 (proteins found in U4/U6 and U4/U6•U5 snRNPs) along with hSnu114 and hPrp6 (U5 and U4/U6•U5 snRNP-specific proteins) were co-precipitated with WT31-YFP illustrating that WT31-YFP is properly incorporated into U4/U6 and U4/U6•U5 snRNPs. In contrast, AD29-YFP did not pull-down

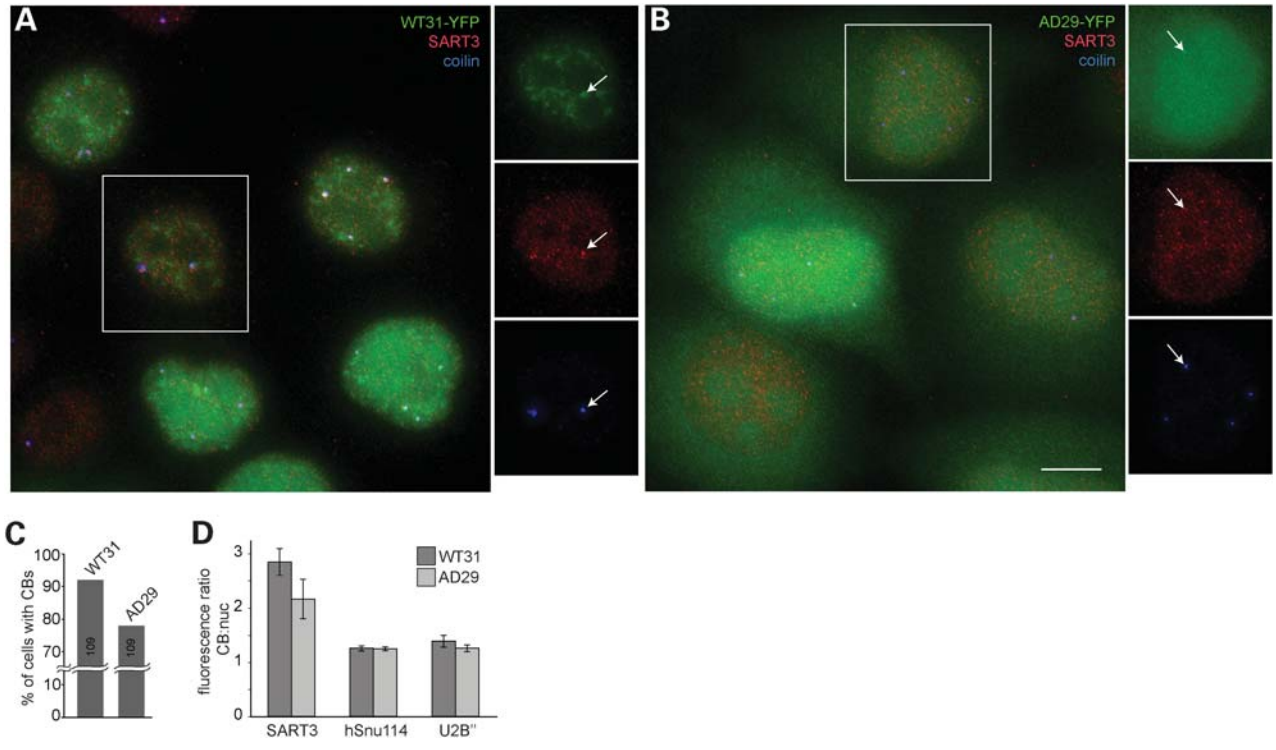

Figure 2. Expression of AD29-YFP affects the formation of Cajal bodies. To reveal how the expression of AD29-YFP affects the formation of Cajal bodies, WT31 (**A**) and AD29 (**B**) cells were stained for the Cajal body marker coilin (blue) and SART3 (red), a marker of the U4/U6 snRNP. Cajal bodies are marked by arrows. Bar represents 10 μm. (**C**) Cells containing Cajal bodies were counted (number of cells counted is given within bars). (**D**) To analyze whether the AD29 mutant influences the localization of snRNPs in Cajal bodies, AD29 and WT31 cells were stained for coilin as a marker of Cajal bodies and either SART3 (U6 and U4/U6 snRNPs), hSnu114 (U5 snRNP and tri-snRNP) or U2B″ (U2 snRNP) and the fluorescence ratio of Cajal bodies to nucleoplasm calculated. Expression of AD29 affected accumulation of SART3 in Cajal bodies. The average of three experiments and SEM are shown.

any of the tested U4/U6-specific proteins signifying that the single-point mutation is sufficient to disrupt the interaction between AD29 and the U4/U6 snRNP. However, AD29 precipitated with its U5-specific binding partner hPrp6. This finding extends the *in vitro* binding studies (9,31) and shows in human cells that AD29 interacts with hPrp6. Of interest, we repeatedly detected limited amounts of hSnu114 pulled down by AD29-YFP suggesting that under the immunoprecipitation assay conditions, the AD29 mutant might still be capable of interaction with the U5 snRNP.

To confirm that the AD29 mutant is impaired in its ability to incorporate into snRNPs, we prepared nuclear extracts from AD29 or WT31 stable cell lines. These extracts were subjected to glycerol gradient fractionation and the presence of AD29-YFP or WT31-YFP in individual fractions analyzed (Fig. 3D). Consistent with our previous findings, the AD29 mutant was mainly restricted to the top of the gradient and its sedimentation behavior was similar to bovine serum albumin that has a comparable molecular weight (data not shown). These data further demonstrate that the mutant is not a stable component of snRNP complexes.

Over-expression of hPrp6 is able to rescue some defects in AD29 expressing cells

Although the interaction between AD29 and snRNPs is dramatically reduced, this mutant is still able to instigate a dominant negative effect on both cell growth and Cajal body formation (Figs 1 and 2). It has been shown that AD29 binds strongly to hPrp6 *in vitro* (31) and our data show that AD29 is able to interact with hPrp6 *in vivo* (Fig. 3). Thus, it is plausible that AD29 might sequester free U5 snRNP or hPrp6 and that in turn changes the dynamics of tri-snRNP formation. To test this hypothesis, we expressed hPrp6-CFP in AD29 cells and measured the appearance of Cajal bodies (Fig. 4A–C). Expression of hPrp6-CFP but not CFP alone increased the number of cells that contained Cajal bodies to a level comparable to parental HeLa or WT31 cells. This result indicates that the negative effect AD29 has on Cajal body formation can be overcome by the expression of hPrp6.

To further test whether hPrp6 can also rescue the AD29-induced growth phenotype, AD29 cells were transfected with hPrp6-CFP and their proliferation measured as described previously (Fig. 4D). Neighboring AD29 cells that did not express hPrp6-CFP served as an internal negative control. Although the transfection procedure had a general negative effect on cell proliferation (compare Fig. 4D with Fig. 1C), AD29 cells expressing hPrp6-CFP divided faster than their non-transfected neighbors.

The AD29 mutation destabilizes the hPrp31 protein

During live-cell observations, we noticed that the amount of AD29-YFP in individual cells changed significantly during

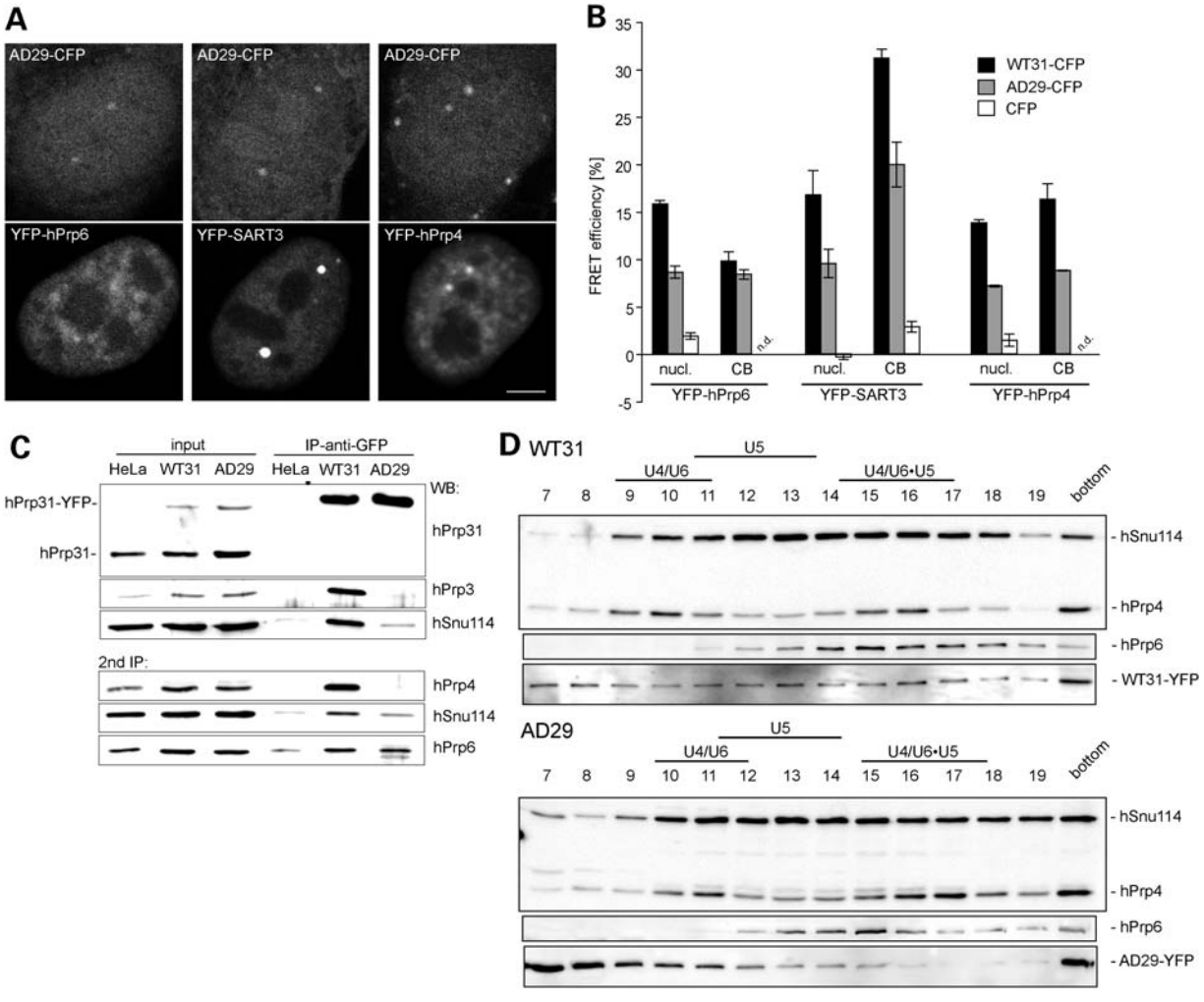

Figure 3. The interaction between AD29 and snRNPs is weakened. (**A**) AD29-CFP was co-expressed with markers of different snRNPs tagged with YFP and their association in the nucleoplasm and Cajal bodies measured by FRET. Bar represents 5 μm. (**B**) FRET efficiency indicates the association of wild-type protein (WT31) or AD29 mutant protein with hPrp6, SART3 or hPrp4. The AD29 mutant exhibited a significantly lower FRET signal with U4/U6 snRNP markers (SART3 and hPrp4) than wild-type protein. FRET measurements of cells expressing an empty CFP vector were used as a negative control. The average of two independent experiments and SEM is plotted. (**C**) AD29-YFP or WT31-YFP was precipitated from extracts made from the WT31 or AD29 stable cell lines using anti-GFP antibodies that cross-react with the YFP variant. Parental HeLa cells (HeLa) were used as a negative control. Two independent immunoprecipitations are shown. WT31-YFP co-precipitated efficiently with U4/U6 (hPrp3 and hPrp4) and U5 (hSnu114 and hPrp6) snRNP-specific proteins demonstrating that it is incorporated into the U4/U6 and U4/U6•U5 snRNPs. In contrast, AD29-YFP co-precipitated U5-specific hPrp6 and also a smaller amount of hSnu114, but none of the tested U4/U6 specific proteins. (**D**) Nuclear extracts were prepared from WT31 or AD29 cells, resolved on glycerol gradients and the position of snRNP-specific proteins visualized by western blotting. In comparison to the wild-type protein, the AD29 mutant does not co-migrate with snRNPs, but is instead concentrated at the top of the gradient signifying that it is not stably incorporated into snRNP complexes.

the 24 h observation period. The observed changes in AD29-YFP accumulation were not connected with any particular cell cycle phase and instead exhibited a rather stochastic behavior indicating that this effect might be a reflection on the dynamics of AD29 expression and degradation. To test the stability of the AD29-YFP protein, cells were treated with the translation inhibitor cycloheximide and YFP fluorescence monitored for 5 h (Fig. 5). While the WT31-YFP fluorescence decreased only marginally, the level of AD29-YFP fluorescence dropped rapidly after only 1 to 2 h incubation in cycloheximide (Fig. 5A–C). The fluorescent signal decreased both in the nucleus and the cytoplasm and no preferential degradation was observed in either of these cell compartments. Similar results were observed when the degradation of the AD29 mutant was analyzed by western blotting (Fig. 5D). While endogenous hPrp31 and WT31-YFP were stably present in cells during the 5 h treatment, AD29-YFP protein disappeared within a couple of hours. Together, these data suggest that the Ala216Pro substitution causes a conformational change that negatively affects the stability of the protein.

DISCUSSION

RP is a heritable disease that affects 1 in 4000 people. So far, there have been over 40 loci identified that carry mutations that cause RP. Generally, most of these genes are directly involved in controlling retina cell metabolism. However,

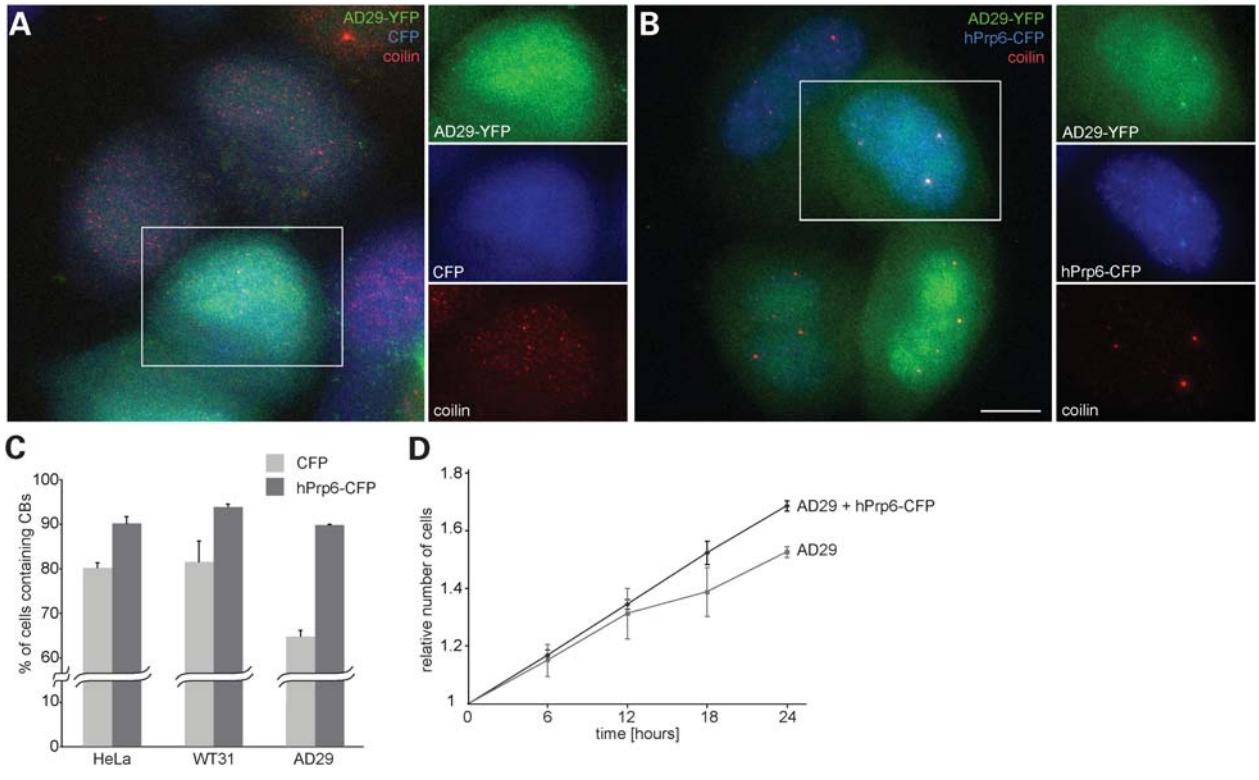

Figure 4. Expression of hPrp6 rescues the AD29 phenotype. The AD29 cell line was transfected with (**A**) CFP or (**B**) hPrp6-CFP. Twenty-four hour post-transfection cells were fixed and stained for the Cajal body marker coilin. In CFP transfected cells, Cajal bodies were smaller and coilin was often dispersed throughout the nucleoplasm with no obvious accumulation. Expression of hPrp6 led to the re-formation of Cajal bodies. Bar represents 10 μm. (**C**) Parental HeLa cells, WT31 or AD29 cells, were transfected with CFP or hPrp6-CFP, stained for coilin and the number of cells with Cajal bodies determined. The average and SEM of two independent experiments is shown. (**D**) The AD29 cells were transfected with hPrp6-CFP and their proliferation measured 20–24 h after transfection. Although transfection conditions negatively affected cell growth, the AD29 cells expressing hPrp6-CFP divided faster than non-transfected cells. An average of three experiments with SEM is shown.

three genes that encode general RNA splicing factors that are ubiquitously expressed have also been implicated in RP. In addition, the gene encoding the putative splicing factor PAP1 is also mutated in RP (4). The mechanism underlying how mutations in splicing factors trigger RP has been extensively investigated during the last couple of years. Such studies has shown that mutations in HPRP3 and HPRP8 can influence snRNP assembly and that many mutations in HPRP31 lead to the degradation of its mRNA by the nonsense-mediated decay pathway, consequently lowering the expression of functional hPrp31 protein.

Here we investigated the hPrp31 point mutation found in the AD29 family that does not apparently activate the mRNA degradation pathway but instead codes for an alanine to proline substitution at residue 216. It has been shown *in vitro* and by two-hybrid analysis that this amino acid change does not interfere with the hPrp31–hPrp6 interaction (9,31). In addition, a structural analysis of the U4snRNA/15.5K/hPrp31 complex revealed that the Ala216 residue is not directly involved in the interaction between hPrp31 and U4 snRNA or 15.5K; however, the effect of the AD29 mutation on the hPrp31 and U4 snRNP interaction has never been tested (9). Here we have demonstrated that the AD29 mutation dramatically alters the ability of hPrp31 to interact with U4/U6 snRNPs. Analysis of the association of AD29 and U4/U6 snRNPs *in situ* by FRET revealed that this association was reduced by half. Further, the AD29 mutant precipitated the U5 snRNP, specifically the hPrp6 and hSnu114 proteins but not any of the tested U4/U6 markers. Finally, the AD29 mutant was mainly concentrated at the top of a glycerol gradient indicating that it is not a stable component of snRNPs. These data together indicate that the mutant has a limited ability to associate with U4/U6 snRNPs. In addition, the interaction between AD29 and snRNPs is weak and does not withstand the conditions during snRNP immunoprecipitation and gradient centrifugation. As the mutant protein is partially localized in the cytoplasm, one explanation for reduced interaction with snRNPs could be a defect in nuclear import. However, the Ala216Pro substitution does not affect the nuclear localization signal or interaction with importin β1 and direct measurements of nuclear import did not reveal any differences between wild-type and mutant proteins (32,33). Therefore, we assume that reduced nuclear localization is rather an effect than a cause of reduced AD29 binding to snRNPs.

To date, it is unclear whether the AD29 mutant can bind U4/U6 and U5 snRNPs simultaneously and form the tri-snRNP or whether the mutant binds U4/U6 and U5 snRNPs independently and prevents tri-snRNP formation. Based on the fact that AD29 interacts with hPrp6 *in vivo* as assayed by both

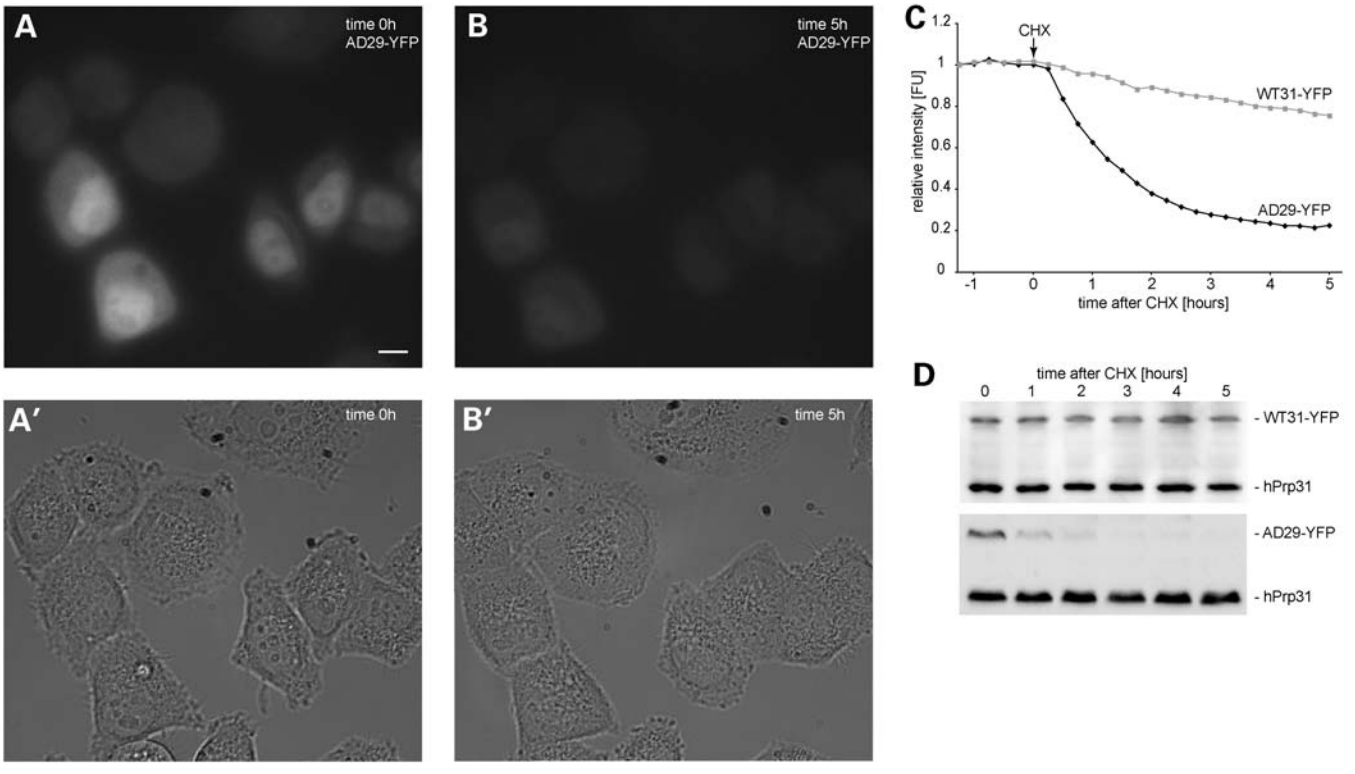

Figure 5. The AD29 protein is rapidly degraded inside cells. (**A**–**C**) To compare the stability of AD29-YFP to WT31-YFP, proteo-synthesis was inhibited by cycloheximide in WT31 or AD29 cell lines and YFP fluorescence measured every 15 min for 5 h. (A and A′) AD29 cells at time 0 h and (B and B′) 5 h after cycloheximide addition. (A and B) YFP fluorescence (A′ and B′) bright-field images. Bar represents 10 μm. (C) Graph of relative YFP fluorescence after protein synthesis inhibition. YFP fluorescence did not exhibit any significant decrease before addition of cycloheximide, 15 min post addition of cycloheximide AD29-YFP fluorescence ($n = 28$ cells) began decreasing indicative of the rapid degradation of the AD29-YFP protein. In contrast, WT31-YFP protein ($n = 22$ cells) exhibited only a slow decay during the course of the 5 h experiment. (**D**) Protein synthesis was inhibited as before and proteins detected by western blotting using anti-hPrp31 antibodies that recognize both endogenous and tagged hPrp31 variants. The results show the relative stability of WT31-YFP compared to AD29-YFP that is rapidly degraded after 2 h.

FRET and immunoprecipitation (Fig. 3) and that over-expression of hPrp6 is able to rescue the AD29 phenotype, we speculate that free AD29 transiently binds via hPrp6 to the U5 snRNP. This interaction prevents the proper association with the U4/U6 snRNP and changes the dynamics of tri-snRNP formation resulting in the observed phenotypes: reduced cellular proliferation (Fig. 1) and disruption of Cajal body formation (Fig. 2). Both phenotypes are likely to be dominant as we did not observe any changes in the expression of endogenous hPrp31 or other tested snRNP proteins (Fig. 3 and data not shown).

Besides the effects of AD29 expression on cell growth and nuclear morphology, we also observed the rapid degradation of the AD29 mutant in HeLa cells. Despite the fact that these results were acquired using cell culture expressing normal levels of endogenous hPrp31, such observation raise two alternative models for RP. The first model predicts that the AD29 mutant is rapidly degraded in all cell types including retina cells and RP symptoms are caused by the insufficiency of functional hPrp31. This hypothesis would be in accordance with previous findings that demonstrated that large deletions of the HPRP31 gene and mutations that destabilize hPrp31 mRNA cause RP (23–25). Additionally, this model would also explain the incomplete penetrance of the AD29 mutation (3).

An alternative hypothetical model would require specific stabilization and/or high expression of the mutant in retina cells. In this case, the mutant would only be able to exert its dominant negative effect on snRNP metabolism and cell viability, when it is present in cells as is the case of our model system. These defects can be reverted by over-expressing the hPrp31 binding partner, hPrp6 whose expression might represent an additional factor that determines whether RP symptoms are manifested in affected individuals. To distinguish between these two models, further investigation is required to determine whether the AD29 mutant is present in targeted retina cells.

MATERIALS AND METHODS

Cells and antibodies

HeLa cells were cultured in Dulbecco's modified Eagle medium supplemented with 10% fetal calf serum, penicillin and streptomycin (Gibco BRL). Cells were transfected with Fugene HD (Roche) according to the manufacture's protocol. Stable HeLa cell lines were created by transfecting cells with the hPrp31-YFP (13) or AD29-YFP plasmids. To obtain individual YFP positive cell, G418 resistant cells were sorted by

FACS. After selection, the antibiotics were omitted from the cell culture medium.

The following antibodies were used: rabbit anti-SART3/p110 antibodies (14), mAb anti-coilin (5P10) (34) kindly provided by M. Carmo-Fonseca, rabbit antibodies against hPrp31 (U4/U6-61K) (11), hPrp4 (U4/U6-60K) (35), hSnu114 (U5-116K) (36) and hPrp3 kindly provided by R. Lührmann. Monoclonal antibodies against U2B″ were purchased from Progen and anti-hPrp6 antibodies (H-300) from Santa Cruz Biotechnology.

Mutation and protein tagging

SART3-YFP-C3, hPrp4-YFP-C1, hPrp31-CFP-C3 and hPrp31-YFP-C3 were described previously (13). The full-length hPrp6 was amplified by high fidelity PCR (Phusion, Finnzymes) from an EST clone and subsequently sub-cloned into ECFP-C3 or EYFP-C3 vectors derived from EGFP-C3 (Clontech) by using EcoRI/HindIII restriction sites. Correct sequences were confirmed by sequencing.

The point G646C mutation within the hPrp31 sequence was introduced by PCR mutagenesis using the ExSite Mutagenesis kit (Stratagene), primers 646-For: 5′-TTCATCCCACCCAA CCTGTCCATCAT and 646-Rev: 5′-GGACATCCGGGA CTCCACATACTC and hPrp31-CFP-C3 as a template (13). The correct sequence was verified by sequencing. Subsequently, the AD29 mutant was re-cloned into the EYFP-C3 vector using EcoRI/BamHI restriction sites.

Indirect immunofluorescence

Cells were fixed in 4% paraformaldehyde/PIPES (Sigma) for 10 min, permeabilized for 5 min with 0.2% Triton X-100 (Sigma) and incubated with the appropriate primary antibodies. Secondary anti-rabbit antibodies conjugated with FITC or TRITC and anti-mouse antibodies conjugated with TRITC or Cy5 (Jackson ImmunoResearch Laboratories) were used. Images were collected using the DeltaVision microscope system (Applied Precision) coupled with the Olympus IX70 microscope equipped with an oil immersion objective 60x 1.42NA using the same settings for each sample. Stacks of 25 z-sections with 200 nm z-step were collected per sample and subjected to mathematical deconvolution using the measured point spread function (SoftWorx, Applied Precision). Mean intensities in Cajal bodies and nucleoplasm were quantified using SoftWorx as described previously (13). Twenty to 40 cells containing ~40–100 Cajal bodies were analyzed in each experiment.

Live cell imaging

Cells were plated on glass bottomed Petri dishes (MatTek) and after 20–24 h imaged using the DeltaVision microscope system coupled with the Olympus IX70 microscope equipped with an oil immersion objective 40x 1.3NA and an environmental chamber controlling CO_2 level and temperature. Images were taken every 30 min for 24 h using YFP excitation and emission filters (Applied Precision). To measure the effects of hPrp6-CFP expression on AD29 cell growth, the same microscope set up was used and YFP/CFP filters were used. Eight to 12 positions were imaged simultaneously using the Multi-point visiting function. There were ~30–75 cells per experiment at time 0 h. The number of YFP or YFP/CFP positive cells were counted at each time point and plotted accordingly.

For protein stability measurements, cells were placed under the DeltaVision microscopic system as descried above and images were taken every 15 min for 75 min using YFP filters. Cycloheximide was added to the medium at a final concentration of 30 μg/ml and cells were imaged as before for an additional 5 h. Relative YFP fluorescence of each cell with respect to the start point was calculated and an average of all cells was plotted.

Western blotting

Cells were washed with ice-cold PBS, scraped and pelleted at 1000*g* for 5 min before being resuspended in 30 μl PBS. This was followed by the addition of 30 μl of 2x protein sample buffer and incubation at 95°C for 5 min. Cell extracts were subsequently homogenized by passage through a 22 G needle. Proteins were resolved on a 10% polyacrylamide gel, blotted onto a nitrocellulose membrane and incubated with anti-hPrp31 antibodies followed by incubation with goat anti-rabbit antibodies coupled with horseradish peroxidase (Jackson ImmunoResearch Laboratories). The SuperSignal West Pico/Femto Chemiluminiscent Substrate (Pierce) was used to generate luminiscence.

FRET measurement

HeLa cells were transfected with constructs encoding fluorescently tagged proteins using Fugene HD, grown for 24–26 h and fixed at room temperature in 4% paraformaldehyde/PIPES (Sigma) for 10 min. After rinsing with Mg-PBS (PBS supplemented with 10 mM Mg^{2+}) and water, cells were embedded in glycerol containing DABCO. FRET was measured by the acceptor photobleaching method as previously described (13) using the Leica SP5 confocal microscope. Intensities of CFP (excited by 405 nm laser set to 5–10% of maximum power) and YFP (excited by 514 nm laser line set to 2% of maximum power) were measured. Following this, YFP was bleached in a region of interest by three to five intensive (30% maximum power) pulses of 514 nm laser line and CFP and YFP fluorescence measured again. Apparent FRET efficiency was calculated according to the equation $FRET_{efficiency}$ (%) = $(CFP_{after} - CFP_{before}) \times 100/CFP_{after}$. Unbleached regions of the same cell were used as a negative control. Ten cells were measured per each FRET pair.

Immunoprecipitation

HeLa, WT31 or AD29 cells were grown on 15 cm Petri dishes, placed on ice, washed three times with ice cold Mg-PBS and harvested into NET-2 buffer (50 mM TRIS–Cl pH 7.5, 150 mM NaCl, 0.05% Nonidet P-40) supplemented with a complete mix of protease inhibitors (Roche) and pulse-sonicated for 90 s on ice. Cell extracts were centrifuged at 13 000 rpm and the supernatant incubated with Protein-G Sepharose beads (GE Healthcare) coated with goat anti-GFP antibodies

(raised against bacterially expressed full-length EGFP and obtained from David Drechsel, MPI-CBG, Dresden, Germany) for 4 h at 4°C. Captured complexes were extracted by bead incubation in protein sample buffer for 5 min at 95°C and the precipitated proteins were detected by western blotting.

Glycerol gradient ultracentrifugation

Nuclear extracts were prepared according to (37), diluted in gradient buffer (20 mM HEPES/KOH pH 8, 150 mM NaCl, 1.5 mM MgCl2, 0.5 mM dithiothreitol) and fractionated in a linear 10–30% glycerol gradient by centrifugation at 32 000 rpm for 17 h using the SW-41 rotor (Beckman). The gradient was divided into 20 fractions (~620 μl) and proteins from these fractions analyzed by western blotting.

ACKNOWLEDGEMENTS

We thank Karla Neugebauer in whose laboratory we performed pilot experiments. We are grateful to Reinhard Lührmann and Maria Carmo-Fonseca for gifts of antibodies. We also thank Petr Těšina for comments on the manuscript and Alicia Corlett for language proofreading.

Conflict of Interest statement. None declared.

FUNDING

This work was supported by grants from Max Planck Society (the Partner group program) and from the Academy of Sciences of the Czech Republic (KAN200520801, AV0Z50520514).

REFERENCES

1. Chakarova, C.F., Hims, M.M., Bolz, H., Abu-Safieh, L., Patel, R.J., Papaioannou, M.G., Inglehearn, C.F., Keen, T.J., Willis, C., Moore, A.T. *et al.* (2002) Mutations in HPRP3, a third member of pre-mRNA splicing factor genes, implicated in autosomal dominant retinitis pigmentosa. *Hum. Mol. Genet.*, **11**, 87–92.
2. McKie, A.B., McHale, J.C., Keen, T.J., Tarttelin, E.E., Goliath, R., van Lith-Verhoeven, J.J., Greenberg, J., Ramesar, R.S., Hoyng, C.B., Cremers, F.P. *et al.* (2001) Mutations in the pre-mRNA splicing factor gene PRPC8 in autosomal dominant retinitis pigmentosa (RP13). *Hum. Mol. Genet.*, **10**, 1555–1562.
3. Vithana, E.N., Abu-Safieh, L., Allen, M.J., Carey, A., Papaioannou, M., Chakarova, C., Al-Maghtheh, M., Ebenezer, N.D., Willis, C., Moore, A.T. *et al.* (2001) A human homolog of yeast pre-mRNA splicing gene, PRP31, underlies autosomal dominant retinitis pigmentosa on chromosome 19q13.4 (RP11). *Mol. Cell*, **8**, 375–381.
4. Mordes, D., Luo, X., Kar, A., Kuo, D., Xu, L., Fushimi, K., Yu, G., Sternberg, P. Jr and Wu, J.Y. (2006) Pre-mRNA splicing and retinitis pigmentosa. *Mol. Vis.*, **12**, 1259–1271.
5. Pena, V., Rozov, A., Fabrizio, P., Lührmann, R. and Wahl, M.C. (2008) Structure and function of an RNase H domain at the heart of the spliceosome. *EMBO J.*, **27**, 2929–2940.
6. Grainger, R.J. and Beggs, J.D. (2005) Prp8 protein: at the heart of the spliceosome. *RNA*, **11**, 533–557.
7. Will, C.L. and Lührmann, R. (2006) Spliceosome structure and function. Gesteland, R.F., Cech, T.R. and Atkins, J.F. (eds), *The RNA World*, Third edn, Cold Spring Harbor Laboratory Press, New York, pp. 369–400.
8. Keen, T.J., Hims, M.M., McKie, A.B., Moore, A.T., Doran, R.M., Mackey, D.A., Mansfield, D.C., Mueller, R.F., Bhattacharya, S.S., Bird, A.C. *et al.* (2002) Mutations in a protein target of the Pim-1 kinase associated with the RP9 form of autosomal dominant retinitis pigmentosa. *Eur. J. Hum. Genet.*, **10**, 245–249.
9. Liu, S., Li, P., Dybkov, O., Nottrott, S., Hartmuth, K., Lührmann, R., Carlomagno, T. and Wahl, M.C. (2007) Binding of the human Prp31 Nop domain to a composite RNA-protein platform in U4 snRNP. *Science*, **316**, 115–120.
10. Nottrott, S., Urlaub, H. and Lührmann, R. (2002) Hierarchical, clustered protein interactions with U4/U6 snRNA: a biochemical role for U4/U6 proteins. *EMBO J.*, **21**, 5527–5538.
11. Makarova, O.V., Makarov, E.M., Liu, S., Vornlocher, H.P. and Lührmann, R. (2002) Protein 61K, encoded by a gene (PRPF31) linked to autosomal dominant retinitis pigmentosa, is required for U4/U6·U5 tri-snRNP formation and pre-mRNA splicing. *EMBO J.*, **21**, 1148–1157.
12. Schaffert, N., Hossbach, M., Heintzmann, R., Achsel, T. and Lührmann, R. (2004) RNAi knockdown of hPrp31 leads to an accumulation of U4/U6 di-snRNPs in Cajal bodies. *EMBO J.*, **23**, 3000–3009.
13. Stanek, D. and Neugebauer, K.M. (2004) Detection of snRNP assembly intermediates in Cajal bodies by fluorescence resonance energy transfer. *J. Cell Biol.*, **166**, 1015–1025.
14. Stanek, D., Rader, S.D., Klingauf, M. and Neugebauer, K.M. (2003) Targeting of U4/U6 small nuclear RNP assembly factor SART3/p110 to Cajal bodies. *J. Cell Biol.*, **160**, 505–516.
15. Klingauf, M., Stanek, D. and Neugebauer, K.M. (2006) Enhancement of U4/U6 small nuclear ribonucleoprotein particle association in Cajal bodies predicted by mathematical modeling. *Mol. Biol. Cell*, **17**, 4972–4981.
16. Stanek, D., Pridalova-Hnilicova, J., Novotny, I., Huranova, M., Blazikova, M., Wen, X., Sapra, A.K. and Neugebauer, K.M. (2008) Spliceosomal small nuclear ribonucleoprotein particles repeatedly cycle through Cajal bodies. *Mol. Biol. Cell*, **19**, 2534–2543.
17. Stanek, D. and Neugebauer, K.M. (2006) The Cajal body: a meeting place for spliceosomal snRNPs in the nuclear maze. *Chromosoma*, **115**, 343–354.
18. Carmo-Fonseca, M., Pepperkok, R., Carvalho, M.T. and Lamond, A.I. (1992) Transcription-dependent colocalization of the U1, U2, U4/U6, and U5 snRNPs in coiled bodies. *J. Cell Biol.*, **117**, 1–14.
19. Lemm, I., Girard, C., Kuhn, A.N., Watkins, N.J., Schneider, M., Bordonne, R. and Lührmann, R. (2006) Ongoing U snRNP biogenesis is required for the integrity of Cajal bodies. *Mol. Biol. Cell*, **17**, 3221–3231.
20. Sleeman, J.E., Ajuh, P. and Lamond, A.I. (2001) snRNP protein expression enhances the formation of Cajal bodies containing p80-coilin and SMN. *J. Cell Sci.*, **114**, 4407–4419.
21. Yuan, L., Kawada, M., Havlioglu, N., Tang, H. and Wu, J.Y. (2005) Mutations in PRPF31 inhibit pre-mRNA splicing of rhodopsin gene and cause apoptosis of retinal cells. *J. Neurosci.*, **25**, 748–757.
22. Mordes, D., Yuan, L., Xu, L., Kawada, M., Molday, R.S. and Wu, J.Y. (2007) Identification of photoreceptor genes affected by PRPF31 mutations associated with autosomal dominant retinitis pigmentosa. *Neurobiol. Dis.*, **26**, 291–300.
23. Rio Frio, T., Wade, N.M., Ransijn, A., Berson, E.L., Beckmann, J.S. and Rivolta, C. (2008) Premature termination codons in PRPF31 cause retinitis pigmentosa via haploinsufficiency due to nonsense-mediated mRNA decay. *J. Clin. Invest.*, **118**, 1519–1531.
24. Abu-Safieh, L., Vithana, E.N., Mantel, I., Holder, G.E., Pelosini, L., Bird, A.C. and Bhattacharya, S.S. (2006) A large deletion in the adRP gene PRPF31: evidence that haploinsufficiency is the cause of disease. *Mol. Vis.*, **12**, 384–388.
25. Kohn, L., Bowne, S.J., S. Sullivan L., Daiger, S.P., Burstedt, M.S., Kadzhaev, K., Sandgren, O. and Golovleva, I. (2008) Breakpoint characterization of a novel approximately 59 kb genomic deletion on 19q13.42 in autosomal-dominant retinitis pigmentosa with incomplete penetrance. *Eur. J. Hum. Genet.* [Epub ahead of print].
26. Rivolta, C., McGee, T.L., Rio Frio, T., Jensen, R.V., Berson, E.L. and Dryja, T.P. (2006) Variation in retinitis pigmentosa-11 (PRPF31 or RP11) gene expression between symptomatic and asymptomatic patients with dominant RP11 mutations. *Hum. Mutat.*, **27**, 644–653.
27. Vithana, E.N., Abu-Safieh, L., Pelosini, L., Winchester, E., Hornan, D., Bird, A.C., Hunt, D.M., Bustin, S.A. and Bhattacharya, S.S. (2003) Expression of PRPF31 mRNA in patients with autosomal dominant retinitis pigmentosa: a molecular clue for incomplete penetrance? *Invest. Ophthalmol. Vis. Sci.*, **44**, 4204–4209.

28. Graziotto, J.J., Inglehearn, C.F., Pack, M.A. and Pierce, E.A. (2008) Decreased levels of the RNA splicing factor Prpf3 in mice and zebrafish do not cause photoreceptor degeneration. *Invest. Ophthalmol. Vis. Sci.*, **49**, 3830–3838.
29. Gonzalez-Santos, J.M., Cao, H., Duan, R.C. and Hu, J. (2008) Mutation in the splicing factor Hprp3p linked to retinitis pigmentosa impairs interactions within the U4/U6 snRNP complex. *Hum. Mol. Genet.*, **17**, 225–239.
30. Boon, K.L., Grainger, R.J., Ehsani, P., Barrass, J.D., Auchynnikava, T., Inglehearn, C.F. and Beggs, J.D. (2007) prp8 mutations that cause human retinitis pigmentosa lead to a U5 snRNP maturation defect in yeast. *Nat. Struct. Mol. Biol.*, **14**, 1077–1083.
31. Wilkie, S.E., Vaclavik, V., Wu, H., Bujakowska, K., Chakarova, C.F., Bhattacharya, S.S., Warren, M.J. and Hunt, D.M. (2008) Disease mechanism for retinitis pigmentosa (RP11) caused by missense mutations in the splicing factor gene PRPF31. *Mol. Vis.*, **14**, 683–690.
32. Deery, E.C., Vithana, E.N., Newbold, R.J., Gallon, V.A., Bhattacharya, S.S., Warren, M.J., Hunt, D.M. and Wilkie, S.E. (2002) Disease mechanism for retinitis pigmentosa (RP11) caused by mutations in the splicing factor gene PRPF31. *Hum. Mol. Genet.*, **11**, 3209–3219.
33. Wilkie, S.E., Morris, K.J., Bhattacharya, S.S., Warren, M.J. and Hunt, D.M. (2006) A study of the nuclear trafficking of the splicing factor protein PRPF31 linked to autosomal dominant retinitis pigmentosa (ADRP). *Biochim. Biophys. Acta*, **1762**, 304–311.
34. Almeida, F., Saffrich, R., Ansorge, W. and Carmo-Fonseca, M. (1998) Microinjection of anti-coilin antibodies affects the structure of coiled bodies. *J. Cell Biol.*, **142**, 899–912.
35. Lauber, J., Plessel, G., Prehn, S., Will, C.L., Fabrizio, P., Groning, K., Lane, W.S. and Lührmann, R. (1997) The human U4/U6 snRNP contains 60 and 90kD proteins that are structurally homologous to the yeast splicing factors Prp4p and Prp3p. *RNA*, **3**, 926–941.
36. Fabrizio, P., Laggerbauer, B., Lauber, J., Lane, W.S. and Lührmann, R. (1997) An evolutionarily conserved U5 snRNP-specific protein is a GTP-binding factor closely related to the ribosomal translocase EF-2. *EMBO J.*, **16**, 4092–4106.
37. Dignam, J.D., Lebovitz, R.M. and Roeder, R.G. (1983) Accurate transcription initiation by RNA polymerase II in a soluble extract from isolated mammalian nuclei. *Nucleic Acids Res.*, **11**, 1475–1489.

OPEN ACCESS Freely available online

PLoS one

Histone Deacetylase Activity Modulates Alternative Splicing

Jarmila Hnilicová, Samira Hozeifi, Eva Dušková, Jaroslav Icha, Tereza Tománková, David Staněk*

Department of RNA Biology, Institute of Molecular Genetics AS CR, Prague, Czech Republic

Abstract

There is increasing evidence to suggest that splicing decisions are largely made when the nascent RNA is still associated with chromatin. Here we demonstrate that activity of histone deacetylases (HDACs) influences splice site selection. Using splicing-sensitive microarrays, we identified ~700 genes whose splicing was altered after HDAC inhibition. We provided evidence that HDAC inhibition induced histone H4 acetylation and increased RNA Polymerase II (Pol II) processivity along an alternatively spliced element. In addition, HDAC inhibition reduced co-transcriptional association of the splicing regulator SRp40 with the target fibronectin exon. We further showed that the depletion of HDAC1 had similar effect on fibronectin alternative splicing as global HDAC inhibition. Importantly, this effect was reversed upon expression of mouse HDAC1 but not a catalytically inactive mutant. These results provide a molecular insight into a complex modulation of splicing by HDACs and chromatin modifications.

Citation: Hnilicová J, Hozeifi S, Dušková E, Icha J, Tománková T, et al. (2011) Histone Deacetylase Activity Modulates Alternative Splicing. PLoS ONE 6(2): e16727. doi:10.1371/journal.pone.0016727

Editor: Juan Valcarcel, Centre de Regulació Genòmica, Spain

Received December 16, 2010; **Accepted** January 8, 2011; **Published** February 2, 2011

Funding: This project was supported by grants from the Max Planck Society (the Partner group program), the Czech Science Foundation (P305/10/0424) and from the Academy of Sciences of the Czech Republic (KAN200520801, AV0Z50520514). The funders had no role in study design, data collection and analysis, decision to publish, or preparation of the manuscript.

Competing Interests: The authors have declared that no competing interests exist.

* E-mail: stanek@img.cas.cz

Introduction

Pre-mRNA splicing is an essential step in eukaryotic gene expression and its regulation vastly increases the coding potential of our genome. Splicing is catalyzed by the spliceosome which consists of spliceosomal small ribonucleoproteins (snRNPs) and additional splicing factors [1]. The critical step in splicing is intron recognition; this is achieved through the association of the splicing machinery with pre-mRNA via RNA-RNA and protein-RNA interactions. Interestingly, there is an increasing body of evidence suggesting that these interactions are not the only determinants of the splice-site definition [2].

There are many examples of a close coupling between transcription and splicing ([3,4] reviewed in [5,6]). Several splicing factors interact with RNA polymerase II (Pol II), which is important for their recruitment to pre-mRNA and through the combination of Pol II processivity and promoter identity, splice-site selection is influenced ([7,8,9,10] reviewed in [11]). This regulation involves a co-transcriptional definition of splice-sites, spliceosome assembly and splicing [12,13]. Indeed, the major regulators of splicing, snRNPs and SR proteins, are found at the site of active transcription [14,15,16,17,18], demonstrating that the splicing machinery assembles while the pre-mRNA is still associated with the DNA template. Such an observation suggests that chromatin modification might potentially play a regulatory role in splicing.

In yeast, the histone acetyltransferase found in the SAGA complex, Gcn5 is involved in co-transcriptional recruitment of the U2 snRNP [19]. In higher eukaryotes, the SWI/SNF chromatin remodeling complex associates with pre-mRNA and regulates alternative splicing of endogenous genes [20,21] and treatment with histone deacetylase inhibitor trichostatin A (TSA) affects minigene alternative splicing [8]. Additionally, splicing factors interact directly with modified histones, although the significance of these interactions for splicing regulation remains unclear [22,23]. Recently, genome-wide nucleosome mapping revealed that nucleosome localization correlates with exon positioning and may be involved in exon recognition [24,25,26,27]. The role of nucleosome packing was supported by finding that siRNA-induced formation of heterochromatin influenced alternative splicing [28]. H3K36 tri-methylation differs at alternative and consecutive exons and affects alternative splicing through splicing factor recruitment [29,30,31,32]. In addition, cell membrane depolarization resulted in altered RNA polymerase II transcription and chromatin modifications, correlating with alternative splicing changes [30]. In this study we examined whether enzymes catalyzing histone deacetylation can modulate alternative splicing of human genes.

Results

HDAC activity regulates alternative splicing

In order to explore the effects of HDAC activity on alternative splicing we treated cells with the potent HDAC inhibitor, sodium butyrate (NaB) and monitored splicing changes by exon arrays. The analysis revealed that the splicing of 683 genes (out of 17,771 human genes included in the analysis) was altered upon HDAC inhibition (Table S1). Targeted genes are mainly involved in signaling (transmembrane transporters and receptors), transcription regulation, apoptosis, cell cycle and cell organization, all processes that regulate cell fate and differentiation (Fig. 1a). Interestingly, one of the target genes was encoding the Tau protein, which is abundantly expressed in central nervous system

and enhanced inclusion of exon 10 causes neurodegenerative diseases as frontotemporal dementia with Parkinsonism linked to chromosome 17 (FTDP-17) [33]. The NaB treatment reduced expression of the splice variant that is upregulated during the disease (Fig. 1c). Exons with high splicing change (≥3 fold) were further analyzed with respect to their inclusion or exclusion (Fig. 1b). While we found a partial preference for overall exon inclusion (389 included/294 excluded) there was a strong correlation between increased gene expression and alternative events with a partial bias towards exon exclusion in up-regulated genes. Recently, a similar relationship was observed when a smaller set of genes was analyzed after UV irradiation [34]. These data suggest that HDAC inhibition did not only alter transcription but also substantially affected splicing pattern. To confirm exon-array results 16 target genes were further analyzed by conventional RT-PCR. Thirteen genes exhibited alternative splicing changes predicted by exon-arrays. Splicing pattern of nine of them is shown in Fig. 1c together with two control exons with no splicing change (Fig. 1d).

Histone H4 acetylation correlates with alternative splicing

One of the genes most affected by HDAC inhibition was fibronectin (*FN1*). Given that fibronectin's alternative splicing variants are well described and have been extensively studied [35,36,37], we decided to use this gene to further characterize the role of HDACs in alternative splicing. As a model we analyzed exon 25 (called EDB or EDII) that was influenced by HDAC inhibition and exon 33 (called EDA or EDI) that did not alter splicing pattern upon NaB treatment. Moreover, one of the major advantageous is that proteins regulating splicing of the EDB exon were identified. It was shown that SR proteins, in particular SRp40, and PTB are important for EDB inclusion [38,39,40,41].

To test a potential mechanism via HDACs influence alternative splicing we first analyzed whether HDAC inhibition affected expression of general splicing proteins (namely snRNP specific proteins) and splicing regulators (SR proteins or PTB) (Fig. 2a,b). Using the monoclonal antibody m104 that recognizes a set of

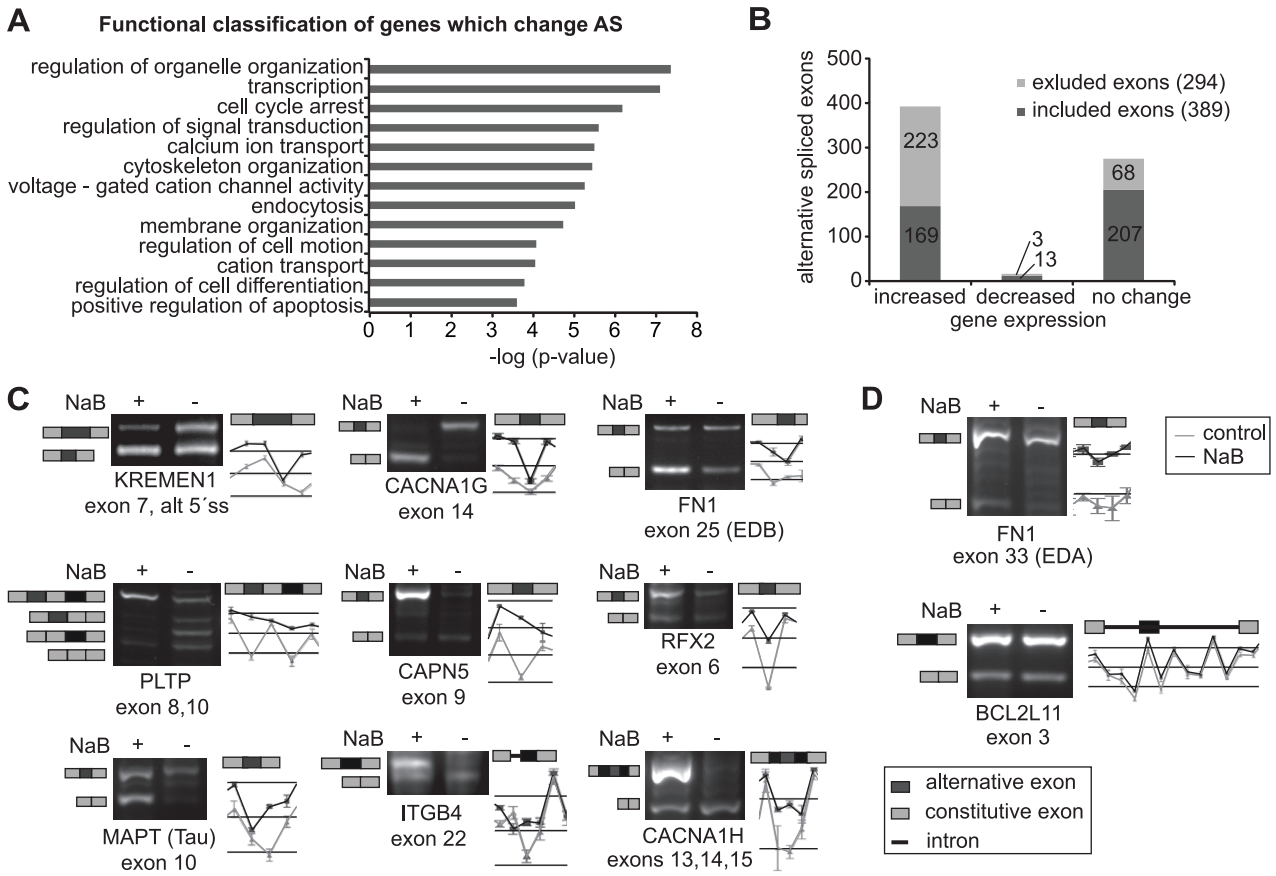

Figure 1. HDAC inhibition induces global changes in alternative splicing. HDAC activity was inhibited by treating cells with sodium butyrate (NaB) and splicing changes monitored by exon arrays. The splicing pattern of over 680 genes was changed (see Table S1). (A) Gene ontology analysis was performed with genes from the microarray annotation file as a background, enrichment score is the -log (p-value) of the chi-square test. Functional groups of over-represented genes with enrichment score >3 are shown. (B) Exons with high change (≥3-fold) were analyzed with respect to their inclusion or exclusion and divided into three groups according to the expression of a gene where the alternative exons are localized. (C) Several genes identified as top hits by microarray were confirmed by RT-PCR. Alternative exons were skipped after NaB treatment in three genes (*CACNA1G, FN1* –exon 24 and *MAPT).* In *KREMEN1* alternative 5'splice site was used and in *CAPN5, RFX2, ITGB4, PLTP* and *CACNA1H* alternative exons were included after HDAC inhibition. A graphic illustration of microarray data representing the same genomic loci as RT-PCR is shown next to the gels (non-treated cells - grey line; NaB treatment - black line). Exon array data show expression of individual alternative exons and neighboring constitutive exons. Relative decrease of the signal from alternative exon probes indicates alternative exon skipping, e.g. *CACNA1G* alternative exon signal from control cells (grey line) is higher compared to the surrounding constitutive exons than signal from NaB treated cells (black line). Although *CACNA1G* gene expression is elevated in NaB treated cells, the expression of alternative exon decreased, because this exon is preferentially skipped. (D) Two control exons that did not change splicing pattern upon NaB treatment.
doi:10.1371/journal.pone.0016727.g001

phosphorylated SR proteins including SRp40 [42] we showed that HDAC inhibition did not significantly alter the level of phosphorylated SR proteins (Fig. 2a). In addition, we used a HeLa cell line stably expressing SRp40-GFP from a bacterial artificial chromosome (BAC) that preserved endogenous SRp40 regulatory elements [43]. No change in SRp40-GFP expression was observed following the NaB treatment (Fig. 2b). Moreover, we did not observe any difference in expression of PTB, Pol II or core spliceosomal components hSnu114, hPrp4, U5-40K and SmB. It was shown recently that several splicing regulators including SRp40 are acetylated [44]. Therefore, we probed acetylation level of SRp40 before and after HDAC inhibition but did not find any significant changes in SRp40 acetylation status (Fig. 2c).

To further test whether the HDAC inhibition caused overexpression of other splicing factors that may potentially regulate fibronectin alternative splicing, cellular protein synthesis was inhibited in conjunction with HDAC activity. The inhibition of protein synthesis itself did not have any significant effect on EDB splicing. Further, we did not observe any differences in the splicing of the EDB exon whether cells were treated in combination with the ribosomal and HDAC inhibitors or HDAC inhibitor alone (Fig. 2d). These data indicated that NaB treatment did not influence splicing via altered expression or modification of regulatory proteins.

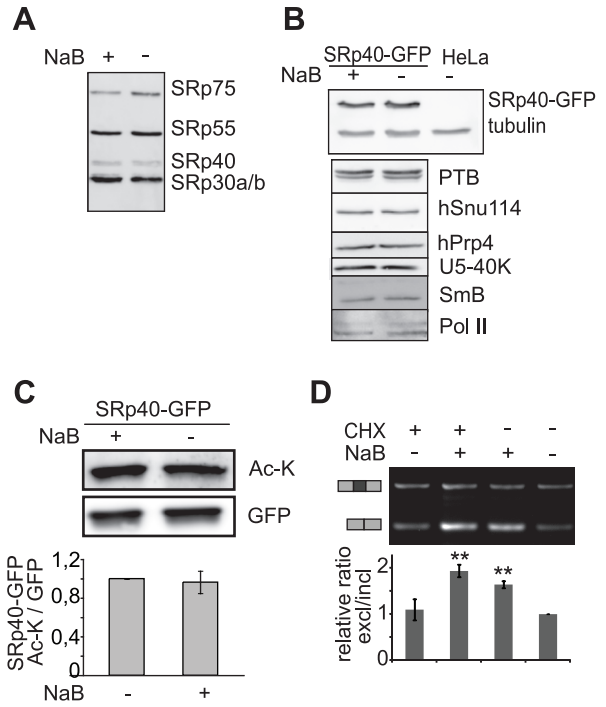

Figure 2. HDAC inhibition does not alter phosphorylation, acetylation or expression of SRp40. (A) HeLa cells or (B) HeLa cells stably expressing SRp40-GFP from BAC were treated for 15 h with NaB and levels of SR proteins were analyzed by Western blotting with the m104 antibody recognizing an SR protein phospho-epitope (A) or anti-GFP antibody (B). In addition, HDAC inhibition did not alter expression of several splicing proteins or RNA polymerase II. (C) SRp40-GFP was immunoprecipitated from SRp40-GFP stable cell line before and after HDAC inhibition and acetylation assayed by anti-acetyl lysine antibody. No significant change was observed after six hours NaB treatment. Representative Western blot and the average of three independent experiments is shown. (D) Inhibition of protein synthesis does not affect alternative splicing of the EDB exon in the *FN1* gene. Cells were treated for 9 h with cycloheximide (*CHX*), sodium butyrate (*NaB*) or both and EDB splicing assayed by RT-PCR and RT-qPCR (graph). Inhibition of HDAC by NaB had a similar effect on EDB skipping after CHX treatment. A representative RT-PCR (gel) and the average of three independent quantitative RT-PCR experiments (graph) are shown including SEM, ** indicates $p \leq 0.01$ of the t-test with respect to non-treated cells.
doi:10.1371/journal.pone.0016727.g002

Next, we performed a detailed analysis of chromatin marks along the *FN1* gene including the EDA exon where we did not detect any change in alternative splicing after NaB treatment. First we determined the level of acetylated histone H3 and H4. Acetylation of histone H3 was maximal at the promoter and dropped in the body of the gene. HDAC inhibition resulted in decreased H3 acetylation at the promoter (likely reflecting clearance of the promoter; see Fig. 3h) and partial increase within the gene (Fig. 3a). In non-treated cells general H4 acetylation was highest at the promoter. After HDAC inhibition, general H4 acetylation was more uniform and high all over the gene (Fig. 3b). Interestingly, the increase of H4 acetylation was significantly higher at the EDB exon than at the EDA exon, whose splicing did not respond to HDAC inhibition. Notably, different lysine residues within histone H4 contributed differently to the general H4 acetylation with highest increase at the lysines 8 and 12 (Fig. 3c–f). Next, we analyzed the level of lysine 36 tri-methylation at histone H3 as this modification was recently described as a marker of exon associated chromatin that influenced alternative splicing [30,31,32]. H3K36 tri-methylation increased partially within the gene body, including the alternative exon (Fig. 3g). At the same time no change was found in general nucleosome occupancy within the body of the gene (Fig. 3h). Together, these data show that HDAC inhibition has a global effect on chromatin modifications within the *FN1*.

As the maximal changes observed were in the acetylation of histone H4, we tested whether this modification correlated with alternative splicing. First, we measured the dynamics of H4 acetylation after HDAC inhibition in HeLa cells (Fig. 4a). Histone acetylation rapidly increased after 3 h of treatment and reached maximal levels within 6–9 h. However, little splicing effects were observed within this time period (Fig. 4b and data not shown). This discrepancy could be caused by mRNA being synthesized and spliced before HDAC inhibition. Thus, the presence of this mRNA might delay the detection of any splicing changes. To reduce the effect of mRNA spliced before HDAC inhibition, cells were incubated for 6 h with DRB, a reversible inhibitor of Pol II. Following this incubation, the Pol II inhibitor was removed and the cells were treated with NaB for an additional 6 h and EDB inclusion analyzed (Fig. 4b). The subsequent results show that as soon as 6 h post HDAC inhibition, the splicing of *de novo* synthesized pre-mRNA was altered. To further test the correlation between histone H4 acetylation and *FN1* splicing, we analyzed H4 acetylation in a retinoblastoma derived cell line Y79 that almost exclusively included the alternative exon (Fig. 4c). Using three different loci of the fibronectin gene, we show that general histone H4 acetylation is reduced in Y79 cells with respect to HeLa cells (Fig. 4d).

Pol II processivity changes after HDAC inhibition

Our data suggest a link between alternative splicing and H4 acetylation. It was previously shown that H4 acetylation was associated with Pol II processivity [45]. Moreover, there have been several observations that suggested a close relationship between Pol II dynamics and alternative splicing [7,46]. Based on these observations we decided to analyze whether HDAC inhibition affects Pol II processivity. We probed Pol II processivity at several *FN1* gene loci by measuring the ratio between two pre-mRNA fragments as described previously [30] (Fig. 5a). Our results

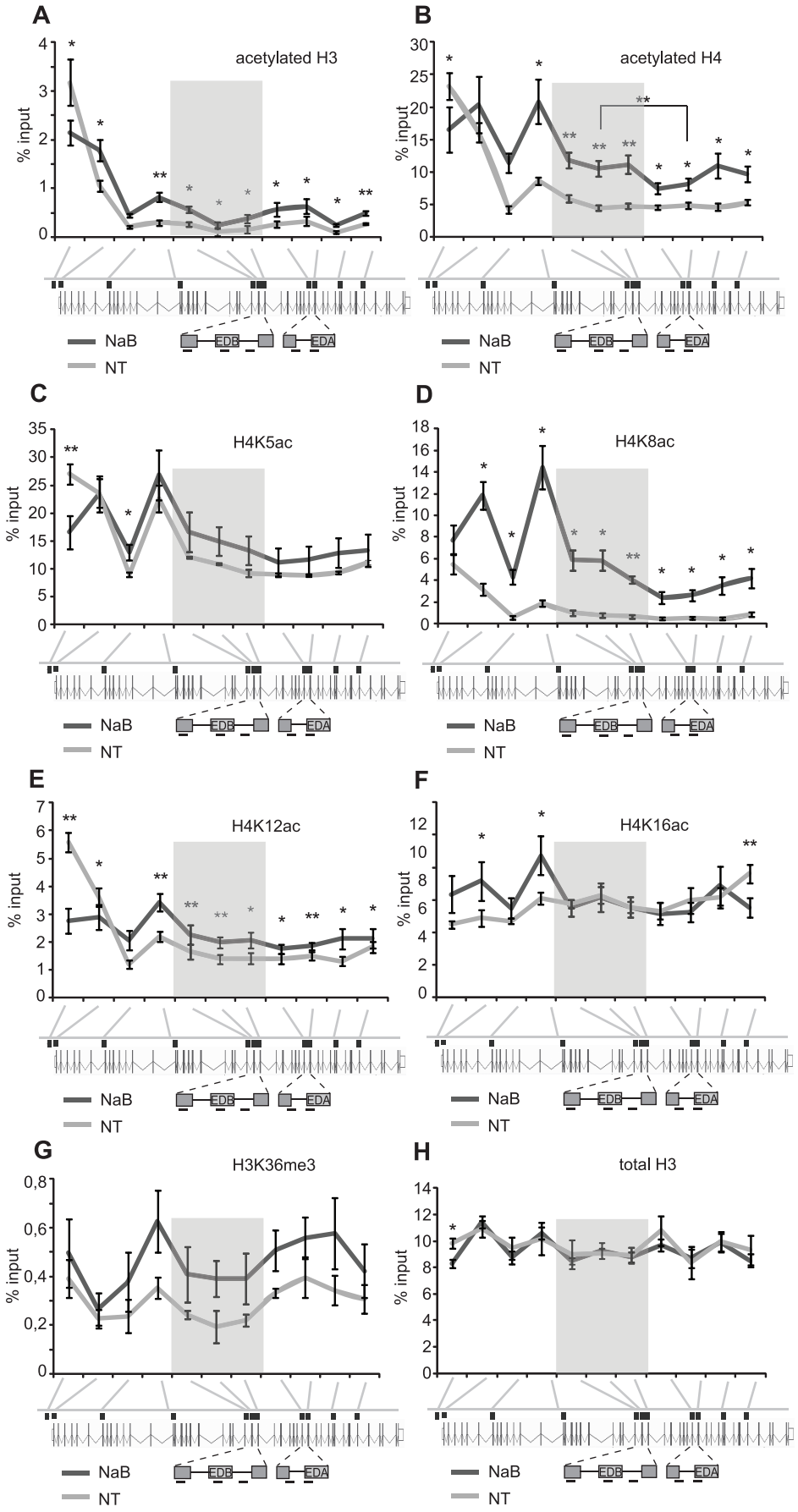
A
acetylated H3
% input
NaB
NT
EDB
EDA
B
acetylated H4
% input
NaB
NT
EDB
EDA
C
H4K5ac
% input
NaB
NT
EDB
EDA
D
H4K8ac
% input
NaB
NT
EDB
EDA
E
H4K12ac
% input
NaB
NT
EDB
EDA
F
H4K16ac
% input
NaB
NT
EDB
EDA
G
H3K36me3
% input
NaB
NT
EDB
EDA
H
total H3
% input
NaB
NT
EDB
EDA

Figure 3. HDAC inhibition induces histone acetylation along the *FN1* gene. Chromatin immunoprecipitations were performed 6 h after HDAC inhibition with NaB using antibodies against (A) acetylated H3, (B) acetylated H4, (C) acetylated H4 lysine 5, (D) acetylated H4 lysine 8, (E) acetylated H4 lysine 12, and (F) acetylated H4 lysine 16. In addition, (G) tri-methylated lysine 36 histone H3, and (H) total H3 were probed. Probes detecting gene loci around alternative EDB exon are shaded. The average of at least three experiments is shown including SEM, ** indicates $p \leq 0.01$ and * $p \leq 0.05$ of the t-test.
doi:10.1371/journal.pone.0016727.g003

showed the highest increase of Pol II processivity in proximity of the EDB exon that was excluded but only small change at the alternative EDA exon that did not change splicing after HDAC inhibition.

Next, we determined the distribution of total Pol II as well as Pol II phophorylated at the C-terminal domain along the fibronectin gene after HDAC inhibition (Fig. 5b–d). Consistent with elevated levels of fibronectin mRNA (~5-fold, see Table S1), we observed an increased occupancy of total Pol II and Pol II phosphorylated at Ser-5 at the promoter indicating a higher frequency of transcription initiation (Fig. 5b,c). Surprisingly, we found lower Ser-2 phosphorylation along the gene upon HDAC inhibition with EDB exon as the only exception, which likely reflects accumulation of total Pol II at the EDB exon (Fig. 5d). In addition, we observed accumulation of total Pol II at the EDB exon and the intronic sequence downstream of the EDB exon. Together with measurements of Pol II processivity these data indicated that HDAC inhibition resulted in increased Pol II processivity at upstream and downstream introns and slow down at the EDB exon. HDAC inhibition thus had a complex effect on Pol II distribution, phosphorylation and processivity along the fibronectin gene.

HDAC inhibition decreases the association of SRp40 with the *FN1* gene

The EDB exon is regulated by several *cis*-regulatory elements. A couple SRp40 binding sites were found within the EDB exon and the downstream intron, while PTB sites were identified upstream of the alternative exon. It was reported that EDB exon is recognized and spliced co-transcriptionaly [12] and that SR proteins directly associate with the nascent RNA at the transcription site [17]. Therefore, we decided to test whether HDAC inhibition influenced the interaction of SRp40 or PTB with the nascent RNA at the transcription site. To detect SRp40 at the transcription unit, we used a recently developed system that utilizes GFP tagged SR proteins and chromatin immunoprecipitation (ChIP) [17]. This report showed that GFP tagged SR proteins are expressed at the same or at lower levels than the

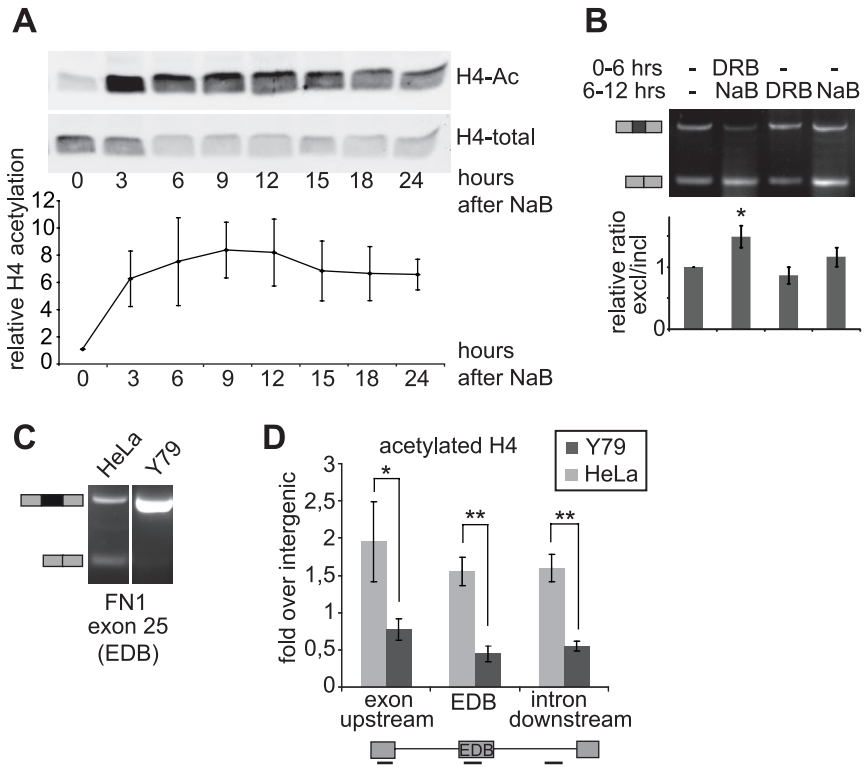

Figure 4. H4 acetylation correlates with EDB exon skipping. (A) The dynamics of histone H4 acetylation was assayed by Western blotting at different times after NaB treatment. A representative blot and the average of three experiments are shown including SEM. (B) EDB splicing was assayed six hours after HDAC inhibition. To reduce the possible effects of mRNA synthesis before HDAC inhibition, cells were treated with the Pol II inhibitor, DRB before the addition of HDAC inhibitor (*NaB*). The same amount of total RNA was used in each reaction. Following Pol II inhibition changes in EDB splicing were detected six hours post NaB treatment. A representative RT-PCR (gel) and the average of three independent quantitative RT-PCR experiments (graph) are shown including SEM. (C) EDB inclusion was analyzed in two different cell lines (Hela and Y79) using RT-PCR. (D) Histone H4 acetylation in HeLa and Y79 was assayed by chromatin immunoprecipitation at the EDB exon and the surrounding regions (see graphical representation of the gene loci below the graph). The average of three experiments is shown including SEM, ** indicates $p \leq 0.01$ and * $p \leq 0.05$ of the t-test.
doi:10.1371/journal.pone.0016727.g004

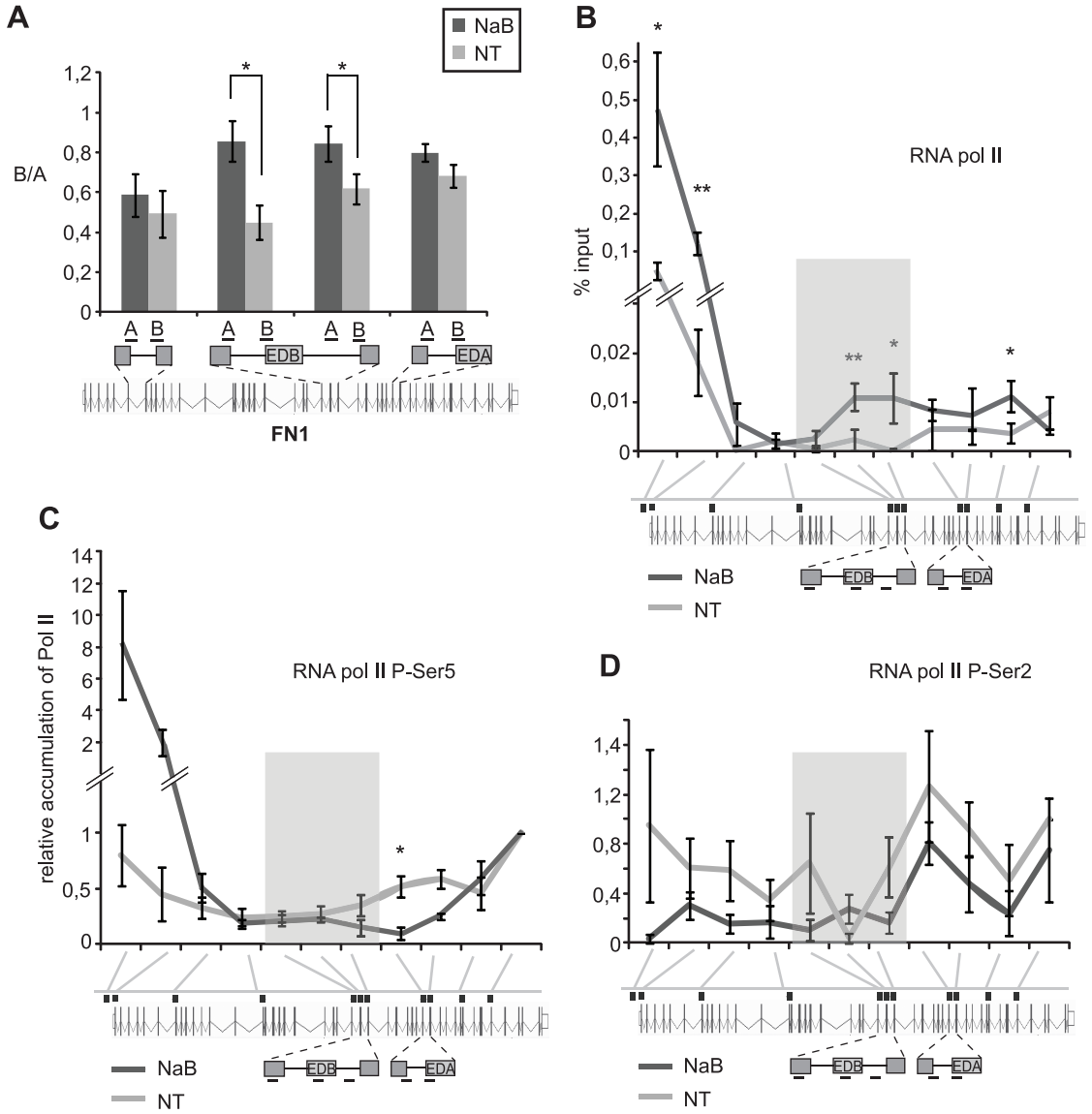

Figure 5. Pol II processivity correlates with exon skipping. (A) Pol II processivity was determined as a ratio of two pre-mRNA sequences (B:A) along several regions of the *FN1* gene. The abundance of given pre-mRNA locus was determined by quantitative PCR. The increased ratio after NaB treatment indicates higher Pol II processivity over the assayed region. Pol II exhibited high processivity increased significantly upstream and downstream of the EDB exon but not over consecutively spliced intron or alternative EDA exon that was not affected by NaB treatment. The average of three experiments is shown including SEM, * indicates $p \leq 0.05$ the t-test. (B-D) HDAC inhibition affects Pol II distribution. HDAC activity was inhibited by NaB for six hours and distribution of (B) total Pol II, (C) Pol II phosphorylated at the C-terminal domain Ser-5, and (D) Pol II phosphorylated at the C-terminal domain Ser-2 was assayed along the gene by chromatin immunoprecipitation. Probes detecting gene loci around alternative EDB exon are shaded. The tested gene loci are the same as in fig. 3. The average of three experiments is shown including SEM, ** indicates $p \leq 0.01$ and * $p \leq 0.05$ of the t-test.
doi:10.1371/journal.pone.0016727.g005

endogenous protein and that the behavior of this tagged variant is indistinguishable from its endogenous counterpart. Our results revealed that SRp40 association with the *FN1* gene decreased upon HDAC inhibition, with the most significant decrease at the alternative EDB exon (Fig. 6a). The observed decrease was not a result of overall reduction of SRp40 protein level because HDAC inhibition did not alter SRp40 expression (Fig. 2b). In contrast, we did not detect any significant changes in association of PTB or general splicing Sm proteins over the alternative EDB exon indicating that changes in SRp40 interaction were not due to general changes in gene accessibility (Fig. 6b,c). These data indicated that HDAC activity influenced co-transcriptional association of SRp40 with the EDB exon.

HDAC1 activity modulates fibronectin alternative splicing

To test whether the observed effects on alternative splicing were specific for NaB or whether it was a general property of HDAC inhibitors we reduced HDAC activity using three different inhibitors - TSA, valproic acid (VPA) and NaB and determined their effect on splicing of the fibronectin exon EDB. TSA is a pan-HDAC isoform inhibitor that *in vitro* displays nM potency against HDAC classes I (HDAC 1, 2, 3 and 8) and II (HDAC 4, 5, 6, 7, 9 and 10) with the exception of HDAC8, which is in the low μM range [47]. VPA is an established drug in the long-term therapy of epilepsy. It is a class I selective HDAC inhibitor, which *in vitro* inhibits HDAC 1, 2, 3 and 8 in the mM range [48]. Finally,

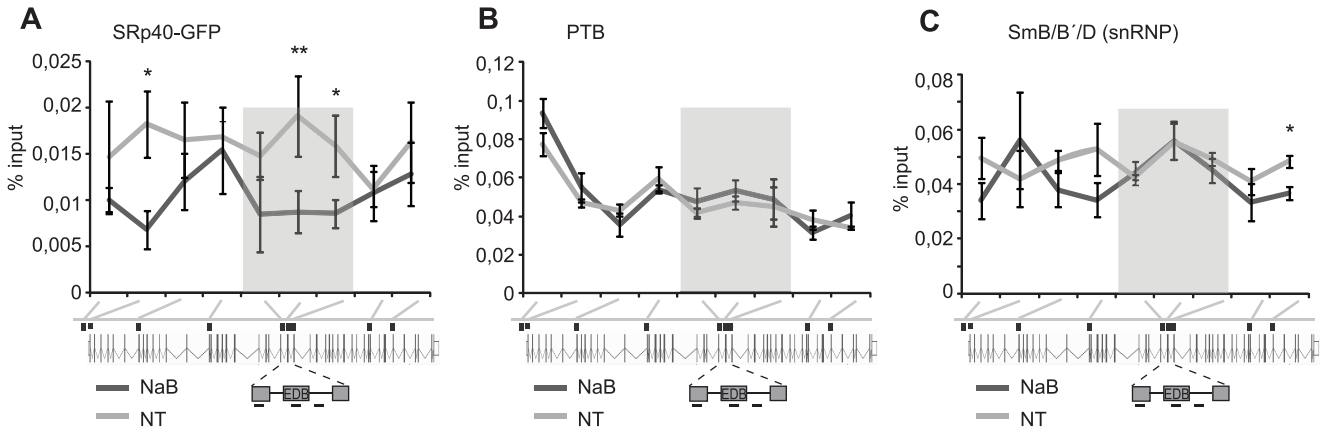

Figure 6. HDAC inhibition reduces SRp40 association with the EDB exon. (A) SRp40-GFP stably expressed from a BAC cell line was immunoprecipitated using an anti-GFP antibody. SRp40 interaction with the *FN1* gene was measured in cells treated for 6 h with NaB and in control cells. No changes in distribution of another splicing regulator PTB (B) or general splicing factors Sm proteins (C) were detected. Probes detecting gene loci around alternative EDB exon are shaded. The average of 3-5 experiments is shown, including SEM, ** indicates p≤0.01 and * p≤0.05 of the t-test.
doi:10.1371/journal.pone.0016727.g006

sodium butyrate, a short-chain fatty acid sodium salt, primarily inhibits class I HDACs, but also HDAC 10 [47]. Following the treatment of cells with each HDAC inhibitor we observed the exclusion of the EDB exon in all cases, albeit with differing efficiencies, which might reflect the fact that targets of these inhibitors were not fully overlapping (Fig. 7a). The effect on alternative splicing was detectable after 12 h of HDAC inhibition and sustained for an additional 12 h. The smallest exclusion was observed after VPA treatment and Western blot analysis of H4 acetylation revealed that VPA had the smallest effect on H4 acetylation (data not shown). These results correlated with previous finding that different inhibitors regulated acetylation of core histones with different efficiencies [44].

To further investigate the role of HDACs in alternative splicing, two highly expressed enzymes from the HDAC class I family, HDAC 1 and 2, were knocked-down by RNAi (Fig. S1). Similar to HDAC inhibition, depletion of HDAC1 but not HDAC2 had a strong effect on fibronectin splicing, resulting in EDB skipping (Fig. 7b). To demonstrate the splicing effect of the RNAi treatment was specific to HDAC1, we used RNAi-resistant mouse HDAC1, which reverted the EDB splicing pattern (Fig. 7c and Fig. S1a). The requirement for HDAC1 activity was further supported by expression of HDAC1 mutant carrying an inactivating mutation within the active site [49], which was unable to rescue the splicing phenotype after RNAi treatment. These results together with HDAC inhibition data demonstrate that the enzymatic activity of HDAC1 is important for the regulation of fibronectin alternative splicing.

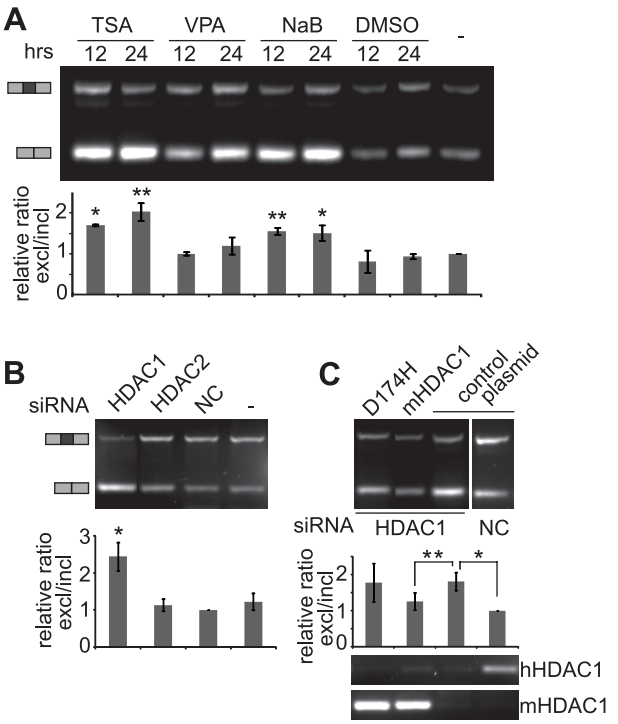

Figure 7. HDAC1 depletion affects EDB splicing. (A) Cells were treated with three different HDAC inhibitors (trichostatin A - TSA, valproic acid - VPA and sodium butyrate - NaB) for 12 h and 24 h. Their effect on fibronectin alternative EDB exon splicing was analyzed by RT-PCR (gel) or quantitative RT-PCR (graph). DMSO and non-treated cells served as negative controls. (B) HDAC1 and HDAC2 were down-regulated using siRNA and the resulting EDB splicing assayed. Depletion of HDAC1 but not HDAC2 resulted in EDB exon skipping. For knock-down efficiency see Fig. S1. (C) Endogenous HDAC1 was knocked-down by siRNA. The EDB skipping phenotype was rescued by expressing the mouse HDAC1 homologue (*mHDAC1*) but not an inactive mouse HDAC1 mutant (*D174H*). *NC* - negative control siRNA, *control plasmid* - GFP transfected cells. Expression of endogenous human (*hHDAC1*) and ectopically expressed mouse HDAC1 (*mHDAC1*) is shown below the graph. Graphs represent the average of three independent experiments measured by quantitative RT-PCR including SEM, ** indicates p≤0.01 and * p≤0.05 of the t-test.
doi:10.1371/journal.pone.0016727.g007

Discussion

There is an increasing amount of evidence to show that chromatin modifications play a vital role in pre-mRNA splicing. However, little is known about the mechanism and factors involved in this coupling. In this study, we show that alternative splicing of a hundreds of genes is regulated by HDAC activity. Recently published *in vitro* data indicate that several HDAC inhibitors work by stalling the splicing reaction, suggesting that protein acetylation might have a role in regulating splicing activity. However, Kuhn and his co-workers did not identify a potential protein target, leaving the mechanism of HDAC inhibitor action on splicing open [50]. In our study, we did not observe any

decrease in global mRNA production indicating that general splicing was not inhibited after HDAC inhibition with NaB. Thus, it remains to be clarified whether the observed *in vitro* effects of HDAC inhibitors apply to *in vivo* as well. Interestingly, about half of the proteins found in the spliceosome are acetylated but the functional role of these acetylations in splicing is yet to be established [44]. In addition, Mathias Mann and his colleagues tested two different HDAC inhibitors (SAHA targeting both HDAC classes I and II and MS-275 targeting class I) and found surprisingly low overlap of proteins with enhanced acetylation (43 out of 1750 proteins). Interestingly, histones were among the common targets and their acetylation increased after treatment with both drugs [44]. Here, we showed that at least two different inhibitors had the same effect on fibronectin splicing suggesting that both act via increased acetylation of histones as shared targets of different HDAC inhibitors. Moreover, we analyzed acetylation of the splicing regulator SRp40 but did not detect any changes upon HDAC inhibition. Despite that we cannot absolutely rule out the possibility that HDACs affect splicing via deacetylation of splicing proteins.

Recently it was shown in yeast that histone acetyltransferase Gcn5 affects co-transcriptional recruitment of U2 snRNPs [19]. The authors proposed that H3 acetylation at the promoter is responsible for the association of splicing factors with Pol II, resulting in their recruitment to the transcription unit. Our results with HDAC inhibitors suggest that histone acetylation can play a more direct role within the gene body. Histone acetylation around alternatively spliced elements affects splicing through the alteration of Pol II processivity that consequently modulates co-transcriptional association of splicing regulators with the nascent RNA.

The coupling between the elongation rate and alternative splicing was previously indicated by several studies. It was shown that the mutation in Pol II affecting the speed of synthesis, introduction of a pause site into the DNA template or depletion of transcription elongation factors influence alternative splicing outcome of transiently expressed reporter genes [7,11,28,30,46,51,52]. However, a direct molecular link between transcription dynamics and alternative splicing has not been described. Karla Neugebauer and her colleagues showed that reduction of RNA synthesis rate by camptothecin increases association of general splicing factors with the transcription unit indicating a kinetic coupling between RNA synthesis and interaction of splicing factors with the nascent RNA [16]. Here we describe that increase of Pol II dynamics in the vicinity of the alternative EDB exon correlates with reduced co-transcriptional recruitment of SRp40 supporting the model of kinetic coupling between transcription and splicing. It was shown that co-transcriptional association of SR proteins with the transcription unit is RNA dependent and determined by the RNA recognition domain [17]. Here we show that SR protein interaction with the transcription unit also depends on HDAC activity. In addition, SRp40 distribution does not correlate with Pol II occupancy, indicating that SRp40 does not interact primarily with Pol II.

More than 20 years ago it was hypothesized that splice-site selection is accomplished within a short window after transcription when RNA is naked and splicing factors can interact with target sequences [53]. Since then, co-transcriptional recognition of splice-sites was further supported by the study of Roberts et al. [52] and the significance of co-transcriptional splice-site recognition was recently demonstrated using the EDB exon that is recognized and spliced co-transcriptionally [12,13]. Here we propose that co-transcriptional recruitment of splicing factor is modulated by histone modifications and Pol II processivity, which provides a link between chromatin modifications, transcription and splicing. Because NaB treatment leads to exclusion as well as inclusion of alternative exons we speculate that HDAC inhibition reduces the interaction of splicing enhancers (in the case of exon exclusion) or silencers (in the case of exon inclusion).

Our data also provide an example of how global changes in chromatin structure can result in local changes within specific genes. Global analysis of alternative splicing further revealed that many genes whose alternative splicing is regulated by HDACs belong to families of proteins that are involved in signaling and cell organization; processes that are tightly connected with cell differentiation. The dynamic interplay between chromatin structure, transcription and splicing might explain why some genes are alternatively spliced in different cell types that contain the same or a similar set of splicing regulators and as such might represent an efficient method for global splicing regulation during development and cell differentiation. In addition, many genes affected by HDAC inhibitor are involved in regulation of membrane potential, a process linked to signal transduction in neurons. Thus, HDAC inhibitors (e.g. VPA) used in epilepsy treatment might act via modulation of splicing pattern in patient neurons. For example, misbalanced splicing of Tau protein is a primary cause of frontotemporal dementias. Interestingly, Tau gene is on the list of genes whose splicing is modulated by HDAC inhibition. HDAC inhibitors thus might serve as a drug that acts via alteration of splicing pattern, which can increase their therapeutic potential.

Materials and Methods

Cell culture and treatments

HeLa and HeLa-GFP-SRp40 cells were cultured in DMEM supplemented with 10% fetal calf serum, penicillin and streptomycin (Invitrogen) and treated with 50 μM DRB (5,6-Dichlorobenzimidazole 1-β-D-ribofuranoside), 5 mM sodium butyrate, 5 mM valproic acid, 330 nM trichostatin A (all from Sigma) or cycloheximide (50 μg/ml, Calbiochem). Y79 human retinoblastoma cells (ATCC HTB-18, a kind gift of Martina Zikova, IMG ASCR) were cultured in RPMI with 10% fetal calf serum, penicillin and streptomycin. HeLa-GFP-SRp40 cell line was a gift from Ina Poser and Tony Hyman from (Max Planck Institute of Molecular Cell Biology and Genetics, Germany).

Antibodies

The anti-RNA polymerase II H5 monoclonal antibody (recognizing phosphoserine 2) and H14 antibody (recognizing phosphoserine 5) were purchased from Covance, polyclonal antibodies against acetylated lysine 16 histone H4, Pol II (clone H-224) and mouse anti-GFP antibody (used for Western blotting) were from Santa Cruz. Monoclonal antibodies specific for HDAC1, polyclonal for acetyl-histone H4, acetyl-histone H3, H4K5ac H4K8ac and H4K12ac were all purchased from Upstate. Anti-H3, anti-H3K36me3 and 8WG16 anti-RNA polymerase II antibody (used for chromatin immunoprecipitations), anti-HDAC2 and anti-PTB antibodies were purchased from Abcam. hSnu114, hPrp4 and U5-40K antiserum was a gift from R. Lührmann (Max Planck Institute of Biophysical Chemistry, Göttingen, Germany), monoclonal m104 antibody recognizing phosphorylated SR proteins was a gift from K. Neugebauer (Max Planck Institute of Molecular Cell Biology and Genetics, Germany), anti-tubulin antibody was kindly provided by Pavel Draber (Institute of Molecular Genetics ASCR, Prague, Czech Republic), goat anti-GFP antibody used for ChIP was received from David Drechsel (Max Planck Institute of Molecular Cell Biology and Genetics, Germany) and the monoclonal anti-PTB antibody (BB7, used for chromatin immunoprecipitations) was

provided by Douglas L. Black (Howard Hughes Medical Institute, Los Angeles, USA). The anti-Sm antibody Y12 was produced from a hybridoma cell line (a gift of Karla Neugebauer, Max Planck Institute for Molecular Cell Biology, Dresden, Germany; [54]) in the antibody facility at the Institute of Molecular Genetics ASCR. The polyclonal pan anti-acetyl lysine antibody was obtained from Immunechem. Nonspecific mouse IgG and anti-mouse IgM were both purchased from Sigma.

Plasmids and siRNA transfection

Mouse HDAC1 cDNA (gift form Konstantinos Anastassiadis, TUD, Dresden, Germany) was subcloned into EGFP-N1 with SalI/NotI. The D174H mutation was introduced by PCR site-directed mutagenesis as described previously [55]. List of primers used in this study is listed in List S1. Plasmids were transfected with FuGENE HD (Roche Applied Science) according to manufacture's protocol. Preannealed siRNA duplexes were obtained from Ambion: HDAC1 5′-GGGAUACUUUUAUG-CAACCtt-3′; HDAC2 5′-GCCACUGCCGAAGAAAUGAtt-3′; The negative control 1 siRNA from Ambion was used as a negative control. Oligofectamine (Invitrogen) was used for siRNA transfection according to the manufacture's protocol. Cells were incubated for 48 h (78 h for rescue experiments) before further treatment.

RNA isolation and RT PCR

Total RNA was purified with TRIzol (Invitrogen), reverse transcribed using SuperScript III (Invitrogen) and cDNA amplified by Taq polymerase (MBI Fermentas). Primers used for RT-PCR and qPCR are listed in List S1.

Quantitative real-time PCR

The ratio of mRNA with EDB exon skipped/included was calculated from relative Ct values of primers 41196 (*FN1* exon 24) and 42658 (*FN1* exon 25, EDB) according to $R_{treatment} = 2^{(CtEDB - CtEDBupstream)}$ and normalized to control cells ($R = R_{treated}/R_{control}$). RNA polymerase II processivity was calculated from relative Ct values of primer pairs A (upstream) and B (downstream) according to pre-mRNA $ratio_{distal/proximal} = 2^{(CtA - CtB)}$.

Exon arrays

HeLa cells were treated with 5 mM NaB for 15 h and their RNA was isolated with TRIzol. For each sample, 1 µg of total RNA was processed, amplified, and labeled according to the Affymetrix GeneChip Whole Transcript (WT) Sense Target Labeling Assay (P/N 701880 Rev. 5). This protocol resulted in biotinylated sense strand cDNA samples, which were subsequently hybridized to GeneChip Human Exon 1.0 ST Array (Affymetrix, Inc., U.S.). Washing, staining, and scanning of the arrays was done according to the Affymetrix GeneChip Expression Wash, Stain, and Scan User Manual (P/N 702731) protocol. The data were analysed with the Partek Genomics Suite 6.4 software (Partek Incorporated, U.S.) using the RMA (Robust Multi-Array) algorithm. Only probesets that were present in the 'core' meta-probe list (17 800 RefSeq genes and full-length GenBank mRNAs) were used to identify alternative splicing events with Alt-splice ANOVA. A list of genes with alternative splicing was generated by using alternative splicing p-values corresponding to the 0.005 FDR criterion as a cutoff. To identify differentially expressed genes a p-value of 0.05 FDR was used as a cutoff.

Changes in exon expression were normalized to the changes in gene expression $(NaB_{exon\ expression}/NT_{exon\ expression})/(NaB_{gene\ expression}/NT_{gene\ expression})$ and all exons with values ≥ 3 were considered as included, exons $\leq 1/3$ as excluded. All data are MIAME compliant and that the raw data has been deposited in a MIAME compliant database (GEO, the accession numbers is GSE17397) available at the Gene Expression Omnibus (GEO) (http://www.ncbi.nlm.nih.gov/geo/info/linking.html).

ChIP assays

Y79 or Hela cells (treated with 5 mM NaB for 6 h) were washed with PBS, crosslinked with 1% formaldehyde/PBS for 15 min at room temperature and the reaction was stopped by the addition of glycine (final conc. 125 mM). Cells were scraped into RIPA buffer (150 mM NaCl, 1% NP-40, 0.5% deoxycholate, 0.1% SDS, 50 mM Tris-HCl, pH 8.0, 5 mM EDTA, 0.5 mM PMSF, complete protease inhibitor cocktail (Calbiochem), 50 mM NaF and 0.2 mM sodium orthovanadate) and sonicated to generate ~500 nt chromatin fragments. The same total amount of protein (1 mg or 0.3 mg for histone H3) was used for immunoprecipitation. Immunoprecipitation with the appropriate antibodies (20 µg anti-P-ser 2 and anti-P-ser 5 RNA Pol II, 5 µg anti-RNA pol II, 12 µg goat anti-GFP, 5 µl anti-PTB, 500 µl Y12 cell supernatant and 3 µg anti-H3 per reaction) was performed at 4°C overnight. Subsequently, the beads were rinsed twice with RIPA, four times with 100 mM Tris-HCl, pH 8.5, 500 mM LiCL, 1% Nonidet P-40, 1% deoxycholic acid, twice again with RIPA and twice with TE. Protein-DNA complexes were eluted with 1% SDS for 10 minutes at 65°C, decrosslinked in the presence of 200 mM NaCl for 5 h at 65°C and treated with 20 µg proteinase K for 30 min at 45°C. DNA was phenol/chloroform extracted, precipitated and amplified by quantitative real-time PCR on a LightCycler 480 System (Roche Applied Science). Data sets were normalized to ChIP input values, and the relative proportions of gene fragments obtained from ChIP with a nonspecific antibody were subtracted from the values obtained from templates derived from ChIP with the specific antibody: $2^{(Ct(input) - Ct(spec))} - 2^{(Ct(input) - Ct(unspec))}$. To measure the level of phosphorylated RNA pol II the signal obtained for gene regions was further normalized to the value obtained in non-treated cells with the primer pair *FN1* 65438. To compare the level of acetylated histone H4 on *FN1* in HeLa and Y79 cells the signal obtained for *FN1* was normalized to the primer pair amplifying an intergenic region on chromosome 10 where no annotated genes could be found [16].

Native ChIP assays

Hela cells (treated with 5 mM NaB for 6 h) were scraped into PBS and resuspended in 0.3 M sucrose, 60 mM KCl, 15 mM NaCl, 5 mM $MgCl_2$, 0.1 mM EGTA, 0,2% NP-40, 15 mM Tris-HCl, pH 7.7, 0.5 mM DTT, complete protease inhibitor cocktail (Calbiochem) and 5 mM NaB. Nuclei were released by passage through a 22 G needle and loaded on a sucrose gradient (1.2 M sucrose, 60 mM KCl, 15 mM NaCl, 5 mM $MgCl_2$, 0.1 mM EGTA, 15 mM Tris-HCl, pH 7.7, 0.5 mM DTT, protease inhibitors and 5 mM NaB) and centrifuged for 20 min at 2000 g, 4°C. Pellets were resuspended in Mnase digestion buffer (0.32 M sucrose, 1 mM $CaCl_2$, 4 mM $MgCl_2$, 15 mM Tris-HCl pH 7.7 and protease inhibitors) and digestion performed for 6 min at 37°C (1U Mnase/30 µg chromatin). Reactions were stopped by EDTA (final concentration 10 mM) and centrifuged. The supernatant was taken and the pellet resuspended in 0.2 mM EDTA, 1 mM Tris/HCl, pH 7.7, incubated for 1 h at 4°C, centrifuged again and both supernatants mixed. ~100 µg of chromatin was diluted in nChIP buffer (50 mM NaCl, 5 mM EDTA, 50 mM Tris/HCl, pH 7.7) and incubated overnight at 4°C with appropriate antibody (10 µg anti-acetyl H3, 6 µg anti-

H3K36me3, 4 µg anti-H4K16ac, 10 µg nonspecific IgG, 5 µl anti-acetyl H4, 6 µl anti-H4K12ac and 5 µl anti-H4K5ac and anti-H4K8ac). The beads were washed once with nChIP buffer, then twice in the same buffer with increasing salt concentration (75 mM NaCl, 125 mM NaCl, 175 mM NaCl). Complexes were eluted with 1% SDS for 15 min at room temperature, treated with 20 µg proteinase K for 30 minutes at 45°C and DNA was recovered with the QIAGEN PCR Purification Kit, quantified by qPCR and signal compared to the input and non-specific antibody: $2^{(Ct(input) - Ct(spec))}$ -$2^{(Ct(input) - Ct(unspec))}$.

Western blotting and immunoprecipitation

Western blotting and immunoprecipitation was performed as described previously [55]. Protein extraction from TRIzol after RNA isolation was done according to manufacturer's protocol.

Supporting Information

Figure S1 HDAC1 activity regulates fibronectin alternative splicing. (A) Before cells were transfected with wild type mouse HDAC1 or a control plasmid, endogenous HDAC1 was knocked-down by siRNA. Subsequently, EDB splicing was analyzed by RT-PCR. Expression of HDAC1 after siRNA treatment was assayed by Western blotting. The anti-HDAC1 antibody cross-reacted with mouse HDAC1, which resulted in an increased signal in the last line. Snu114 served as a loading control. (B) Reduction of HDAC2 expression after siRNA treatment. Total RNA and proteins were isolated from cells treated with HDAC2 siRNA, negative control siRNA or untreated. The relative amount of HDAC2 mRNA was assayed by RT-qPCR and protein by Western blotting.
(EPS)

List S1 Supplementary primer list.
(DOC)

Table S1 Alternative spliced genes decreased expression.
(XLS)

Acknowledgments

We thank Reinhard Lührmann, David Drechsel, Ina Poser, Tony Hyman, Karla Neugebauer, Douglas Black, Pavel Draber, Marta Miaczynska and Konstantinos Anastassiadis for gifts of reagents. We also thank Julia Jarrells for help with microarrays, Petr Svoboda, Karla Neugebauer and Stanek's lab members for helpful comments and Alicia Corlett for proofreading.

Author Contributions

Conceived and designed the experiments: JH DS. Performed the experiments: JH SH ED TT JI. Analyzed the data: JH SH. Wrote the paper: JH DS.

References

1. Wahl MC, Will CL, Luhrmann R (2009) The spliceosome: design principles of a dynamic RNP machine. Cell 136: 701–718.
2. Irimia M, Rukov JL, Roy SW (2009) Evolution of alternative splicing regulation: changes in predicted exonic splicing regulators are not associated with changes in alternative splicing levels in primates. PLoS One 4: e5800.
3. Hicks MJ, Yang CR, Kotlajich MV, Hertel KJ (2006) Linking splicing to Pol II transcription stabilizes pre-mRNAs and influences splicing patterns. PLoS Biol 4: e147.
4. Das R, Dufu K, Romney B, Feldt M, Elenko M, et al. (2006) Functional coupling of RNAP II transcription to spliceosome assembly. Genes Dev 20: 1100–1109.
5. Perales R, Bentley D (2009) "Cotranscriptionality": the transcription elongation complex as a nexus for nuclear transactions. Mol Cell 36: 178–191.
6. Moore MJ, Proudfoot NJ (2009) Pre-mRNA processing reaches back to transcription and ahead to translation. Cell 136: 688–700.
7. de la Mata M, Alonso CR, Kadener S, Fededa JP, Blaustein M, et al. (2003) A slow RNA polymerase II affects alternative splicing in vivo. Mol Cell 12: 525–532.
8. Nogues G, Kadener S, Cramer P, Bentley D, Kornblihtt AR (2002) Transcriptional activators differ in their abilities to control alternative splicing. J Biol Chem 277: 43110–43114.
9. Das R, Yu J, Zhang Z, Gygi MP, Krainer AR, et al. (2007) SR proteins function in coupling RNAP II transcription to pre-mRNA splicing. Mol Cell 26: 867–881.
10. de la Mata M, Kornblihtt AR (2006) RNA polymerase II C-terminal domain mediates regulation of alternative splicing by SRp20. Nat Struct Mol Biol 13: 973–980.
11. Kornblihtt AR (2006) Chromatin, transcript elongation and alternative splicing. Nat Struct Mol Biol 13: 5–7.
12. Pandya-Jones A, Black DL (2009) Co-transcriptional splicing of constitutive and alternative exons. RNA 15: 1896–1908.
13. Neugebauer KM (2002) On the importance of being co-transcriptional. J Cell Sci 115: 3865–3871.
14. Lacadie SA, Rosbash M (2005) Cotranscriptional spliceosome assembly dynamics and the role of U1 snRNA:5′ss base pairing in yeast. Mol Cell 19: 65–75.
15. Kotovic KM, Lockshon D, Boric L, Neugebauer KM (2003) Cotranscriptional recruitment of the U1 snRNP to intron-containing genes in yeast. Mol Cell Biol 23: 5768–5779.
16. Listerman I, Sapra AK, Neugebauer KM (2006) Cotranscriptional coupling of splicing factor recruitment and precursor messenger RNA splicing in mammalian cells. Nat Struct Mol Biol 13: 815–822.
17. Sapra AK, Anko ML, Grishina I, Lorenz M, Pabis M, et al. (2009) SR protein family members display diverse activities in the formation of nascent and mature mRNPs in vivo. Mol Cell 34: 179–190.
18. Gornemann J, Kotovic KM, Hujer K, Neugebauer KM (2005) Cotranscriptional spliceosome assembly occurs in a stepwise fashion and requires the cap binding complex. Mol Cell 19: 53–63.
19. Gunderson FQ, Johnson TL (2009) Acetylation by the transcriptional coactivator Gcn5 plays a novel role in co-transcriptional spliceosome assembly. PLoS Genet 5: e1000682.
20. Batsche E, Yaniv M, Muchardt C (2006) The human SWI/SNF subunit Brm is a regulator of alternative splicing. Nat Struct Mol Biol 13: 22–29.
21. Tyagi A, Ryme J, Brodin D, Ostlund Farrants AK, Visa N (2009) SWI/SNF associates with nascent pre-mRNPs and regulates alternative pre-mRNA processing. PLoS Genet 5: e1000470.
22. Sims RJ, 3rd, Millhouse S, Chen CF, Lewis BA, Erdjument-Bromage H, et al. (2007) Recognition of trimethylated histone H3 lysine 4 facilitates the recruitment of transcription postinitiation factors and pre-mRNA splicing. Mol Cell 28: 665–676.
23. Loomis RJ, Naoe Y, Parker JB, Savic V, Bozovsky MR, et al. (2009) Chromatin binding of SRp20 and ASF/SF2 and dissociation from mitotic chromosomes is modulated by histone H3 serine 10 phosphorylation. Mol Cell 33: 450–461.
24. Schwartz S, Meshorer E, Ast G (2009) Chromatin organization marks exon-intron structure. Nat Struct Mol Biol 16: 990–995.
25. Tilgner H, Nikolaou C, Althammer S, Sammeth M, Beato M, et al. (2009) Nucleosome positioning as a determinant of exon recognition. Nat Struct Mol Biol.
26. Spies N, Nielsen CB, Padgett RA, Burge CB (2009) Biased chromatin signatures around polyadenylation sites and exons. Mol Cell 36: 245–254.
27. Nahkuri S, Taft RJ, Mattick JS (2009) Nucleosomes are preferentially positioned at exons in somatic and sperm cells. Cell Cycle 8: 3420–3424.
28. Allo M, Buggiano V, Fededa JP, Petrillo E, Schor I, et al. (2009) Control of alternative splicing through siRNA-mediated transcriptional gene silencing. Nat Struct Mol Biol 16: 717–724.
29. Hon G, Wang W, Ren B (2009) Discovery and annotation of functional chromatin signatures in the human genome. PLoS Comput Biol 5: e1000566.
30. Schor IE, Rascovan N, Pelisch F, Allo M, Kornblihtt AR (2009) Neuronal cell depolarization induces intragenic chromatin modifications affecting NCAM alternative splicing. Proc Natl Acad Sci U S A 106: 4325–4330.
31. Kolasinska-Zwierz P, Down T, Latorre I, Liu T, Liu XS, et al. (2009) Differential chromatin marking of introns and expressed exons by H3K36me3. Nat Genet 41: 376–381.
32. Luco RF, Pan Q, Tominaga K, Blencowe BJ, Pereira-Smith OM, et al. (2010) Regulation of Alternative Splicing by Histone Modifications. Science 327: 996–1000.
33. Zhou J, Yu Q, Zou T (2008) Alternative splicing of exon 10 in the tau gene as a target for treatment of tauopathies. BMC Neurosci 9 Suppl 2: S10.
34. Munoz MJ, Perez Santangelo MS, Paronetto MP, de la Mata M, Pelisch F, et al. (2009) DNA damage regulates alternative splicing through inhibition of RNA polymerase II elongation. Cell 137: 708–720.

35. White ES, Baralle FE, Muro AF (2008) New insights into form and function of fibronectin splice variants. J Pathol 216: 1–14.
36. Caputi M, Casari G, Guenzi S, Tagliabue R, Sidoli A, et al. (1994) A novel bipartite splicing enhancer modulates the differential processing of the human fibronectin EDA exon. Nucleic Acids Res 22: 1018–1022.
37. Kornblihtt AR, Pesce CG, Alonso CR, Cramer P, Srebrow A, et al. (1996) The fibronectin gene as a model for splicing and transcription studies. FASEB J 10: 248–257.
38. Du K, Peng Y, Greenbaum LE, Haber BA, Taub R (1997) HRS/SRp40-mediated inclusion of the fibronectin EIIIB exon, a possible cause of increased EIIIB expression in proliferating liver. Mol Cell Biol 17: 4096–4104.
39. Lim LP, Sharp PA (1998) Alternative splicing of the fibronectin EIIIB exon depends on specific TGCATG repeats. Mol Cell Biol 18: 3900–3906.
40. Norton PA, Hynes RO (1993) Characterization of HeLa nuclear factors which interact with a conditionally processed rat fibronectin pre-mRNA. Biochem Biophys Res Commun 195: 215–221.
41. Norton PA (1994) Polypyrimidine tract sequences direct selection of alternative branch sites and influence protein binding. Nucleic Acids Res 22: 3854–3860.
42. Zahler AM, Lane WS, Stolk JA, Roth MB (1992) SR proteins: a conserved family of pre-mRNA splicing factors. Genes Dev 6: 837–847.
43. Poser I, Sarov M, Hutchins JR, Heriche JK, Toyoda Y, et al. (2008) BAC TransgeneOmics: a high-throughput method for exploration of protein function in mammals. Nat Methods 5: 409–415.
44. Choudhary C, Kumar C, Gnad F, Nielsen ML, Rehman M, et al. (2009) Lysine acetylation targets protein complexes and co-regulates major cellular functions. Science 325: 834–840.
45. LeRoy G, Rickards B, Flint SJ (2008) The double bromodomain proteins Brd2 and Brd3 couple histone acetylation to transcription. Mol Cell 30: 51–60.
46. Kadener S, Fededa JP, Rosbash M, Kornblihtt AR (2002) Regulation of alternative splicing by a transcriptional enhancer through RNA pol II elongation. Proc Natl Acad Sci U S A 99: 8185–8190.
47. Blackwell L, Norris J, Suto CM, Janzen WP (2008) The use of diversity profiling to characterize chemical modulators of the histone deacetylases. Life Sci 82: 1050–1058.
48. Khan N, Jeffers M, Kumar S, Hackett C, Boldog F, et al. (2008) Determination of the class and isoform selectivity of small-molecule histone deacetylase inhibitors. Biochem J 409: 581–589.
49. Taplick J, Kurtev V, Kroboth K, Posch M, Lechner T, et al. (2001) Homo-oligomerisation and nuclear localisation of mouse histone deacetylase 1. J Mol Biol 308: 27–38.
50. Kuhn AN, van Santen MA, Schwienhorst A, Urlaub H, Luhrmann R (2009) Stalling of spliceosome assembly at distinct stages by small-molecule inhibitors of protein acetylation and deacetylation. RNA 15: 153–175.
51. Barboric M, Lenasi T, Chen H, Johansen EB, Guo S, et al. (2009) 7SK snRNP/P-TEFb couples transcription elongation with alternative splicing and is essential for vertebrate development. Proc Natl Acad Sci U S A 106: 7798–7803.
52. Roberts GC, Gooding C, Mak HY, Proudfoot NJ, Smith CW (1998) Co-transcriptional commitment to alternative splice site selection. Nucleic Acids Res 26: 5568–5572.
53. Eperon LP, Graham IR, Griffiths AD, Eperon IC (1988) Effects of RNA secondary structure on alternative splicing of pre-mRNA: is folding limited to a region behind the transcribing RNA polymerase? Cell 54: 393–401.
54. Lerner EA, Lerner MR, Janeway CA, Jr., Steitz JA (1981) Monoclonal antibodies to nucleic acid-containing cellular constituents: probes for molecular biology and autoimmune disease. Proc Natl Acad Sci U S A 78: 2737–2741.
55. Huranova M, Hnilicova J, Fleischer B, Cvackova Z, Stanek D (2009) A mutation linked to retinitis pigmentosa in HPRP31 causes protein instability and impairs its interactions with spliceosomal snRNPs. Hum Mol Genet 18: 2014–2023.

Nucleus 2:3, 1-7; May/June 2011; © 2011 Landes Bioscience

Where splicing joins chromatin

Jarmila Hnilicová and David Staněk*

Department of RNA Biology; Institute of Molecular Genetics; Academy of Sciences of the Czech Republic; Prague, Czech Republic

Key words: chromatin, exon, alternative splicing, transcription, snRNP, histone methylation, histone acetylation, nucleosome

Abbreviations: HDAC, histone deacetylase; snRNP, small ribonucleoprotein particle; hnRNP, heterogeneous nuclear ribonucleoprotein

There are numerous data suggesting that two key steps in gene expression—transcription and splicing influence each other closely. For a long time it was known that chromatin modifications regulate transcription, but only recently it was shown that chromatin and histone modifications play a significant role in pre-mRNA splicing. Here we summarize interactions between splicing machinery and chromatin and discuss their potential functional significance. We focus mainly on histone acetylation and methylation and potential mechanisms of their role in splicing. It seems that whereas histone acetylation acts mainly by alterating the transcription rate, histone methylation can also influence splicing directly by recruiting various splicing components.

Pre-mRNA Splicing Regulation

The vast majority of our genes has a puzzle-like structure where short coding sequences (exons) must be correctly identified and joined together while surrounding much longer non-coding sequences (introns) have to be removed before a mature mRNA is exported to the cytoplasm and translated. A typical human gene contains 8 introns of average length ~3.4 kb but much larger examples were found (e.g., the last intron of glypican 5 gene is 721 kb in length).[1] In contrast to long introns, exons are short having an average length of 145 bp and represent only a small fraction of primary pre-mRNA transcripts. An extreme example is the largest human gene *CNTNAP2* encoding Caspr2 protein which spans over 2.3 Mb (!) but its spliced mRNA is only 10 kb long because 99.6% of the *CNTNAP2* gene sequence corresponds to introns.[2]

To further complicate matters, exons and introns are not always recognized identically and, for example, a particular exon can be skipped in a fraction of mature mRNAs. This process, called alternative splicing, produces different mRNA isoforms from one gene which significantly increases the coding potential of our genome. It is estimated that in human cells almost 95% of genes are alternatively spliced[3,4] and that there are on average 7 different alternative splicing events per single gene leading to different mRNA variants.[4] The complexity of the process puts pressure on cells to regulate splicing precisely. Then how is alternative splicing regulated?

Introns contain consensus splice sites at both ends. However, compared to yeasts, most splice site sequences in higher metazoans are degenerate and additional regulatory sequences in pre-mRNA are needed to help basal splicing machinery (the spliceosome) to recognize correct splice sites.[5] These regulatory sequences are bound by many different splicing regulatory proteins which are able to interact with the splicing complex. The combinatorial interplay among splicing factors results in the usage (or skipping) of individual splice sites. Some of the splicing regulatory proteins are widely expressed in different tissues (such as PTB or SR proteins) while the others are highly tissue specific (for example, Nova proteins are expressed almost exclusively in neurons). The differences in the expression of splicing regulatory proteins are believed to be responsible for tissue-specific alternative splicing.[6]

The splicing code—the sum of all splicing related features in a pre-mRNA sequence—can explain a majority of differences in alternative splicing between individual tissues (e.g., 74% out of 97 tested alternative splicing events specific for the central nervous system and muscle tissue were properly predicted based on a pre-mRNA sequence).[7] Although the splicing code model was effective to estimate whether the alternative exon was included or skipped it was less precise in the prediction of the level of inclusion/exclusion when tested by Barash et al. which indicates a presence of additional regulatory signals.[7]

Splicing is Cotranscriptional and Occurs in the Vicinity of Chromatin

Intron recognition and removal likely occur in the cell nucleus very shortly after intron transcription. Splicing complexes associate with pre-mRNA immediately after the target sequences are synthesized and splicing of many introns is completed before pre-mRNA transcription termination.[8-15] This was shown not only for long human genes but also for many yeast genes, which are much shorter than human genes and are spliced cotranscriptionally as well.[16-21] Moreover, splicing can induce pausing of RNA polymerase II during transcription[21] and RNA polymerase II was shown to pause in terminal exons, which increases the time window for cotranscriptional splicing.[16]

This suggests that transcription and splicing are coupled not only in time, but also functionally. It was shown that the

*Correspondence to: David Staněk; Email: stanek@img.cas.cz
Submitted: 03/09/11; Revised: 04/18/11; Accepted: 04/19/11
DOI: XXXXXXXXXXX

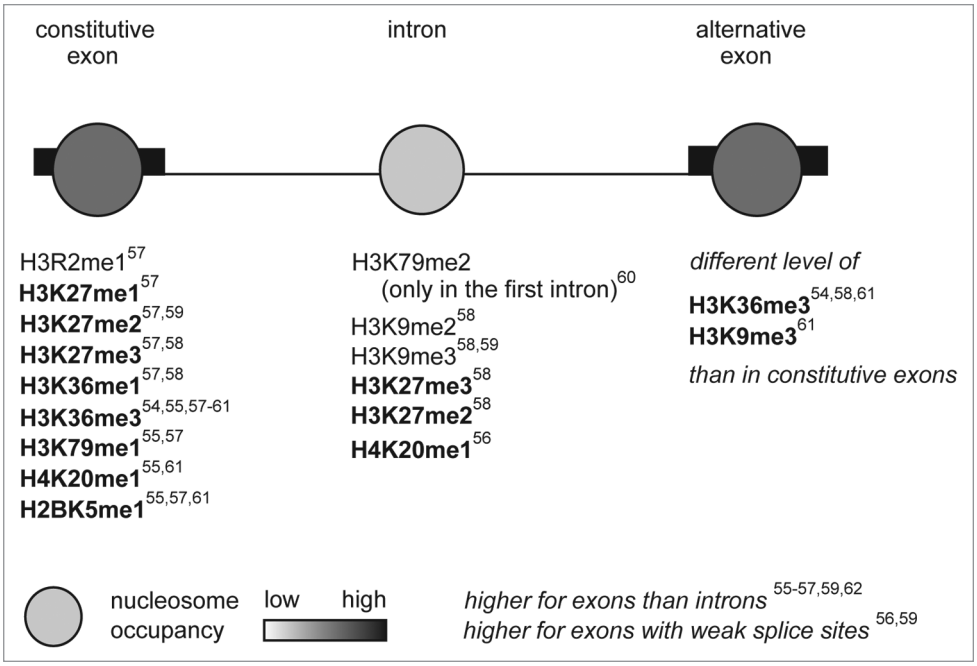

Figure 1. Different sets of chromatin modifications were identified at exons and at introns. The enrichment of a specific histone mark depends on the position of an exon within a gene (e.g., H2BK5me1 and H4K20me1 are found preferentially at exons toward the 5′ end of genes),[61] or it can depend on gene expression (highlighted in bold), e.g., H3K27me3 is high at exons of low expressed genes, but it was reported to be elevated at introns of highly expressed genes.[58]

promoter composition and the speed of transcription can influence splicing.[22-33] The speed of transcription affects the dynamics of presentation of individual splice and regulatory sites to the splicing machinery, which then results in using different splice sites not only in transfected minigenes but also in endogenous genes.[34-43] The carboxyterminal domain of RNA polymerase II itself can also contribute to splicing factors recruitment which then might influence alternative splicing.[44,45]

Average eukaryotic RNA polymerase II elongation rate vary from ~1.5–4.5 kb/min,[8,14,46-49] which means that an average intron is transcribed in 1–3 minutes. An average splicing event takes 30 seconds to accomplish[19,20,50,51] and therefore it is very likely that recognition of splice sites as well as intron excision occur when pre-mRNA is still in close proximity to the chromatin of its own gene, and this makes it possible for chromatin modifications to influence splicing.

Chromatin Marks Affecting Splicing

In cells, DNA is packed together with histones in nucleosomes. Each nucleosome consists of an octamer composed of four core histones (H2A, H2B, H3 and H4) and 147 bp DNA, which is wrapped around this octamer. Histones can be posttranslationally modified on many sites, especially at their N-terminal ends that protrude out of the nucleosomal core. Regulation of gene activity via nucleosome positioning and histone modifications has been well established.[52,53] However, it seems that nucleosome positions and modifications are also important for exon recognition. In the genome, nucleosomes are preferentially found at exons and exon-positioned nucleosomes carry a specific set of histone modifications (see **Fig. 1**),[54-62] although the latter statement is still a matter of a debate.[63,64] Three histone marks were shown to affect splicing and/or to mediate interaction of histones with splicing factors: methylation, acetylation and phosphorylation (see **Table 1**). These modifications differ in the charge they introduce into the chromatin. While methylations are electrostatically neutral and their action is mediated via specific protein readers, it is supposed that histone acetylation, which adds a negative charge, can itself affect nucleosomal stability and make chromatin more accessible (reviewed in ref. 61). Histone phosphorylation, which brings a negative charge, can regulate the binding of SR proteins to the chromatin during the cell cycle but its role in splicing regulation is unclear.[65] The modifications also differ substantially in their turnover: the addition and removal of acetylation is rapid and most acetyl residues are exchanged within minutes, phosphorylations can last up to several hours and methylations, the most stable ones, can be present even for days.[66]

Histone Acetylation Induces Changes in the Alternative Splicing

Histone acetylation can be easily increased in cells by histone deacetylase (HDAC) inhibitors and the treatment with HDAC inhibitors influences an alternative splicing pattern of transiently expressed minigene splicing reporters.[36] Recently, we showed that HDAC inhibition changes alternative splicing of ~700 endogenous human genes. In addition, HDAC1 depletion affected the splicing pattern of the fibronectin gene.[38] The correlation between histone acetylation and alternative splicing was also observed with the *NCAM* gene, whose alternative splicing is regulated by depolarization of neuronal membranes.[67] In this instance, it is worthy to note that many genes that changed alternative splicing after HDAC inhibition were encoding various ion channels and regulators of cell cycle or apoptosis.[38] Thus it seems that acetylation preferentially modulates alternative splicing of genes that must react quickly to changing conditions.

The mechanism by which acetylation modulates splicing has been connected to RNA polymerase II processivity. Increased RNA polymerase II processivity, which is induced by histone acetylation, modulates the association of splicing regulators with the nascent RNA as was shown in the case of the fibronectin gene and the splicing regulator SRp40 (SRSF5).[38] However, in yeast

Table 1. Interaction of chromatin and splicing machinery

Histone modification	Interacting protein	Link to splicing
H3K4me3	Chd1	Chd1 associates with SRp20 (SRSF3)[119] and U2 snRNP (via SF3 subunits) and increases efficiency of pre-mRNA splicing[86]
H3K4me3	Sgf29	Sgf29 interacts with SF3B5 (SF3b10) and SF3B3 (SF3b130) subunits of U2 snRNP[87]
H3K9me3	PTB, hnRNP A1, hnRNP A/B, hnRNP A2/B1, hnRNP K, hnRNP L	PTB and most of the hnRNP proteins are direct regulators of alternative splicing but it is not known whether the association of hnRNP proteins with H3K9me3[87] affects splicing
methylated H3K9	HP1 (HP1a)	HP1 binds to Drosophila hnRNP proteins (PEP, DDP1, HRB87F)[114]
H3K36me3	MRG15	MRG15 recruits PTB; tethering of PTB to chromatin changes alternative splicing[88]
methylated H3K79	TP53BP1	TP53BP1 immunoprecipitates U1 and U2 snRNA (but also other small RNAs)[120]
histone H3 (not phosphorylated at serine 10)	SRp20 (SRFS3), SF2/ASF (SRSF1)	Both SR proteins participate in constitutive and alternative splicing, but the role of interaction with histone H3 in splicing is not known[65]
DNA methylation	MeCP2	MeCP2 regulates alternative splicing[121]

the deletion of histone deacetylases or the histone acetyltransferase Gcn5 influenced cotranscriptional recruitment of spliceosomal proteins without obvious changes in RNA polymerase II distribution along the gene.[68,69] It is then possible that histone acetylation also affects splicing directly via the recruitment of spliceosomal subunits, without altering transcription elongation.

Mutual Influence between Splicing Machinery and Chromatin

The spliceosome assembles from five small ribonucleoprotein particles (snRNPs) that assemble on the pre-mRNA in a stepwise manner.[17,18,50,70-75] Each snRNP consists of several proteins and one small nuclear RNA (snRNA) according to which the snRNPs are named.[76] First, the U1 snRNP binds to the pre-mRNA and recognizes the 5' splice site. Then, the U2 snRNP binds to the vicinity of the 3' splice site, closely followed by the U4/U6•U5 tri-snRNP. After tri-snRNP incorporation the spliceosome undergoes extensive rearrangements that result in the formation of an active complex that catalyzes both steps of the splicing reaction. The U1 and U2 snRNP binding is important for the accuracy of splicing as this defines the intron. U1 and U2 snRNPs associate with pre-mRNA quickly and they are already present when RNA polymerase transcribes only hundreds of nucleotides downstream of splice sites.[11,17,74,75] This implies that snRNPs are in close vicinity to chromatin and their association with pre-mRNA could be influenced by chromatin and vice versa, snRNPs themselves might influence the chromatin state. One example of plausible mutual influence is discussed below.

5' Splice Site Influences Transcription and Chromatin

U1 snRNA interacts with chromatin[77] and it has been shown that the presence of functional 5' splice site in the gene can affect chromatin state.[78] However, U1 snRNA—chromatin interaction might reflect only the role of U1 snRNA in transcription. The U1 snRNA associates with proteins from two general transcription factor complexes, TFIID and TFIIH.[77,79] In the TFIIH complex U1 snRNA enhances transcription presumably through the interaction with cyclin H and regulation of the cyclin H associated kinase CDK7,[79,80] which phosphorylates carboxyterminal domain of RNA polymerase II. It was shown that the functional 5' splice site near the promoter enhances the assembly of general transcription factors at this promoter.[78] If the presence of U1 snRNA (and U1 snRNP) stimulates transcription then intron-containing genes should be transcribed more than intron-less genes. This is true in *Saccharomyces cerevisiae* where almost half of all introns found in the genome are located in highly expressed genes coding ribosomal proteins (95 out of 132 of these genes contain introns).[70,81] Moreover, deletion of introns from two non-ribosomal yeast genes decreases the expression of these genes.[82] In mammalian cells, the presence of intron with functional splice sites also increases gene expression.[78,82-85]

Interestingly, the presence of a functional 5' splice site can increase gene specific H3K9 acetylation and H3K4me3,[78] which are chromatin marks associated with active transcription. In another study, the level of H3K4me3 at the minigene decreased when both splice sites were mutated compared to the minigene containing intron with functional splice sites, however the reported difference was quite small.[83] It is not known whether these changes in the chromatin state are coupled generally with splicing or whether they are specifically related to U1 snRNP recruitment. Moreover, it is difficult to distinguish between the cause and the consequence in these observations. Chromatin modifications might reflect only changes in transcription and the increase of H3K4 trimethylation and histone H3 acetylation occurs independently of splicing. An example of mutual dependence is H3K4me3: the level of H3K4me3 correlates with transcription activity and is enhanced by the presence of a functional 5' splice site within the gene but in turn this chromatin modification affects splicing (see below).

H3K4me3 Associates with U2 snRNP

Association of the U2 snRNP with chromatin is mediated by trimethylated lysine 4 histone H3.[86,87] In addition, the functional significance of H3K4me3 for splicing was shown.[86,88] Several complexes that methylate lysine 4 of histone H3 in human cells share the same structural subunits.[89] The depletion of one of these

subunits, Ash2, leads to the decrease of overall H3K4me3.[90,91] Ash2 depletion causes a decrease of splicing efficiency immediately after induction of transcription[86] and Ash2 overexpression affects alternative splicing.[88]

U2 snRNP binds to chromatin via the chromatin remodeling protein Chd1 that binds H3K4me3 and enhances pre-mRNA splicing efficiency within a short time window after activation of gene transcription.[86] U2 snRNP subunits also interact with another H3K4me3 reader, Sgf29 protein.[87] Considering that H3K4me3 is frequently elevated around transcription start sites,[92-97] it is surprising that this particular histone modification interacts with U2 snRNP. However, the level of H3K4me3 positively correlates with gene expression indicating that U2 snRNP might be recruited preferentially to highly expressed genes.[93,94,97]

As mentioned before, U2 snRNP recruitment to the transcription unit is also regulated by the histone acetyltransferase Gcn5.[68] Although Gcn5 participates in a number of protein complexes the most important for U2 snRNP recruitment seems to be the SAGA complex.[68,98] Gcn5 in the SAGA complex acetylates predominantly histones at promoters[68] that subsequently serve as an anchor stabilizing the binding of the whole SAGA complex to the promoter.[99] Interestingly, yeast Msl1 (a homologue of mammalian U2B", one of the U2 snRNP proteins) was also found at promoters.[68] Sgf29 and Chd1, both of the proteins interacting with U2 snRNP in human cells, are conserved in yeasts and they are components of the yeast SAGA complex.[98] It is possible that Gcn5 plays a role in the recruitment of the SAGA complex to promoters and that SAGA complex subunits are bringing the U2 snRNP. In human cells, the STAGA complex (homologue of the yeast SAGA complex) interacts with the U2 snRNP specific protein SF3B3 (SF3b130).[100]

MRG15: Chromatin Binding Protein that Recruits Splicing Regulator PTB

PTB is an example of a splicing regulator that was shown to associate with chromatin and, more importantly, to modulate through this association alternative splicing of a number of genes.[88] PTB binds chromatin via MRG15 protein and this interaction preferentially regulates splicing of pre-mRNAs with weak PTB binding sites. MRG15 contains chromodomain that is able to bind H3K36me3 [101] and H3K36me3 level on a particular gene correlates with PTB recruitment to pre-mRNAs transcribed from this gene.[88] Interestingly, MRG15 does not only bind H3K36me3, but also interacts with H3K4me3.[87] A simple MRG15 knock-down influences alternative splicing of more than 180 genes independently of PTB.[88] This suggests that there might be an alternative mechanism that does not depend on PTB, although many of these alternative splicing changes might be due to the indirect effects caused by altered expression of splicing regulators after MRG15 knockdown. MRG15 is a component of several chromatin modifying complexes. These complexes contain histone acetylases Tip60 [102,103] and hMOF,[104] histone deacetylases such as HDAC1 or HDAC2 [105,106] and histone demethylases.[107,108] Eaf3, a yeast orthologue of MRG15, associates with RNA polymerase II[109] and is important for histone deacetylation during transcription elongation that inhibits the internal transcription initiation inside coding sequences of genes.[110,111] In mammalian cells, a similar complex that consist of both HDAC1 and MRG15 was identified recently and it was shown to affect progression of RNA polymerase II through transcribed regions.[106] Thus, MRG15 significantly participates in regulation of chromatin acetylation and transcription, processes that were shown to modulate splicing outcome (see above) and it would be interesting to know whether MRG15 alone is able to affect alternative splicing directly through modulation of chromatin.

hnRNP Proteins and H3K9 Methylation

H3K9 methylation, which recruits the HP1 protein, is important for the formation and maintenance of heterochromatin. Although average levels of H3K9me3 and H3K9me2 correlate with gene silencing, both histone modifications can be also detected in some actively transcribed genes.[61,93,112,113] Recently, PTB, together with other splicing regulators hnRNPs (hnRNP A1, hnRNP L, hnRNP K, hnRNP A2/B1, hnRNP A/B), were identified as proteins able to recognize H3K9me3.[87] In Drosophila, several other hnRNP proteins interact with HP1 and heterochromatin.[114] What can be the reason for such an association? One of the H3K9me3 recognizing proteins, hnRNP K, binds to large intergenic noncoding RNAs (linc-RNAs) and the complex of linc-RNA and hnRNP K is an effector of p53 signaling and represses transcription of hundreds of genes.[115] When PTB-RNA interactions were analyzed genome-wide by CLIP-seq method, a substantial fraction of tags (almost 30%) was mapped to intergenic regions, implying that PTB may also bind to noncoding RNAs.[116] PTB was also detected at the promoter of the *HMGA2* gene containing a very specific ~60 bp polypyrimidine/polypurine element but it is unclear whether binding to this promoter is mediated by chromatin.[117,118] It is intriguing to speculate that the association of hnRNP proteins with the chromatin might regulate transcription. In addition, hnRNP proteins binding to HP1 are involved in heterochromatin formation in Drosophila.[114]

H3K9me2 and H3K9me3 were also reported to be enriched at introns in contrast to exons.[58,59] hnRNP proteins associated with chromatin then might help to define intronic sequences. In human cells, the increase of heterochromatin marks (H3K9me2, H3K27me3) together with the presence of HP1α leads to changes in alternative splicing of the fibronectin gene.[40] Recently, it was shown that association of HP1γ with H3K9me3 modulates alternative splicing of several genes including *CD44*.[113] Although the induced heterochromatin formation near the alternative exons reduces the processivity of RNA polymerase II which causes the increased inclusion of alternative exon, it is still possible that methylation of H3K9 influences splicing of certain genes directly via tethering of splicing factors. Interestingly, exons enriched in the H3K9me3 are preferentially excluded from mature mRNAs indicating again the role of H3K9me3 in the regulation of splicing.[61]

Perspectives

The major task in the near future will be to reveal molecular details and mechanism(s) through which chromatin modifications affect pre-mRNA splicing. This knowledge is important not only from a theoretical point of view but might be essential for practical medical usage. Many small molecules that influence chromatin modifications serve as therapeutical agents and thus there is a hope that these compounds might help to treat splicing related diseases as well. The better we understand the connection between splicing and chromatin the higher chance to identify such a drug.

Acknowledgments

We thank Stanek's lab members for helpful comments. Projects in David Stanek's lab are supported by grants from the Czech Science Foundation (P305/10/0424) and from the Academy of Sciences of the Czech Republic (KAN200520801, AV0Z50520514).

References

1. Lander ES, Linton LM, Birren B, Nusbaum C, Zody MC, Baldwin J, et al. Initial sequencing and analysis of the human genome. Nature 2001; 409:860-921.
2. Scherer S. A short guide to the human genome. Cold Spring Harbor NY: Cold Spring Harbor Laboratory Press 2008; 34.
3. Wang ET, Sandberg R, Luo S, Khrebtukova I, Zhang L, Mayr C, et al. Alternative isoform regulation in human tissue transcriptomes. Nature 2008; 456:470-6.
4. Pan Q, Shai O, Lee LJ, Frey BJ, Blencowe BJ. Deep surveying of alternative splicing complexity in the human transcriptome by high-throughput sequencing. Nat Genet 2008; 40:1413-5.
5. Wang Z, Burge CB. Splicing regulation: from a parts list of regulatory elements to an integrated splicing code. RNA 2008; 14:802-13.
6. Black DL. Mechanisms of alternative pre-messenger RNA splicing. Annu Rev Biochem 2003; 72:291-336.
7. Barash Y, Calarco JA, Gao W, Pan Q, Wang X, Shai O, et al. Deciphering the splicing code. Nature 2010; 465:53-9.
8. Singh J, Padgett RA. Rates of in situ transcription and splicing in large human genes. Nat Struct Mol Biol 2009; 16:1128-33.
9. Tennyson CN, Klamut HJ, Worton RG. The human dystrophin gene requires 16 hours to be transcribed and is cotranscriptionally spliced. Nat Genet 1995; 9:184-90.
10. Pandya-Jones A, Black DL. Co-transcriptional splicing of constitutive and alternative exons. RNA 2009; 15:1896-908.
11. Listerman I, Sapra AK, Neugebauer KM. Cotranscriptional coupling of splicing factor recruitment and precursor messenger RNA splicing in mammalian cells. Nat Struct Mol Biol 2006; 13:815-22.
12. Zhang G, Taneja KL, Singer RH, Green MR. Localization of pre-mRNA splicing in mammalian nuclei. Nature 1994; 372:809-12.
13. Bauren G, Wieslander L. Splicing of Balbiani ring 1 gene pre-mRNA occurs simultaneously with transcription. Cell 1994; 76:183-92.
14. Wada Y, Ohta Y, Xu M, Tsutsumi S, Minami T, Inoue K, et al. A wave of nascent transcription on activated human genes. Proc Natl Acad Sci USA 2009; 106:18357-61.
15. Bittencourt D, Dutertre M, Sanchez G, Barbier J, Gratadou L, Auboeuf D. Cotranscriptional splicing potentiates the mRNA production from a subset of estradiol-stimulated genes. Mol Cell Biol 2008; 28:5811-24.
16. Carrillo Oesterreich F, Preibisch S, Neugebauer KM. Global analysis of nascent RNA reveals transcriptional pausing in terminal exons. Mol Cell 2010; 40:571-81.
17. Lacadie SA, Rosbash M. Cotranscriptional spliceosome assembly dynamics and the role of U1 snRNA:5'ss base pairing in yeast. Mol Cell 2005; 19:65-75.
18. Gornemann J, Kotovic KM, Hujer K, Neugebauer KM. Cotranscriptional spliceosome assembly occurs in a stepwise fashion and requires the cap binding complex. Mol Cell 2005; 19:53-63.
19. Lacadie SA, Tardiff DF, Kadener S, Rosbash M. In vivo commitment to yeast cotranscriptional splicing is sensitive to transcription elongation mutants. Genes Dev 2006; 20:2055-66.
20. Alexander RD, Barrass JD, Dichtl B, Kos M, Obtulowicz T, Robert MC, et al. RiboSys, a high-resolution, quantitative approach to measure the in vivo kinetics of pre-mRNA splicing and 3'-end processing in *Saccharomyces cerevisiae*. RNA 2010; 16:2570-80.
21. Alexander RD, Innocente SA, Barrass JD, Beggs JD. Splicing-dependent RNA polymerase pausing in yeast. Mol Cell 2010; 40:582-93.
22. Auboeuf D, Honig A, Berget SM, O'Malley BW. Coordinate regulation of transcription and splicing by steroid receptor coregulators. Science 2002; 298:416-9.
23. Kadener S, Cramer P, Nogues G, Cazalla D, de la Mata M, Fededa JP, et al. Antagonistic effects of T-Ag and VP16 reveal a role for RNA pol II elongation on alternative splicing. EMBO J 2001; 20:5759-68.
24. Kadener S, Fededa JP, Rosbash M, Kornblihtt AR. Regulation of alternative splicing by a transcriptional enhancer through RNA pol II elongation. Proc Natl Acad Sci USA 2002; 99:8185-90.
25. Kornblihtt AR. Promoter usage and alternative splicing. Curr Opin Cell Biol 2005; 17:262-8.
26. Moldon A, Malapeira J, Gabrielli N, Gogol M, Gomez-Escoda B, Ivanova T, et al. Promoter-driven splicing regulation in fission yeast. Nature 2008; 455:997-1000.
27. Cramer P, Caceres JF, Cazalla D, Kadener S, Muro AF, Baralle FE, Kornblihtt AR. Coupling of transcription with alternative splicing: RNA pol II promoters modulate SF2/ASF and 9G8 effects on an exonic splicing enhancer. Mol Cell 1999; 4:251-8.
28. Cramer P, Pesce CG, Baralle FE, Kornblihtt AR. Functional association between promoter structure and transcript alternative splicing. Proc Natl Acad Sci USA 1997; 94:11456-60.
29. Pagani F, Stuani C, Zuccato E, Kornblihtt AR, Baralle FE. Promoter architecture modulates CFTR exon 9 skipping. J Biol Chem 2003; 278:1511-7.
30. Auboeuf D, Dowhan DH, Li X, Larkin K, Ko L, Berget SM, et al. CoAA, a nuclear receptor coactivator protein at the interface of transcriptional coactivation and RNA splicing. Mol Cell Biol 2004; 24:442-53.
31. Auboeuf D, Dowhan DH, Kang YK, Larkin K, Lee JW, Berget SM, et al. Differential recruitment of nuclear receptor coactivators may determine alternative RNA splice site choice in target genes. Proc Natl Acad Sci USA 2004; 101:2270-4.
32. Rosonina E, Bakowski MA, McCracken S, Blencowe BJ. Transcriptional activators control splicing and 3'-end cleavage levels. J Biol Chem 2003; 278:43034-40.
33. Monsalve M, Wu Z, Adelmant G, Puigserver P, Fan M, Spiegelman BM. Direct coupling of transcription and mRNA processing through the thermogenic coactivator PGC-1. Mol Cell 2000; 6:307-16.
34. Munoz MJ, Perez Santangelo MS, Paronetto MP, de la Mata M, Pelisch F, Boireau S, et al. DNA damage regulates alternative splicing through inhibition of RNA polymerase II elongation. Cell 2009; 137:708-20.
35. de la Mata M, Alonso CR, Kadener S, Fededa JP, Blaustein M, Pelisch F, et al. A slow RNA polymerase II affects alternative splicing in vivo. Mol Cell 2003; 12:525-32.
36. Nogues G, Kadener S, Cramer P, Bentley D, Kornblihtt AR. Transcriptional activators differ in their abilities to control alternative splicing. J Biol Chem 2002; 277:43110-4.
37. Ip JY, Schmidt D, Pan Q, Ramani AK, Fraser AG, Odom DT, et al. Global impact of RNA polymerase II elongation inhibition on alternative splicing regulation. Genome Res 2011.
38. Hnilicova J, Hozeifi S, Duskova E, Icha J, Tomankova T, Stanek D. Histone deacetylase activity modulates alternative splicing. PLoS One 2011; 6:16727.
39. Batsche E, Yaniv M, Muchardt C. The human SWI/SNF subunit Brm is a regulator of alternative splicing. Nat Struct Mol Biol 2006; 13:22-9.
40. Allo M, Buggiano V, Fededa JP, Petrillo E, Schor I, de la Mata M, et al. Control of alternative splicing through siRNA-mediated transcriptional gene silencing. Nat Struct Mol Biol 2009; 16:717-24.
41. Howe KJ, Kane CM, Ares M Jr. Perturbation of transcription elongation influences the fidelity of internal exon inclusion in *Saccharomyces cerevisiae*. RNA 2003; 9:993-1006.
42. Roberts GC, Gooding C, Mak HY, Proudfoot NJ, Smith CW. Co-transcriptional commitment to alternative splice site selection. Nucleic Acids Res 1998; 26:5568-72.
43. Nogues G, Munoz MJ, Kornblihtt AR. Influence of polymerase II processivity on alternative splicing depends on splice site strength. J Biol Chem 2003; 278:52166-71.
44. de la Mata M, Kornblihtt AR. RNA polymerase II C-terminal domain mediates regulation of alternative splicing by SRp20. Nat Struct Mol Biol 2006; 13:973-80.
45. Barboric M, Lenasi T, Chen H, Johansen EB, Guo S, Peterlin BM. 7SK snRNP/P-TEFb couples transcription elongation with alternative splicing and is essential for vertebrate development. Proc Natl Acad Sci USA 2009; 106:7798-803.
46. Darzacq X, Shav-Tal Y, de Turris V, Brody Y, Shenoy SM, Phair RD, et al. In vivo dynamics of RNA polymerase II transcription. Nat Struct Mol Biol 2007; 14:796-806.
47. Boireau S, Maiuri P, Basyuk E, de la Mata M, Knezevich A, Pradet-Balade B, et al. The transcriptional cycle of HIV-1 in real-time and live cells. J Cell Biol 2007; 179:291-304.
48. Mason PB, Struhl K. Distinction and relationship between elongation rate and processivity of RNA polymerase II in vivo. Mol Cell 2005; 17:831-40.
49. Ben-Ari Y, Brody Y, Kinor N, Mor A, Tsukamoto T, Spector DL, et al. The life of an mRNA in space and time. J Cell Sci 2010; 123:1761-74.
50. Huranova M, Ivani I, Benda A, Poser I, Brody Y, Hof M, et al. The differential interaction of snRNPs with pre-mRNA reveals splicing kinetics in living cells. J Cell Biol 2010; 191:75-86.
51. Wetterberg I, Zhao J, Masich S, Wieslander L, Skoglund U. In situ transcription and splicing in the Balbiani ring 3 gene. EMBO J 2001; 20:2564-74.
52. Kouzarides T. Chromatin modifications and their function. Cell 2007; 128:693-705.

53. Radman-Livaja M, Rando OJ. Nucleosome positioning: how is it established and why does it matter? Dev Biol 2009; 339:258-66.
54. Kolasinska-Zwierz P, Down T, Latorre I, Liu T, Liu XS, Ahringer J. Differential chromatin marking of introns and expressed exons by H3K36me3. Nat Genet 2009; 41:376-81.
55. Schwartz S, Meshorer E, Ast G. Chromatin organization marks exon-intron structure. Nat Struct Mol Biol 2009; 16:990-5.
56. Tilgner H, Nikolaou C, Althammer S, Sammeth M, Beato M, Valcarcel J, Guigo R. Nucleosome positioning as a determinant of exon recognition. Nat Struct Mol Biol 2009; 16:996-1001.
57. Andersson R, Enroth S, Rada-Iglesias A, Wadelius C, Komorowski J. Nucleosomes are well positioned in exons and carry characteristic histone modifications. Genome Res 2009; 19:1732-41.
58. Dhami P, Saffrey P, Bruce AW, Dillon SC, Chiang K, Bonhoure N, et al. Complex exon-intron marking by histone modifications is not determined solely by nucleosome distribution. PLoS One 2009; 5:12339.
59. Spies N, Nielsen CB, Padgett RA, Burge CB. Biased chromatin signatures around polyadenylation sites and exons. Mol Cell 2009; 36:245-54.
60. Huff JT, Plocik AM, Guthrie C, Yamamoto KR. Reciprocal intronic and exonic histone modification regions in humans. Nat Struct Mol Biol 2010; 17:1495-9.
61. Hon G, Wang W, Ren B. Discovery and annotation of functional chromatin signatures in the human genome. PLoS Comput Biol 2009; 5:1000566.
62. Nahkuri S, Taft RJ, Mattick JS. Nucleosomes are preferentially positioned at exons in somatic and sperm cells. Cell Cycle 2009; 8:3420-4.
63. Schwartz S, Ast G. Chromatin density and splicing destiny: on the cross-talk between chromatin structure and splicing. EMBO J 2010; 29:1629-36.
64. Tilgner H, Guigo R. From chromatin to splicing: RNA-processing as a total artwork. Epigenetics 2010; 5.
65. Loomis RJ, Naoe Y, Parker JB, Savic V, Bozovsky MR, Macfarlan T, et al. Chromatin binding of SRp20 and ASF/SF2 and dissociation from mitotic chromosomes is modulated by histone H3 serine 10 phosphorylation. Mol Cell 2009; 33:450-61.
66. Barth TK, Imhof A. Fast signals and slow marks: the dynamics of histone modifications. Trends Biochem Sci 2010; 35:618-26.
67. Schor IE, Rascovan N, Pelisch F, Allo M, Kornblihtt AR. Neuronal cell depolarization induces intragenic chromatin modifications affecting NCAM alternative splicing. Proc Natl Acad Sci USA 2009; 106:4325-30.
68. Gunderson FQ, Johnson TL. Acetylation by the transcriptional coactivator Gcn5 plays a novel role in co-transcriptional spliceosome assembly. PLoS Genet 2009; 5:1000682.
69. Gunderson FQ, Merkhofer EC, Johnson TL. Dynamic histone acetylation is critical for cotranscriptional spliceosome assembly and spliceosomal rearrangements. Proc Natl Acad Sci USA 2011; 108:2004-9.
70. Kotovic KM, Lockshon D, Boric L, Neugebauer KM. Cotranscriptional recruitment of the U1 snRNP to intron-containing genes in yeast. Mol Cell Biol 2003; 23:5768-79.
71. Konarska MM, Sharp PA. Electrophoretic separation of complexes involved in the splicing of precursors to mRNAs. Cell 1986; 46:845-55.
72. Bindereif A, Green MR. An ordered pathway of snRNP binding during mammalian pre-mRNA splicing complex assembly. EMBO J 1987; 6:2415-24.
73. Jurica MS, Licklider LJ, Gygi SR, Grigorieff N, Moore MJ. Purification and characterization of native spliceosomes suitable for three-dimensional structural analysis. RNA 2002; 8:426-39.
74. Tardiff DF, Rosbash M. Arrested yeast splicing complexes indicate stepwise snRNP recruitment during in vivo spliceosome assembly. RNA 2006; 12:968-79.
75. Tardiff DF, Lacadie SA, Rosbash M. A genome-wide analysis indicates that yeast pre-mRNA splicing is predominantly posttranscriptional. Mol Cell 2006; 24:917-29.
76. Wahl MC, Will CL, Luhrmann R. The spliceosome: design principles of a dynamic RNP machine. Cell 2009; 136:701-18.
77. Jobert L, Pinzon N, Van Herreweghe E, Jady BE, Guialis A, Kiss T, Tora L. Human U1 snRNA forms a new chromatin-associated snRNP with TAF15. EMBO Rep 2009; 10:494-500.
78. Damgaard CK, Kahns S, Lykke-Andersen S, Nielsen AL, Jensen TH, Kjems J. A 5' splice site enhances the recruitment of basal transcription initiation factors in vivo. Mol Cell 2008; 29:271-8.
79. Kwek KY, Murphy S, Furger A, Thomas B, O'Gorman W, Kimura H, et al. U1 snRNA associates with TFIIH and regulates transcriptional initiation. Nat Struct Biol 2002; 9:800-5.
80. O'Gorman W, Thomas B, Kwek KY, Furger A, Akoulitchev A. Analysis of U1 small nuclear RNA interaction with cyclin H. J Biol Chem 2005; 280:36920-5.
81. Ares M Jr, Grate L, Pauling MH. A handful of intron-containing genes produces the lion's share of yeast mRNA. RNA 1999; 5:1138-9.
82. Furger A, O'Sullivan JM, Binnie A, Lee BA, Proudfoot NJ. Promoter proximal splice sites enhance transcription. Genes Dev 2002; 16:2792-9.
83. Eberle AB, Hessle V, Helbig R, Dantoft W, Gimber N, Visa N. Splice-site mutations cause Rrp6-mediated nuclear retention of the unspliced RNAs and transcriptional downregulation of the splicing-defective genes. PLoS One 2010; 5:11540.
84. Fong YW, Zhou Q. Stimulatory effect of splicing factors on transcriptional elongation. Nature 2001; 414:929-33.
85. Alexander MR, Wheatley AK, Center RJ, Purcell DF. Efficient transcription through an intron requires the binding of an Sm-type U1 snRNP with intact stem loop II to the splice donor. Nucleic Acids Res 2010; 38:3041-53.
86. Sims RJ, 3rd, Millhouse S, Chen CF, Lewis BA, Erdjument-Bromage H, Tempst P, et al. Recognition of trimethylated histone H3 lysine 4 facilitates the recruitment of transcription postinitiation factors and pre-mRNA splicing. Mol Cell 2007; 28:665-76.
87. Vermeulen M, Eberl HC, Matarese F, Marks H, Denissov S, Butter F, et al. Quantitative interaction proteomics and genome-wide profiling of epigenetic histone marks and their readers. Cell 2010; 142:967-80.
88. Luco RF, Pan Q, Tominaga K, Blencowe BJ, Pereira-Smith OM, Misteli T. Regulation of alternative splicing by histone modifications. Science 2010; 327:996-1000.
89. Shilatifard A. Molecular implementation and physiological roles for histone H3 lysine 4 (H3K4) methylation. Curr Opin Cell Biol 2008; 20:341-8.
90. Dou Y, Milne TA, Ruthenburg AJ, Lee S, Lee JW, Verdine GL, et al. Regulation of MLL1 H3K4 methyltransferase activity by its core components. Nat Struct Mol Biol 2006; 13:713-9.
91. Steward MM, Lee JS, O'Donovan A, Wyatt M, Bernstein BE, Shilatifard A. Molecular regulation of H3K4 trimethylation by ASH2L, a shared subunit of MLL complexes. Nat Struct Mol Biol 2006; 13:852-4.
92. Bernstein BE, Kamal M, Lindblad-Toh K, Bekiranov S, Bailey DK, Huebert DJ, et al. Genomic maps and comparative analysis of histone modifications in human and mouse. Cell 2005; 120:169-81.
93. Barski A, Cuddapah S, Cui K, Roh TY, Schones DE, Wang Z, et al. High-resolution profiling of histone methylations in the human genome. Cell 2007; 129:823-37.
94. Heintzman ND, Stuart RK, Hon G, Fu Y, Ching CW, Hawkins RD, et al. Distinct and predictive chromatin signatures of transcriptional promoters and enhancers in the human genome. Nat Genet 2007; 39:311-8.
95. Guenther MG, Levine SS, Boyer LA, Jaenisch R, Young RA. A chromatin landmark and transcription initiation at most promoters in human cells. Cell 2007; 130:77-88.
96. Mikkelsen TS, Ku M, Jaffe DB, Issac B, Lieberman E, Giannoukos G, et al. Genome-wide maps of chromatin state in pluripotent and lineage-committed cells. Nature 2007; 448:553-60.
97. Schneider R, Bannister AJ, Myers FA, Thorne AW, Crane-Robinson C, Kouzarides T. Histone H3 lysine 4 methylation patterns in higher eukaryotic genes. Nat Cell Biol 2004; 6:73-7.
98. Baker SP, Grant PA. The SAGA continues: expanding the cellular role of a transcriptional co-activator complex. Oncogene 2007; 26:5329-40.
99. Hassan AH, Prochasson P, Neely KE, Galasinski SC, Chandy M, Carrozza MJ, Workman JL. Function and selectivity of bromodomains in anchoring chromatin-modifying complexes to promoter nucleosomes. Cell 2002; 111:369-79.
100. Martinez E, Palhan VB, Tjernberg A, Lymar ES, Gamper AM, Kundu TK, et al. Human STAGA complex is a chromatin-acetylating transcription coactivator that interacts with pre-mRNA splicing and DNA damage-binding factors in vivo. Mol Cell Biol 2001; 21:6782-95.
101. Zhang P, Du J, Sun B, Dong X, Xu G, Zhou J, et al. Structure of human MRG15 chromo domain and its binding to Lys36-methylated histone H3. Nucleic Acids Res 2006; 34:6621-8.
102. Cai Y, Jin J, Tomomori-Sato C, Sato S, Sorokina I, Parmely TJ, et al. Identification of new subunits of the multiprotein mammalian TRRAP/TIP60-containing histone acetyltransferase complex. J Biol Chem 2003; 278:42733-6.
103. Doyon Y, Selleck W, Lane WS, Tan S, Cote J. Structural and functional conservation of the NuA4 histone acetyltransferase complex from yeast to humans. Mol Cell Biol 2004; 24:1884-96.
104. Pardo PS, Leung JK, Lucchesi JC, Pereira-Smith OM. MRG15, a novel chromodomain protein, is present in two distinct multiprotein complexes involved in transcriptional activation. J Biol Chem 2002; 277:50860-6.
105. Yochum GS, Ayer DE. Role for the mortality factors MORF4, MRGX and MRG15 in transcriptional repression via associations with Pf1, mSin3A and Transducin-Like Enhancer of Split. Mol Cell Biol 2002; 22:7868-76.
106. Jelinic P, Pellegrino J, David G. A novel mammalian complex containing Sin3B mitigates histone acetylation and RNAPII progression within transcribed loci. Mol Cell Biol 2011.
107. Hayakawa T, Ohtani Y, Hayakawa N, Shinmyozu K, Saito M, Ishikawa F, Nakayama J. RBP2 is an MRG15 complex component and downregulates intragenic histone H3 lysine 4 methylation. Genes Cells 2007; 12:811-26.
108. Lee N, Erdjument-Bromage H, Tempst P, Jones RS, Zhang Y. The H3K4 demethylase lid associates with and inhibits histone deacetylase Rpd3. Mol Cell Biol 2009; 29:1401-10.
109. Govind CK, Qiu H, Ginsburg DS, Ruan C, Hofmeyer K, Hu C, et al. Phosphorylated Pol II CTD recruits multiple HDACs, including Rpd3C(S), for methylation-dependent deacetylation of ORF nucleosomes. Mol Cell 2010; 39:234-46.
110. Joshi AA, Struhl K. Eaf3 chromodomain interaction with methylated H3-K36 links histone deacetylation to Pol II elongation. Mol Cell 2005; 20:971-8.
111. Carrozza MJ, Li B, Florens L, Suganuma T, Swanson SK, Lee KK, et al. Histone H3 methylation by Set2 directs deacetylation of coding regions by Rpd3S to suppress spurious intragenic transcription. Cell 2005; 123:581-92.
112. Vakoc CR, Mandat SA, Olenchock BA, Blobel GA. Histone H3 lysine 9 methylation and HP1gamma are associated with transcription elongation through mammalian chromatin. Mol Cell 2005; 19:381-91.

113. Saint-André V, Batsché E, Rachez C, Muchardt C. Histone H3 lysine 9 trimethylation and HP1γ favor inclusion of alternative exons. Nat Struct Mol Biol 2011; 18:337-44.
114. Piacentini L, Fanti L, Negri R, Del Vescovo V, Fatica A, Altieri F, Pimpinelli S. Heterochromatin protein 1 (HP1a) positively regulates euchromatic gene expression through RNA transcript association and interaction with hnRNPs in Drosophila. PLoS Genet 2009; 5:1000670.
115. Huarte M, Guttman M, Feldser D, Garber M, Koziol MJ, Kenzelmann-Broz D, et al. A large intergenic noncoding RNA induced by p53 mediates global gene repression in the p53 response. Cell 2010; 142:409-19.
116. Xue Y, Zhou Y, Wu T, Zhu T, Ji X, Kwon YS, et al. Genome-wide analysis of PTB-RNA interactions reveals a strategy used by the general splicing repressor to modulate exon inclusion or skipping. Mol Cell 2009; 36:996-1006.
117. Ferguson M, Henry PA, Currie RA. Histone deacetylase inhibition is associated with transcriptional repression of the Hmga2 gene. Nucleic Acids Res 2003; 31:3123-33.
118. Rustighi A, Tessari MA, Vascotto F, Sgarra R, Giancotti V, Manfioletti G. A polypyrimidine/polypurine tract within the Hmga2 minimal promoter: a common feature of many growth-related genes. Biochemistry 2002; 41:1229-40.
119. Tai HH, Geisterfer M, Bell JC, Moniwa M, Davie JR, Boucher L, McBurney MW. CHD1 associates with NCoR and histone deacetylase as well as with RNA splicing proteins. Biochem Biophys Res Commun 2003; 308:170-6.
120. Pryde F, Khalili S, Robertson K, Selfridge J, Ritchie AM, Melton DW, et al. 53BP1 exchanges slowly at the sites of DNA damage and appears to require RNA for its association with chromatin. J Cell Sci 2005; 118:2043-55.
121. Young JI, Hong EP, Castle JC, Crespo-Barreto J, Bowman AB, Rose MF, et al. Regulation of RNA splicing by the methylation-dependent transcriptional repressor methyl-CpG binding protein 2. Proc Natl Acad Sci USA 2005; 102:17551-8.